

Neutronic Optimisations of Breeder Blankets for Fusion Reactors



Jonathan Gregory Shimwell

Department of Physics and Astronomy
University of Sheffield

This dissertation is submitted for the degree of
Doctor of Philosophy

June 2016

I would like to dedicate this thesis to my mum.

Declaration

I hereby declare that the content of this thesis, except where otherwise stated is based on my own original research. This thesis has not been submitted in whole or in part for consideration for any other degree or qualification in this, or any other university. Sections of the research presented in this thesis have been published in:

- Spatially and temporally varying tritium generation in solid-type breeder blankets.
J. Shimwell, L. Morgan, S. Lilley, T. Eade, M. Kovari, S. Zheng and J. McMillan.
Published in Fusion Engineering and Design [171].
- A parameter study of time-varying tritium production in solid-type breeder blankets.
J. Shimwell, M. Kovari, S. Lilley, S. Zheng, L. Morgan, L. Packer and J. McMillan.
Submitted to Fusion Engineering and Design [169].
- Isotopically enriched structural material in nuclear devices.
L. Morgan, J. Shimwell and M. Gilbert.
Published in Fusion Engineering and Design [132].
- Reducing beryllium content in mixed bed solid-type breeder blankets.
J. Shimwell, S. Lilley, L. Morgan, L. Packer, M. Kovari, S. Zheng and J. McMillan.
Published in Fusion Engineering and Design [170].

Acknowledgements

I would like to express my sincere gratitude to the following people:

- Friends and family for their help and support: Helen Gale, Tim Shimwell, Suzi Shimwell, Lidiya Pasuljevic, Brais Lopez Paredes, Dimitrios Kyriazopoulos, Luke Chen, Victor Ambrus and Stephen Sadler.
- My wonderful colleagues: Frances Fox, Andrew Turner, Bethany Colling, Elizabeth Surrey, Jonathan Naish, Christopher Ham, Gemma Hurst, Michael Fleming, Zamir Ghani, Jean-Christophe Sublet, David Ward, Tom O’Gorman, Howard Wilson, Susan Cartwright and Neil Lowrie.
- Fantastic collaborators who have been superb to work with: Lee Morgan, Michael Kovari, Shanliang Zheng, Lee Packer, Tim Eade, Ryuta Kasada and Geoffrey Olynyk.
- Two absolutely great supervisors. Many thanks to John McMillan for supporting my development over the last four years. I am particularly appreciative of contributions made by Steven Lilley during the PhD and preceding MSc project.

The following organisations have also been incredibly helpful.

- The Technology Group at Culham Centre for Fusion Energy.
- The Department of Physics and Astronomy at The University of Sheffield.
- The E-Futures Doctoral Training Centre at The University of Sheffield for providing an outstanding training programme and enhancing my understanding of the world’s need for sustainable energy.

-
- Fusenet the educational arm of EUROfusion for enhancing my understanding of fusion.
 - The York Plasma Institute at the University of York for broadening my fusion knowledge base and hosting me for a project on diagnostics.
 - I would also like to express my gratitude to EPSRC for their financial support.
 - The Sheffield, Abingdon and Oxford branches of Waitrose for providing such excellent food and coffee.

Abstract

Fusion is seen by many as the ultimate energy source, capable of providing safe, clean and sustainable energy. Research has been carried out into fusion since the 1920s and substantial progress has been made. While the ultimate goal of providing energy from fusion remains elusive there is a clear understanding of the tasks that must be achieved to make fusion energy a reality.

Deuterium and tritium (DT) offer a high probability of fusion when compared to any other combination of isotopes. Consequently DT fusion is the focus of all large scale fusion research programmes. As there is no natural source of tritium, fusion reactors are being designed with tritium breeder blankets to ensure self-sufficiency. The research contained within this thesis contributes to the ongoing development of breeder blankets for fusion reactors in terms of reducing their cost and improving their performance. The thesis follows a general theme of varying material composition to better utilise the local neutron spectra within fusion breeder blankets. The novel contributions of this thesis are as follows:

The first contribution of this thesis is a technique that improves the accuracy of simulations involving time varying tritium production [171]. The technique identifies a minimum spacial resolution that should be used when performing burn-up studies in solid-type breeder blankets. Previously the tritium production with respect to time has been overestimated due to lack of spatial segmentation within the breeder blanket.

Following on from this a parameter study was carried out to ascertain a more optimal composition for breeder blankets. The results of this study allows blanket designers to minimise the cost of the blanket while increasing the heat generated or maximising the tritium produced.

The composition of breeder blankets operating with a DD neutron source was also optimised. This allows breeder blankets to create tritium from DD plasmas more efficiently.

The use of DD plasmas to generate tritium is a proposed method of negating the need for an external supply of tritium to start up reactors.

The sustainability of fusion is investigated and a method of reducing the use of beryllium within breeder blankets is presented. Blankets utilising this method were also shown to generate more heat, produce more tritium and showed lower peak heating. Varying the isotopic composition of materials was considered as a method to reduce helium production and improve the material properties without additional activity [132]. For the first, time cost benefit analysis of isotopically tailored materials in fusion reactors has been carried out and various methods to offset the enrichment cost have been identified.

Multilayer blankets are investigated as a method of increasing the tritium production and are shown to achieve tritium production levels that are unobtainable for blankets with a uniform composition. Higher tritium production from blankets is particularly necessary in reactor designs that involve a reduction in the blanket volume.

The composition of structural materials used within breeder blankets was also investigated. New material compositions are considered that offer reduced helium production. Additionally, materials that potentially offer improved material properties (e.g. fracture toughness and yield stress) are shown to be achievable. This is achieved by the addition of enriched Ni or Mo; the enrichment of the natural element allows it to be reintroduced without significant increase in activity.

The final chapter summarises the research carried out, makes recommendations with regards to the design of future breeder blankets and presents further research opportunities.

Table of contents

Table of contents	ix
List of figures	xiii
List of tables	xix
1 Introduction to fusion	1
1.1 Fusion Energy	1
1.1.1 Introduction to fusion	1
1.1.2 Possible fusion reactions	5
1.1.3 Magnetic confinement fusion	7
1.1.4 Progress in magnetic confinement fusion	10
1.1.5 Planned progress	17
1.1.6 Challenges identified	20
1.2 Tritium breeder blankets	23
1.2.1 Introduction	23
1.2.2 Requirements	28
1.2.3 Breeding blanket materials	31
1.2.4 Homogenisation of materials	34
1.3 Sustainability of fusion energy	37
1.3.1 Conclusion	43
1.4 Nuclear simulations	44
1.4.1 Particle transport	45

Table of contents

1.4.2	Nuclear interaction probabilities	48
1.4.3	Interface codes	51
1.5	Summary and prelude	52
2	Time varying tritium production	55
2.1	Introduction	55
2.2	Material and methods	58
2.3	Theory	62
2.4	Results	66
2.5	Conclusion	70
3	Breeder blanket parameter study	73
3.1	Introduction	73
3.2	Materials and methods	76
3.2.1	MCNP model	76
3.2.2	Materials	76
3.2.3	Calculation method	78
3.2.4	Cost estimates	80
3.3	Theory	82
3.4	Results	84
3.5	Conclusion	102
4	Breeder blankets for DD plasmas	105
4.1	Introduction	105
4.2	Materials and methods	110
4.3	Results	113
4.3.1	Storing the tritium produced	115
4.3.2	Refueling the plasma with the tritium produced	116
4.4	Conclusion	118

5 Reducing beryllium content in mixed bed solid-type breeder blankets	121
5.1 Introduction	121
5.2 Theory	124
5.3 Materials and methods	125
5.4 Results	128
5.4.1 Performance of uniform multiplier fraction blankets.	128
5.4.2 Decrease quantity of beryllium	130
5.4.3 Maintain sufficient tritium breeding ratio.	131
5.4.4 Increase energy multiplication	132
5.4.5 Reduced peak heating	133
5.4.6 Improved performance	134
5.5 Conclusion	136
6 Layered breeder blanket	137
6.1 Introduction	137
6.2 Method	138
6.3 Results	142
6.4 Conclusion	148
7 Isotopically Enriched Structural Materials	149
7.1 Introduction	149
7.2 Theory	152
7.3 Materials and methods	155
7.4 Results	158
7.4.1 Additional Mo in Eurofer	158
7.4.2 Additional Ni in Eurofer	159
7.4.3 Helium production in CuCrZr	161
7.5 Costs involved	162
7.6 Conclusion	170

Table of contents

8 Thesis conclusion	171
References	175

List of figures

1.1	Binding energy graph of stable isotopes, calculated from data made available by [31].	2
1.2	The resultant forces acting on the nucleus	3
1.3	Fusion reaction rate versus energy for fuel mixtures under consideration. ENDF/B-VII.1 data [22] was used to construct this graph	6
1.4	Fig1	8
1.5	The arrangement of toroidal (blue), poloidal (green) coils and divertor (yellow) within a Tokamak. Image source [48].	9
1.6	The magnetic coil arrangement of a Stellarator. The coloured plasma represents the strength of the magnetic field created by the coils. Image source [33].	11
1.7	The progress in triple product since the 1970s. Image source [48]	14
1.8	The funding requirements for each of the DEMO scenarios were originally published by [35]. Additional data on US fusion expenditure was provided by [86]. Geoffrey M. Olynyk conceived the original graph which this graph is based on.	15
1.9	Graph compiled from data on UK expenditure on R&D in fusion [86] overlaid with crude oil prices [14]. All values are inflation adjusted.	16
1.10	Likelihood of a tritium producing reaction with lithium isotopes. Data from the ENDF/B-VII.1 library [22].	25

List of figures

1.11 Neutron multiplication reactions with Be, Li and Pb. Data from the ENDF/B-VII.1 library [22].	26
1.12 The interaction cross-section of different fusion fuels.	49
1.13 Different evaluations of the EXFOR data for the $^9\text{Be}(\text{n},2\text{n})$ reaction.	50
2.1 Two differently segmented blankets are shown with alternate blanket layers coloured yellow  and green  <p>xiv</p>	

3.1	The thin blanket tokamak model used. This model was adapted from a tokamak DEMO model developed within the PPPT programme [148]. The vacuum vessel and divertor (grey) ■, toroidal field coils (green) ■, poloidal field coils (yellow) ■, blanket (red) ■, blanket casing (black) ■, and tungsten armour (blue) ■, are included. Image generated using [200].	77
3.2	Radial build of the thin blanket at equatorial level. This model was adapted from a tokamak DEMO model developed within the PPPT programme [148].	78
3.3	The combined costs of Be_{12}Ti , Li_4SiO_4 and ${}^6\text{Li}$ enrichment for different blanket compositions.	81
3.4	The time-averaged TBR values for thick, medium and thin blanket thicknesses and different blanket compositions. A TBR of 1.15 is identified by the red contour line.	85
3.5	The tritium inventory at five years for thick, medium and thin blanket thicknesses, with self-sufficient blanket compositions identified by the red contour line.	87
3.6	Optimal ratio of breeder to multiplier in terms of maximising the TBR as a function of ${}^6\text{Li}$ enrichment.	92
3.7	Cost effective blanket compositions capable of producing different sized start up inventories.	93
3.8	A comparison between costs required for the three blanket thicknesses to produce different sized tritium inventories.	94
3.9	The energy deposited by just neutrons, just photons and combined energy from neutrons and photons within the blanket	98
3.10	The change in TBR over the blanket's five year lifetime.	100
3.11	Blanket compositions that meet specified TBR, heat and cost requirements.	101
4.1	Nuclear interactions that result in the production of tritium.	107
4.2	HCPB DEMO model used. The vacuum vessel, divertor and blanket casing (purple) ■, toroidal field coils (green) ■, poloidal field coils (yellow) ■, blanket (light blue) ■ and the rear casing for the blanket (black) ■.	111

List of figures

4.3	View of HCPB DEMO model showing individual blanket modules. The tungsten first wall armour is also shown (red) ■	111
4.4	A simplified diagram of the system dynamics model used; this diagram only shows the main tritium pathways.	112
4.5	TBR values for different blanket compositions.	114
4.6	TPR values for different blanket compositions.	114
4.7	Time required by each blanket composition to reach a 50:50 DT plasma.	116
4.8	The time required to reach a 50:50 DT plasma with different breeder fractions and 100% ^6Li enrichment. TPR and TBR of the compositions are also shown.	117
4.9	The time required to reach a 50:50 DT plasma with different breeder fractions and 70% ^6Li enrichment. TPR and TBR of the compositions are also shown.	118
5.1	The tokamak model used. The vacuum vessel and divertor (grey) ■, toroidal field coils (green) ■, poloidal field coils (yellow) ■, blanket (red) ■, blanket casing (black) ■ and tungsten armour (blue) ■ are included. Image generated using [200].	125
5.2	Examples of how multiplier fraction varies with blanket depth.	126
5.3	Key performance criteria for different multiplier fractions in a mixed pebble bed breeder blanket utilising uniform multiplier fractions.	129
5.4	Total ^9Be requirements for each blanket composition simulated.	130
5.5	The simulated TBR results for different blanket configurations.	131
5.6	Energy multiplication in the breeder blanket by neutrons and photons.	132
5.7	Peak nuclear heating (photon and neutron) in the variable multiplier fraction blankets.	133
5.8	The diagram shows the region of blanket configurations that offer higher energy multiplication, lower peak heat, less ^9Be usage than the uniform multiplier fraction blanket (optimised for TBR).	135

6.1	Various views of the modified DEMO model used, showing the vacuum vessel, divertor and blanket casing (grey) ■, toroidal field coils (green) □, poloidal field coils (yellow) △, blanket (alternating layers orange ▲ and pink ▼) and tungsten armour (red) ▨ are included. Image generated using [200].	141
6.2	Optimising the composition of a uniform blanket for two different enrichments of ${}^6\text{Li}$	142
6.3	Results showing the TBR values of 24 variations to the starting design. Error bars shown are derived from statistical error data produced by MCNP and show a 1 sigma confidence.	144
6.4	Final composition found when the ${}^6\text{Li}$ enrichment was limited to 100% . .	146
6.5	Final composition found when the ${}^6\text{Li}$ enrichment was limited to 70% . .	146
6.6	Maximum TBR achieved with each iteration of the blanket composition. . .	147
7.1	(n, α) cross-sections for the two stable Cu isotopes. Data from the ENDF/B-VII.1 library [22].	152
7.2	Neutron disappearance cross-sections for the different Ni isotopes.	153
7.3	Neutron disappearance cross-sections for the different Mo isotopes.	154
7.4	View of the HCPB DEMO model used. Individual components of the fusion reactor and the plasma source intensity are shown. The location of the Eurofer within the blanket (A) and the CuCrZr as a plasma facing component (B) are shown. Image source [132].	155
7.5	MCNP F4 tallies showing the neutron spectra for the breeder blanket (position A) and the first wall (position B) shown in Figure 7.4.	157
7.6	The simulated activity of regular Eurofer compared to Eurofer with an additional 2% Mo mass.	158
7.7	The simulated activity of Eurofer containing 2% mass Mo additions with varying isotopic enrichments. For comparison, regular Eurofer and Eurofer with additional natural Mo are also plotted. The figure shows the activity 100 years after the end of irradiation.	159

List of figures

7.8	The activity of regular Eurofer compared to Eurofer with an additional 2% Ni mass.	160
7.9	The activity of Eurofer containing 2% mass Ni additions with varying isotopic enrichments. For comparison regular Eurofer and Eurofer with additional natural Ni are also plotted. The figure shows the activity 100 years after the end of irradiation.	160
7.10	The helium production (${}^3\text{He}$ and ${}^4\text{He}$ collectively) in CrCuZr	161
7.11	The enrichment 40,000kg of Ni to 95% ${}^{64}\text{Ni}$ content would cost at least £ 8.0×10^8 . The lowest cost is achieved with a ${}^{64}\text{Ni}$ tails fraction of 0.0083. . .	164
7.12	Optimising the depletion level of the tails for ${}^{64}\text{Ni}$ enrichment.	164
7.13	Optimising the depletion level of the tails for ${}^{97}\text{Mo}$ enrichment.	164
7.14	Optimising the depletion level of the tails for ${}^{65}\text{Cu}$ enrichment.	164
7.15	The additional availability or temperature required to cover the costs of isotope enrichment.	167
7.16	The cost of different enrichment scenarios and the resulting activity.	169

List of tables

1.1	Summary table of ITER test blankets.	28
1.2	Lattice parameters from [187] and [91]	35
2.1	Material fractions for the homogeneous breeder blanket material.	60
3.1	The dimensions and volumes of the three different breeder blanket scenarios simulated.	78
3.2	Coefficients for use with Equation 3.2 to calculate tritium inventory after five years.	89
3.3	Coefficients for use with Equation 3.2 to calculate time-averaged TBR. . . .	90
3.4	The relative performance of the different blanket thicknesses.	91
4.1	Summary of TBR and TPR values used by previous research.	109
4.2	A summary of the different compositions required to optimise the blanket for different neutron energies.	113
5.1	Material specifications for the homogenised breeder blanket material. . . .	126
6.1	Volume fractions of the materials used in the homogenised breeder zone. .	138
6.2	Comparison of TBR value achievable when using the uniform and non uniform blankets.	147
7.1	Natural abundance of isotopes in each of the three elements that were selected for enrichment, data from [31].	157

Nomenclature

Greek Symbols

τ	Confinement time
K_B	Boltzmann constant
n_i	Number density of ions
amu	Atomic mass units
CGS	Constructive Solid Geometry
D	Deuterium
DEMO	DEMOnstration power plant
dpa	Displacements per atom
ITLAM	Isotopically tailored low activation material
K	Kelvin
LAM	Low activation material
n	Neutron
p	Proton
T	Tritium
TBR	Tritium breeding ratio

Chapter 1

Introduction to fusion

1.1 Fusion Energy

1.1.1 Introduction to fusion

Fusion was first hypothesised by Arthur Eddington who suggested that stars draw their energy from the fusion of hydrogen and helium. It took another 19 years before the process was identified as the proton proton chain by Hans Bethe. Ernest Rutherford, Mark Oliphant and Paul Harteck realised the fusion of deuterium into helium. They discovered tritium and also hypothesised the existence of ${}^3\text{He}$, both of which are promising fusion fuels. Experiments followed to ascertain the energy realised from different combinations of light isotopes and the likelihood of interaction. There are many different fusion reactions possible, although the most promising terrestrial fusion reaction is between deuterium ($\text{D}={}^2\text{H}$) and tritium ($\text{T}={}^3\text{H}$). [122] contains a concise history of fusion research over the last 50 years.

The release of energy through nuclear processes can occur via fission or fusion reactions. Nuclear fusion is the process of combining light atomic nuclei to form heavier nuclei whereas fission is the splitting of larger nuclei to form smaller ones. In either case the products have slightly less mass than the reactants and it is this mass deficit that results in the release of energy. The quantity of energy produced per fusion or fission event is significant and can be calculated using Einstein's famous equation, where the energy in Joules (E) can

be found by knowing the mass difference in kg (Δm) and the speed of light in ms⁻¹ (c).

$$E = \Delta mc^2 \quad (1.1)$$

Another method of calculating the energy released from fission or fusion events is to calculate the change in binding energy between the products and the reactants. Binding energy is the amount of energy required to separate a nucleus into its constituent protons and neutrons. Provided that the new configuration of protons and neutrons is more tightly bound then the reaction will be exothermic.

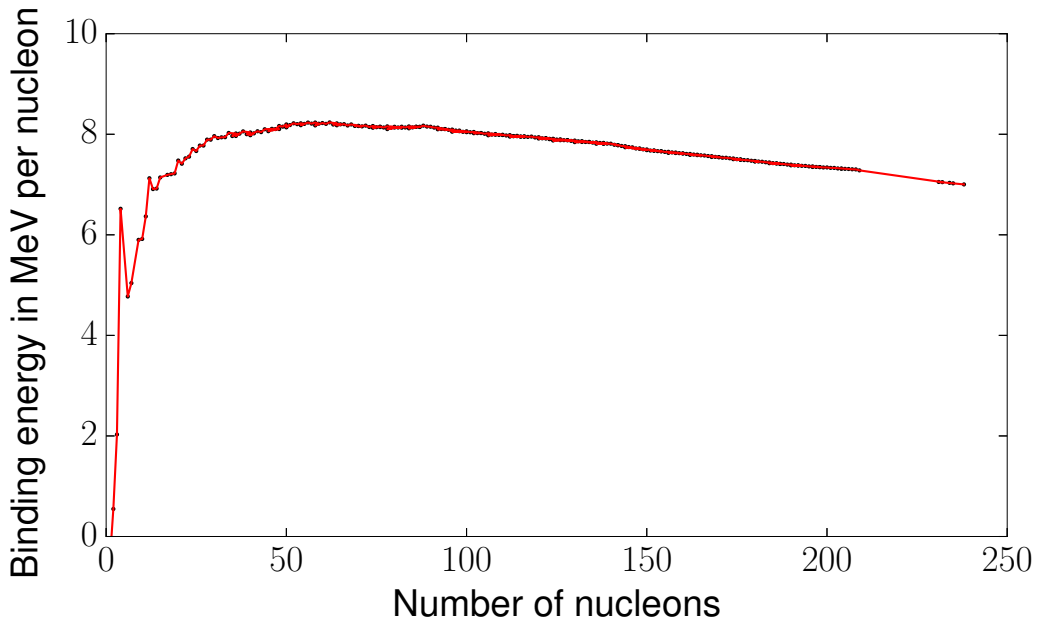


Fig. 1.1 Binding energy graph of stable isotopes, calculated from data made available by [31].

To liberate binding energy via fusion an energy input is required. As nuclei contain positively charged protons they naturally repel other nuclei according to Coulomb's law. The force in Newtons (F) between two point charges can be found by knowing the charge in Coulombs (Q), the separation between the point charges (r) and the electric permittivity of the medium in Farads m⁻¹ (ϵ_0).

$$F = \frac{Q_1 Q_2}{4\pi\epsilon_0 r^2} \quad (1.2)$$

To fuse nuclei they must be accelerated towards each other with sufficient kinetic energy to overcome the Coulomb barrier (see Fig. 1.2). As the nuclei approach each other they are slowed down by the repulsive forces between the two nuclei. If the nuclei are brought to within $\sim 1.5\text{fm}$ then this is sufficiently close for the strong force to act and the two nuclei will be pulled together. This requires the nuclei to have a large kinetic energy available to overcome the potential barrier. To achieve the kinetic energies needed, the fuel must be heated to very high temperatures, during the heating process the atoms are stripped of their electrons and become ionised; this form of matter is known as a plasma. Plasmas are also referred to as ionised gases and the degree of ionisation can vary. Fusion plasmas are generally fully ionised, meaning that all atoms have been fully stripped of their electrons.

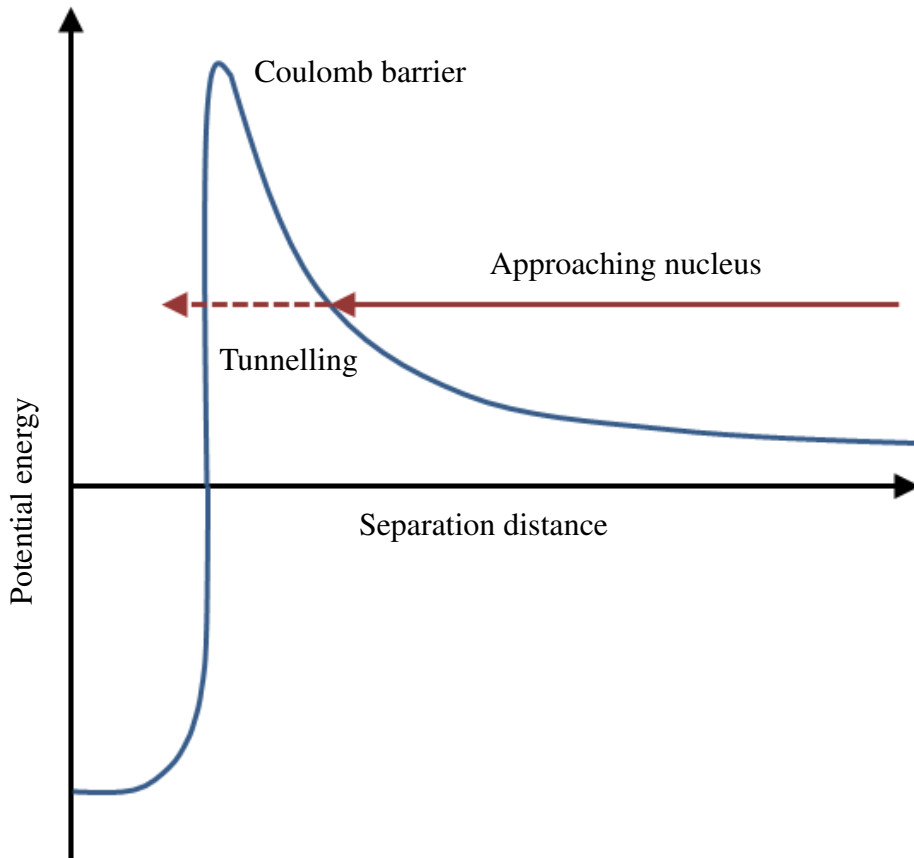


Fig. 1.2 The resultant forces acting on the nucleus

The temperatures required for hydrogen fusion are substantially lower than any other element due to hydrogen having just a single proton. The temperature (T) can be estimated to be 1×10^{10} K by equating potential energy and kinetic energy and knowing the range of the strong force.

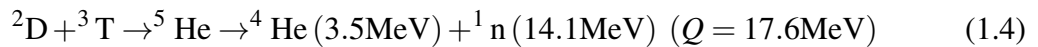
$$\frac{3}{2}k_B T = \frac{Q_1 Q_2}{4\pi\epsilon_0 r} \quad (1.3)$$

The actual temperatures required for fusion are lower than the value suggested by equation 1.3 for two reasons. As the nuclei are brought closer there is a small but increasing chance that nuclei may tunnel through the Coulomb barrier. This is evident in the sun where the core temperature is not sufficient to overcome the fusion barrier. Additionally we can expect the nuclei temperature to have a Maxwellian distribution. This results in particles that are hotter than the average temperature and therefore able to fuse before the bulk of the fuel is up to temperature. With these considerations taken into account, DD fusion occurs at approximately 4.0×10^8 K and DT fusion occurs at 4.5×10^7 K. Once the two nuclei are brought sufficiently close together there are several possible interactions. In the case of a fusion reaction the two nuclei join to form a new nucleus. Usually the newly formed nucleus is unstable and rapidly decays. The decay emits daughter products which contain less mass than the original fuel nuclei. Excess energy liberated by the reaction is carried away in the kinetic energy of the newly formed nuclei.

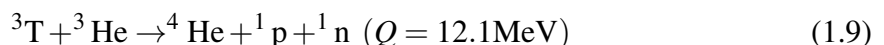
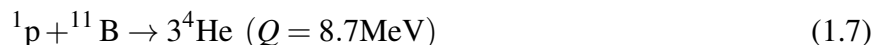
Fusion energy claims several distinct advantages over existing energy generation methods. These are: a potentially abundant fuel supply, inherently safe, low land usage, zero emission of greenhouse gases during operation and negligible production of long lived radioactivity. One attractive feature of fusion energy is the high energy density, at 337 TJ/kg for DT fuel. This compares favourably with chemical fuel sources and even other nuclear energy sources such as uranium at 77TJ/kg. Fusion energy is purported to be the ultimate energy source in many ways; unfortunately there is a stumbling block, fusion is very difficult to achieve.

1.1.2 Possible fusion reactions

There are many different fusion reactions, however deuterium tritium (DT) is considered the most achievable for the first power producing fusion reactors. The reaction products, the energy of the products and the total energy liberated by the reaction (Q) are shown in Equation 1.4.



Although other fusion reactions have desirable characteristics, the main advantage of DT fuel is the large reactivity at relatively low temperatures (see Figure 1.3). Another advantage of DT fuel is the large amount of energy liberated in each reaction (17.6MeV), which tends to be higher than other fuel options. Alternative reactions include the following:



An obvious difficulty with DT fusion is that tritium is an unstable isotope with a half life of 12.3 years and no viable natural resources exist. Fusion reactions involving ^3He also suffer from resource scarcities whereas DD and $^1\text{p} + ^{11}\text{B}$ fusion are far more abundant in resources. Aneutronic fuels such as the $^2\text{D} + ^3\text{He}$ reaction offer the advantage of less activated waste due to the absence of neutrons in the primary reaction. Despite the apparent shortage of fuel, the combination of high energy release, high likelihood of interaction and low threshold energy required for interaction make DT a particularly promising reaction. While other reactions may become more popular in the future, DT has long been established

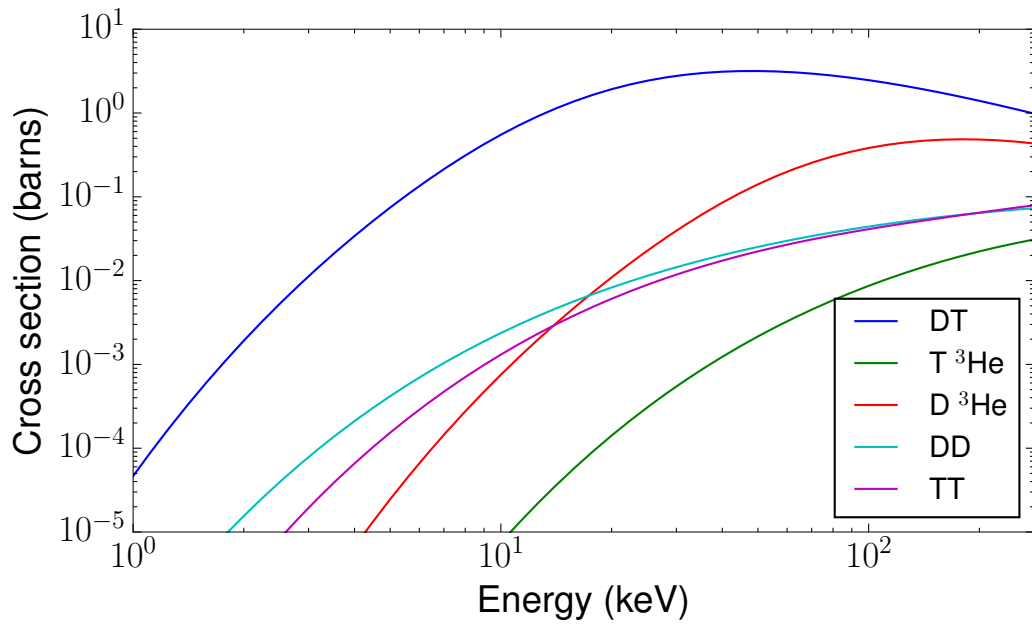


Fig. 1.3 Fusion reaction rate versus energy for fuel mixtures under consideration. ENDF/B-VII.1 data [22] was used to construct this graph

as the most viable fuel source for first generation fusion power producing reactors.

1.1.3 Magnetic confinement fusion

The sun's large mass allows confinement of the plasma via the gravitational force. Naturally this is not an option for terrestrial nuclear fusion and alternative methods of confining the plasma must be considered. There are many novel methods of fusion, however just two main methods have enjoyed the vast majority of research and development. The main methods are Magnetic Confinement Fusion (MCF) and Inertial Confinement Fusion (ICF). Both methods are able to overcome the Coulomb repulsion between the two nuclei by producing fast moving nuclei, however their approach is quite different.

ICF uses lasers or ion drivers to heat and compress a pellet of fuel to fusion relevant conditions for a very short period of time. MCF confines a plasma using magnetic fields so that it can be heated and fusion events occur. Both reactors plan on using DT fusion and will therefore require breeder blankets. ICF reactors will differ from MCF reactors in many respects including the neutronics environment. Nuclei within dense plasmas gain energy via elastic scattering events with alpha particles or neutrons; this occurs more frequently in dense ICF plasmas compared to low density MCF plasmas. When the high energy nuclei fuse they produce neutrons with energy above the Q value of the reaction; these are referred to as suprathermal neutrons. Down scattered neutrons also appear in both ICF and MCF spectra as a result of interactions with the reactor structure such as the first wall. This thesis is concerned with optimising breeder blankets for the neutron spectra experienced in MCF and the results are not applicable to ICF blankets due to the difference in neutron spectra. However, the methods and ideas described could also be applied to ICF devices.

Magnetic confinement is the most developed of the approaches and has come the closest to achieving net energy output with a world record of 65% efficiency [186]. Ions are trapped in a “magnetic bottle” that can take a variety of geometric forms. Early designs called magnetic mirrors (see Figure 1.4) were prevalent in the 1970s; these used magnets to form a cylindrical field configuration which becomes narrower at the ends. Ions would reflect back and forth within the geometry and varying levels of confinement could be achieved. Unfortunately the faster ions were prone to escaping from the ends of the mirror.

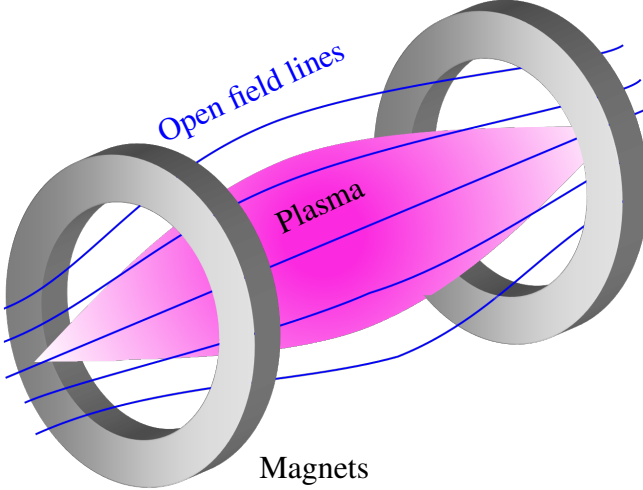


Fig. 1.4 A magnetic mirror, an early magnetic confinement technique.

Other geometries which built on the lessons learnt from magnetic mirrors have been more successful. The magnetic mirror design was adapted by bending the cylindrical field into a torus shape. This formed a geometry with closed magnetic field lines where even faster particles from the high energy tail of a Maxwellian distribution could be contained. The torus confinement geometry has been further refined and several different variations are being considered. The most developed of these is the Tokamak [184] and this design was chosen as the basis of several large international devices.

In this configuration toroidal magnets are used to form a torus shaped magnetic field in which to trap the ions. Relying solely on toroidal fields alone cannot confine the ions indefinitely. Due to the fact that the electrons and ions orbit in different directions, they drift in contrary directions and this leads to charge separation. Charge separation causes the formation of electric fields in the plasma and results in instabilities which cause the plasma to collide with the wall; also known as a disruption. Additional poloidal magnets are required to hold the plasma away from the walls and prevent excessive charge separation. The long-range electrostatic forces between the ions cause the plasma to exhibit collective effects and instabilities readily form in the plasma. Further details of the magnetic confinement configurations and instabilities are well documented [191]. Once contained, the fuel must also

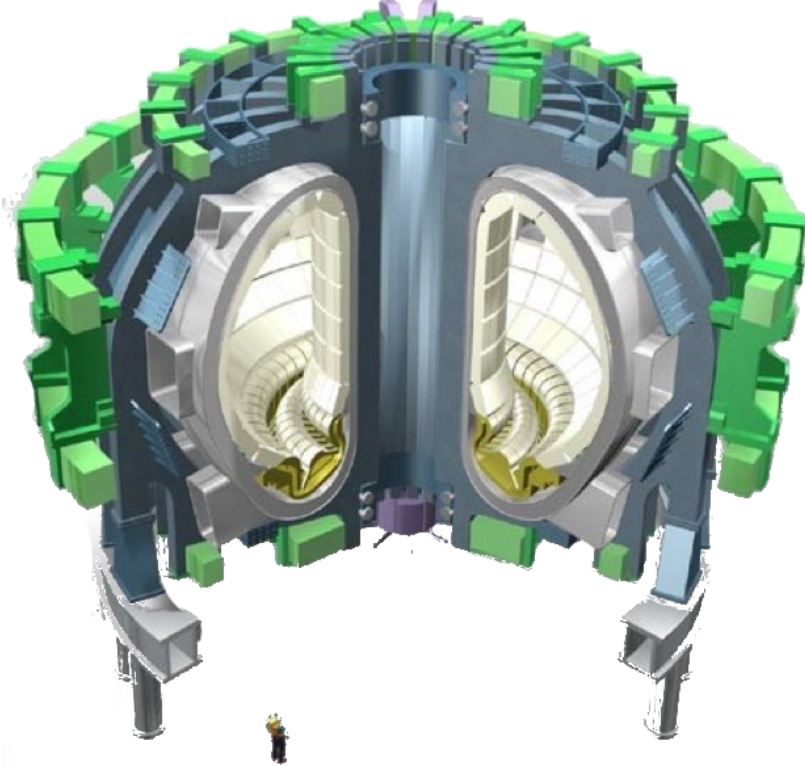


Fig. 1.5 The arrangement of toroidal (blue), poloidal (green) coils and divertor (yellow) within a Tokamak. Image source [48].

be heated to achieve fusion and this is done with ohmic, radio frequency and neutral beam injection methods. As the temperature rises, fusion reactions start within the plasma and in the case of DT fusion, neutrons are emitted into the surrounding material. Temperatures are typically 15keV and increasing the temperature beyond this results in lower DT fusion rates (see Figure 1.3).

1.1.4 Progress in magnetic confinement fusion

Atkinson and Houtermans [8] carried out fusion related experiments in 1929. They made measurements of low mass nuclei and used Einstein's $E = mc^2$ equation to suggest that large amounts of energy could be released by joining them together. Fusion research quickly became the domain of weapons research and international knowledge on the subject was confined to military areas. After a decade of nations independently researching into various Z-pinch devices and magnetic mirror devices, difficulties started to emerge. The need for international cooperation became apparent when scientists noticed that they were researching similar methods and coming up against the same problems. As a consequence nuclear fusion research was declassified at the Atoms for Peace Conference in 1958. Scepticism gave way to enthusiasm and progress has been made in fusion energy research ever since. The first outstanding success of magnetic confinement fusion experiments was achieved in 1968 when Russian scientists announced record high plasma temperatures [7]. This was quickly verified by western scientists and worldwide interest in the Russian Tokamak design grew. In the 1970s small Tokamaks were built across the world [135] and as a consequence they are now the most developed fusion device. This rapid growth in Tokamaks culminated in the construction of five large experiments TFTR, DIII-D, JT-60, Tore Supra and JET in the early 1980s. To date 215 Tokamaks have been built and old Tokamaks are continually being upgraded. Early Tokamaks have suffered from limited pulse duration partly due to the use of copper electromagnets which heat up and expand if used for long durations. More recently new superconducting Tokamaks such as EAST and K-Star have been built and are operational. The next stage in Tokamak development is the completion of ITER, which is currently under construction in France.

As magnetic confinement has matured, more complex reactor designs such as the Wendelstein 7-X Stellarator [194] have been conceived and built. Wendelstein 7-X uses a single set of coils to produce both toroidal and poloidal magnetic fields. This emerging branch of magnetic confinement offers advantages over the more traditional Tokamak. The variation in the magnetic field of torus shaped confinement devices leads to particle drift and charge separation of electrons and nuclei within the plasma. Charge separation leads to an electric

field and instabilities within the plasma. One of the main differences between Tokamaks and Stellarators is the method of suppressing charge separation. While Tokamaks rely on a toroidal current to suppress charge separation Stellarators use rotational transforms of the plasma. Stellarators are inherently better at maintaining steady state operation and are less prone to plasma instabilities. However Tokamaks remain the more developed of the two designs. With impressive results already achieved by the Japanese Stellarator LHD [133], the next break through results are expected to come from the Wendelstein 7-X Stellarator in Germany. Further experimental results are needed before the Wendelstein 7-X Stellarator can be reliably extrapolated to power plant scale [197].

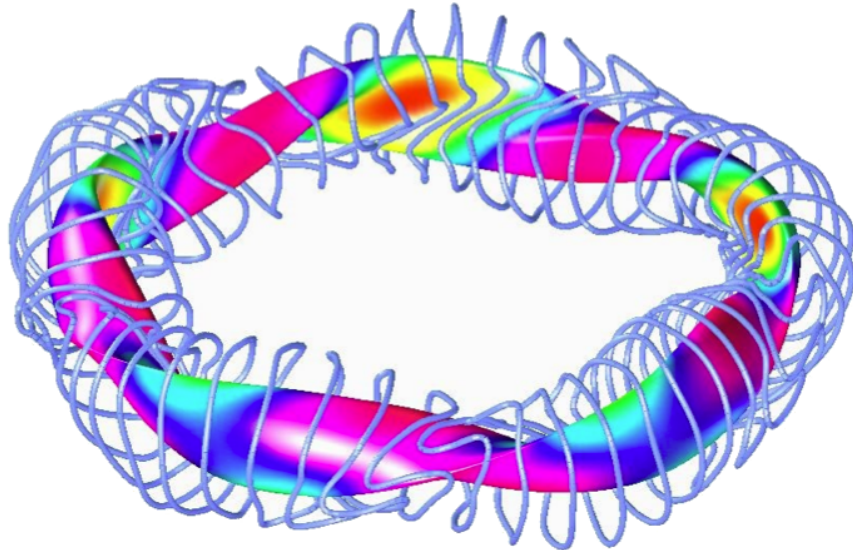


Fig. 1.6 The magnetic coil arrangement of a Stellarator. The coloured plasma represents the strength of the magnetic field created by the coils. Image source [33].

Improvements in plasma parameters, confinement time , temperature and power production have been made. The confinement time (see Equation 1.11) is defined as a function of the total plasma energy content (W) and the total heating power (P).

$$\tau = \frac{W}{P - dW/dt} \quad (1.11)$$

To gauge the general development in fusion energy a figure of merit is required. To this end various methods of measuring the merit of a fusion experiment are available. The Lawson criterion was first derived in 1955 [110] and defines the minimum requirements for number density of ions (n_i) and confinement time (τ) for a reactor to reach a self-sustaining reaction. This depends on the Boltzmann constant (K_B), temperature of the ions (T_i), the energy release per fusion (Q), the fusion cross-section (σ_f) and the relative velocity (v).

Using Equation 1.12, it can be demonstrated that the minimum product of $n_i\tau$ required to achieve a self-sustaining DT fusion reaction is $1.5 \times 10^{20} \text{ m}^{-3}\text{s}$.

$$n_i\tau \geq \frac{12K_B T_i}{Q\langle\sigma_f v\rangle} \quad (1.12)$$

The Lawson criterion helps to ascertain whether net energy is being produced but does not really provide a scale of merit. A more useful measure of merit called the triple product is used. This follows on from the Lawson criterion and provides a scale on which different confinement methods can be compared.

$$\text{Fusion triple product} = n_i\tau T_i \quad (1.13)$$

Since the Geneva declassification in 1958, the achieved triple product has been increased by a factor of 10^7 [122]. Initially, the fusion triple product achieved effectively doubled every 1.8 years but more recently the progress has slowed (See Figure 1.7). The record is currently held by the Japanese fusion device JT-60U which achieved a fusion triple product of $1.5 \times 10^{21} \text{ keVsm}^{-3}$ with a DD plasma [189]. The triple product provides an excellent figure of merit to compare dissimilar reactors but does not provide a suitable scale for practical use in terms of energy produced.

The fusion energy gain factor or Q is perhaps the most usable figure of merit. Q is the ratio of fusion power produced to input power (see Equation 1.14). The heating of the plasma is the main energy input for current fusion reactors. To achieve net energy

production, also referred to as "break even", a value of at least $Q = 1$ is required. The fusion energy produced is in the form of thermal energy. Therefore a more realistic Q value to aim for would be $Q = 10$. This allows for various inefficiencies involved in generating electricity from thermal energy to be taken into consideration. In power producing reactors the energy use for operating the cryoplant and pumping of coolant will also need to be considered. JET achieved a Q value of 0.65 in 1997 [186] and this is the highest value achieved to date.¹

$$Q = \frac{\text{Fusion energy produced (thermal)}}{\text{Heating energy required}} \quad (1.14)$$

Figure 1.7 shows progress in magnetic confinement since the 1970s in terms of the triple product. Q values for 0.1, 1 and 10 are also plotted as arcs on the graph. Progress has been made and the increase in the triple product can easily be observed. Additional challenges in materials and neutronics have emerged as achievable plasma performances approach the requirements for viable power plant performance. Efforts have increased and diversified to meet the needs of these growing disciplines. Recently improvements in the Q value have slowed as the community awaits the input of large devices being built (ITER) and medium devices undergoing upgrades. ITER plans to achieve Q values of at least 10 and this is plotted on the graph for comparison. As part of the preparation and testing of ITER baseline scenarios, existing Tokamaks have been upgraded so that they can better contribute. Tokomaks such as JET and JT-60U (reopening as JT-60 SA) are expected to make additional contributions and help verify ITER modes of operation before ITER operates in DT mode. JET plans to break its own records in fusion power produced and obtain a higher Q value [154]. JT-60 SA aims to reach record high triple products [137].

Because controlled fusion is such a desirable goal, fusion research has attracted its share of erroneous and dubious results. In 1958 scientists working on the ZETA experiment announced fusion had been achieved, only to find they had been mistaken and subsequently retracted the statement. The announcements in 1989 of electrochemically induced fusion

¹Care should be taken not to confuse the Q value with energy released in individual fusion reactions, which is also referred to as Q (see Equation 1.4).

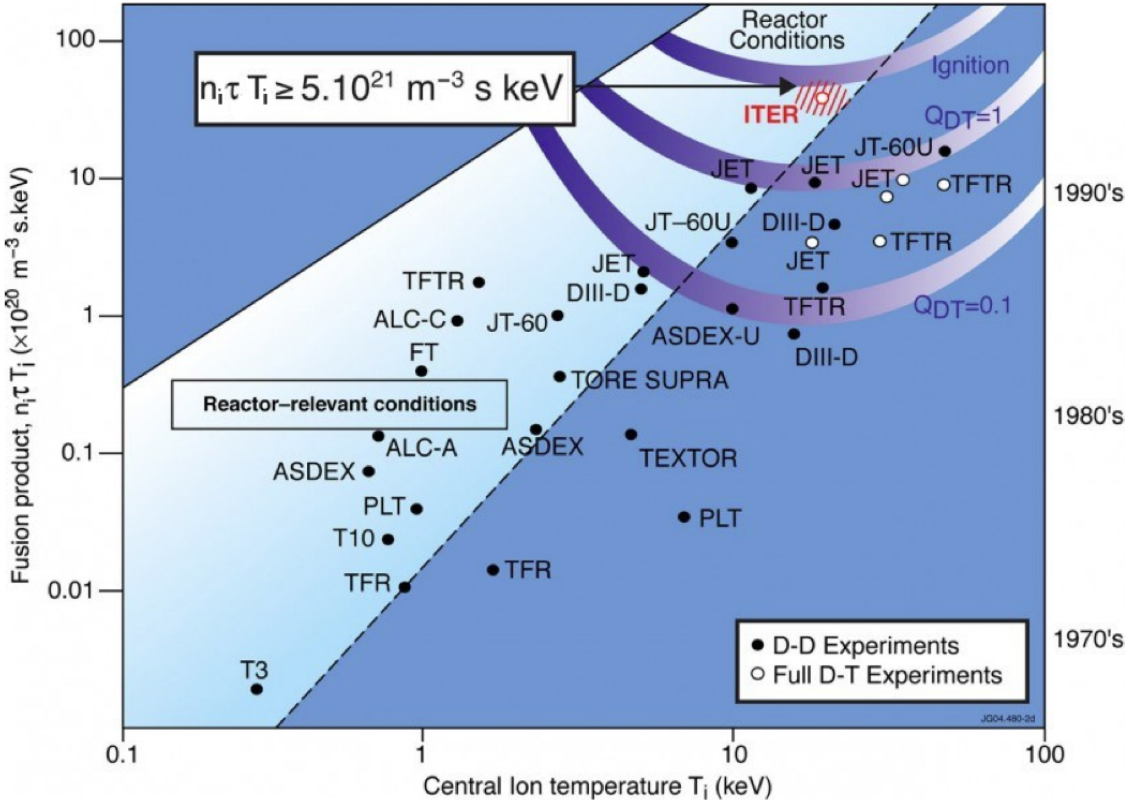


Fig. 1.7 The progress in triple product since the 1970s. Image source [48]

[60] sparked the world's interest in cold fusion and scientists around the globe quickly tried to reproduce the results. The vast majority of the scientific community were unable to reproduce the results. Some labs initially reported similar findings, which later turned out to be erroneous. The authors finally announced that their neutron detector was prone to false readings when exposed to heat. However the public distrust in fusion research was established and the concept of table top fusion was reignited. Cold fusion research continues today, however the field has been renamed Low Energy Nuclear Reaction (LENR) to avoid the negative connotations of "cold fusion".

The cost of building ITER has been continually underestimated and although the reasons behind this have been suitably explained [49], confidence in the whole project has suffered. A question often asked by opponents to fusion energy is "Why is fusion still 40 years away?" This is a reference to the perceived promise made in the 1970s that fusion would be solved within 40 years. The subtleties of the promise of fusion energy within 40 years appear to

have been forgotten. Fortunately for fusion research the conditions of the “fusion within 40 years promise” were published and survive to this day. Several countries conducted studies and published possible scenarios that indicated when commercial fusion would occur. The U.S. performed the most involved study [35] which was republished more recently [36]. As one might expect, the rate of progress of research is heavily dependent on investment. Fusion power stations were predicted to come online between 1990 and 2005 depending on the amount of funding.

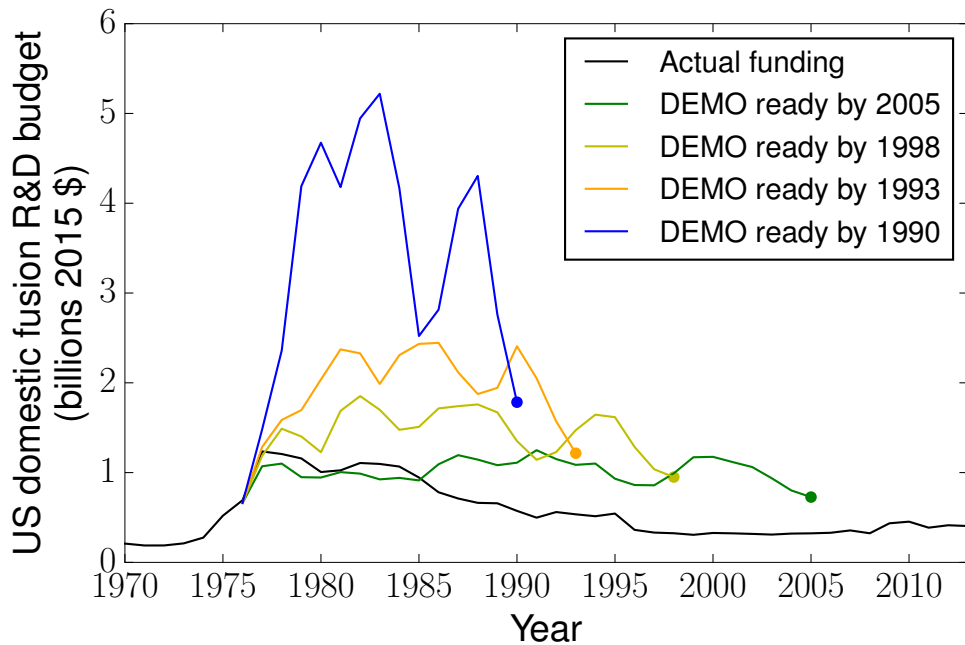


Fig. 1.8 The funding requirements for each of the DEMO scenarios were originally published by [35]. Additional data on US fusion expenditure was provided by [86]. Geoffrey M. Olynyk conceived the original graph which this graph is based on.

Figure 1.8 shows the scenarios suggested by [35] that could lead to commercial fusion. The figure also includes the actual level of US funding which is lower than the required amount to create a US DEMO reactor. Despite low funding there has been progress in fusion research and this is due to worldwide cooperation. In 2010 the worldwide investment in energy R&D was \$15,450 million [86], while the worldwide expenditure on energy was \$6,400,000 million [46]. R&D in energy accounted for 0.2% of the value of the en-

ergy market. Energy R&D budgets and indeed fusion R&D budgets are related to fossil fuel availability and price. During the 1973-1974 oil crisis, expenditure on fusion research increased dramatically (see Figure 1.9). The correlation between oil prices and funding in fusion research does not necessarily imply causation and other factors are certainly involved, however funding revenue does appear to be dependent on the perceived need for fusion energy.

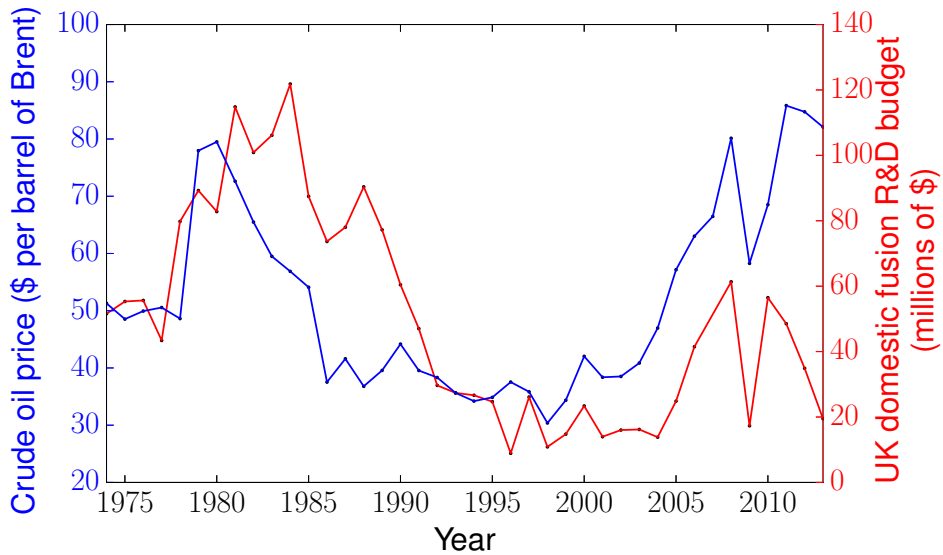


Fig. 1.9 Graph compiled from data on UK expenditure on R&D in fusion [86] overlaid with crude oil prices [14]. All values are inflation adjusted.

Overall progress in magnetic confinement fusion has been impressive and boasts a development rate faster [158] than Moore's law [127] used in the semiconductor industry. The continual improvement in magnetic fusion has allowed it to become the most developed method of achieving fusion. By building upon success fusion energy has emerged from its origins when experiments were conducted using relatively inexpensive recycled spare parts [181] to multibillion pound projects funded by half the world's population. Magnetic fusion has made steps towards achieving the goal of providing a clean, sustainable energy source and merits further development.

1.1.5 Planned progress

Commercialisation of fusion energy is the ultimate goal of fusion research. To best coordinate efforts towards this goal, a roadmap is required. While ITER is a joint effort, the next step in the commercialisation is being planned independently by many countries. China [199], Japan [80], India [175], Korea [108], Russia [103] and the EU [42] have all produced plans to develop a DEMOnstration fusion power plant (DEMO). Several roadmaps to fusion energy have been created by different organisations and all take different approaches. However the various roadmaps share some similarities and generally include: a list of technical challenges still to be met, key milestones that should be accomplished by certain dates, involve results from ITER, a flexible approach that is subject to change in response to physics and budgetary developments, construction of material testing facilities. The most recent and most detailed roadmap to date was published by the EU in 2013 [42]. The EU is a leader in fusion research and hopes its ambitious but pragmatic approach will keep the EU at the forefront of fusion development. There are opportunities for countries outside of the EU to collaborate on projects relating to the EU fusion effort, for example an agreement with Japan ensures cooperation on facilities such as the Satellite Tokamak Programme (STP) and the International Fusion Energy Research Centre (IFERC) [141]. The EU roadmap splits into three distinct parts:

- The first stage is planned to continue up to 2020 and focuses on building ITER.
- The second stage starts in 2021 and continues until 2030 and involves the exploitation of ITER and preparation for DEMO construction.
- The third stage runs from 2031 to 2050 and includes construction and operation of DEMO.

The general stages required for commercial fusion have long been established; these are reiterated clearly in the EU roadmap and have not altered significantly from earlier roadmaps [35]. The EU roadmap carefully balances ambition with risk, to form a pragmatic approach that leads to the production of fusion energy by 2050. A low risk but slow roadmap would mean fully exploiting ITER and learning as much as possible before designing and then

constructing DEMO. A higher risk and potentially quicker roadmap would start designing DEMO before ITER's contribution is complete.

Several existing fusion facilities feature in the EU roadmap; their role is to act as test beds for various ITER operational regimes and new materials. JET and JT 60 SA are the main contributors and are carrying out the testing of various ITER-like components (e.g. beryllium first walls) and plasma scenarios (e.g. partly self heated DT plasmas). Medium fusion devices and technology test facilities are exploring other aspects of commercial fusion, for example Magnum PSI in the Netherlands is investigating plasma-surface interactions. Several facilities have been proposed to be built after ITER; these are the dedicated Divertor Tokamak Test (DTT) Facility [10], Component Test Facility (CTF) [146], the International Fusion Materials Irradiation Facility (IFMIF) [43] [126]. A DTT is proposed to trial various divertor designs such as the Super-X [190] and the Snowflake [157] as well as first wall materials (e.g. tungsten alloys). A CTF would aim to address the main engineering and technological questions remaining after ITER has been exploited. The CTF would aim to establish the fusion engineering and technology needs for practical fusion power. Technology relating to the DT fuel cycle would be a particular focus. IFMIF is focused on material characterisation and would use an accelerator and target based approach to reproduce heat fluxes and neutron fluxes expected in DEMO. FAFNIR is also an accelerator and target based approach that aims to gather information for the fusion materials' engineering database, however the scope and risk is reduced in comparison to IFMIF.

The EU roadmap is built on financial assumptions and is subject to review (first review in 2015). The roadmap aims to move the fusion industry from scientific experiments in laboratories to the industrial sector that will ultimately produce commercial power plants. International cooperation is still heavily promoted between the EU and partner countries. However the roadmap was created partly due to a perceived need to stay at the forefront of fusion research and competition is certainly becoming increasingly apparent as commercial fusion power gets closer. The need for an increase in the number of trained fusion experts (referred to as generation ITER) is also mentioned within the roadmap document.

ITER is the critical facility in the EU roadmap for commercial fusion; it also has its own individual roadmap. The ITER roadmap contains more specifics of its operational agenda and Integrated Project Schedule. Construction of ITER started in 2008 and it has made good progress in many areas, however this one of a kind project has some issues in terms of schedule and expense. Any additional delays in ITER will have an adverse effect on the EU target of fusion power by 2050. To support the European fusion efforts Fusion for Energy (F4E) has been tasked with coordinating the European contribution towards ITER and publishes yearly reports [63] on progress made. ITER is currently undergoing a transitional period which involves appointing a new director, reforming the organisation and reassessing the delivery schedule. The EU roadmap sets out one possible roadmap for commercial magnetic confinement fusion; as mentioned previously there are alternative roadmaps which follow different pathways. Similar key challenges presented in all roadmaps must be met if commercially viable fusion power is to succeed.

1.1.6 Challenges identified

The majority of challenges focus on improvements that must be made to cope with the more demanding reactor conditions inherent in DEMO. Although some roadmaps go as far as listing eight challenges, only the most demanding four are covered in this section. The details of each challenge is briefly discussed below, along with comments on the maturity of possible solutions.

Theory and modelling effort in plasma physics. Plasma turbulence is the main mechanism of energy loss from the fusion plasma. To minimise this energy loss, low turbulence plasma regimes are being developed for ITER. By running various plasma experiments in the smaller Tokamaks available, it has been possible to extrapolate low turbulent stable plasma regimes for ITER. Results from ITER will provide additional data required to extrapolate stable plasma regimes for larger reactors such as DEMO. ITER and DEMO both aim to confine a burning (largely self-heated) plasma; this has never been achieved before and may introduce new unpredicted instabilities. Therefore one of the key remaining challenges is to design low turbulence plasma regimes for the DEMO reactor. Plasma physics has been the focus of fusion research since the first confinement experiments in the 1970s. Theories and simulations have been built up and supported by years of experimental data from a wide range of experimental configurations. Unpredicted instabilities have previously occurred and plasma parameters have been designed to avoid these instabilities in ITER. As computers have improved it has been possible to create increasingly realistic plasma simulations. Fusion plasmas overlap with other areas where plasmas are researched, such as low temperature plasmas and astrophysical plasmas. DEMO sized self heated plasmas are however unprecedented.

Theory and modelling effort in material physics. Plasma wall interaction in the divertor is a major issue. The plasma is separated from the majority of the walls by magnetic fields and contact is made with just one component, the divertor. This contact between the plasma and the divertor is purposeful as it allows exhausted plasma to exit the

torus. Helium can leave the plasma via the divertor; it is important to keep the helium fraction low to avoid dilution of the fusion fuel. The divertor is subject to high heat fluxes in the region of 10MWm^{-2} [17] for typical DEMO reactor designs. A full-tungsten divertor design has undergone an extensive qualification program [79] and has been selected for use in ITER. However, designing a divertor for DEMO is still a current challenge as the heat flux is more intensive. Fifteen different Tokamaks have divertors installed and some are testing novel designs such as the Super-X and the Snowflake divertor. The Tokamak divertors in operation today do not experience the intense heat flux that is expected in DEMO reactors. Research is needed to scale any existing technology so that it can operate in more intense situations.

Neutron damage in reactor materials. Neutrons interacting with materials can cause induced activation, formation of gas bubbles, reduction in thermal conductivity, embrittlement and other material degrading effects. A dedicated neutron source is needed for material development so that materials can be tested under “DEMO like” conditions of around 30dpa. Neutron damage and activation of materials has been a known issue since early fission reactors. The magnitude of the problem depends on both the neutron energy and the number of neutrons interacting. Neutrons produced during fusion (2.45MeV for DD and 14.1MeV for DT) are higher energy than neutrons found in fission (2.1MeV on average in a faster breeder and 0.040eV in a moderated fission reactor). DEMO will also be a very intense source of neutrons. Fission reactors have used reduced activation ferritic/martensitic (RAFM) steels for a number of years. More advanced materials such as ODS steels were developed specifically for fast breeder reactors. Materials such as Eurofer [163] have also been developed specifically for fusion devices. DEMO levels of neutron irradiation are unprecedented and will push material requirements further than before.

Strengthen R&D to ensure tritium self-sufficiency. Tritium is required to sustain the DT reaction and breeder blankets will be expected to produce $\sim 400\text{g}$ of tritium fuel on a daily basis. However self-sufficiency is yet to be experimentally demonstrated. As

well as producing the tritium it will be necessary to extract and separate the tritium. The nuclear physics of neutron interactions and tritium production is well understood and simulation tools are increasingly sophisticated. Simulations have been shown to produce reliable predictions by comparing their results with experimental benchmarks. While there are many fission relevant benchmarks there are limited quantities of relevant benchmarks for DT fusion. Breeder blankets will be demonstrated for the first time in ITER; unfortunately successful blankets at this stage are no guarantee for DEMO like reactors. Alterations will need to be made to the breeder blankets to ensure they are compatible with the higher neutron fluxes in DEMO. Tritium breeder blankets are not installed on any fusion reactor; no fully functional breeder blanket has ever been constructed and no obvious similarities exist in other sectors. The technology involved in fusion breeder blankets is relatively immature.

There are additional challenges involved in fusion energy which are far from trivial [78], however the four challenges previously listed are considered the main challenges and further details are well documented [5]. Each challenge differs in terms of worldwide experience in the topic and maturity of possible solutions.

Where tritium breeding differs from the other main challenges is that while divertors, plasma physics and materials activation all exist to some extent on existing fusion experiments, tritium breeding does not. While the other three challenges require further development of existing technology, tritium breeding requires starting from scratch and will only be trialled for the first time in 2024 when the ITER TBM programme commences. While all the challenges present their own difficulties it is clear that the solution to tritium breeding is the least mature of all.

1.2 Tritium breeder blankets

1.2.1 Introduction

First generation fusion power plants will rely on a supply of DT fuel. As deuterium and tritium are continually used up by the fusion reaction (see Equation 1.4), there is a need to replenish deuterium and tritium to maintain fuel levels. Deuterium is abundant in sea water and can be readily obtained, however tritium is almost non-existent on Earth. Natural sources of tritium are dispersed around the atmosphere and sea; the total amount of tritium on the planet is estimated to be less than 5kg [73]. Tritium used in fusion experiments such as ITER and DEMO will therefore need to be from artificial sources. Tritium has previously been produced for military uses however production for this purpose has now ceased and remaining quantities are unknown. Tritium is currently produced by CANadian Deuterium Uranium (CANDU) heavy water reactors. The costs are high (in excess of \$30,000 per gram) [196] and production quantities are low. CANDU reactors are fission reactors that use deuterium to moderate the neutrons to thermal energies. In CANDU reactors tritium is formed predominantly via neutron capture in deuterium nuclei and a small amount is formed via ternary fission. Another source of tritium in fission reactors is via neutron capture reactions with ^{10}B which is used as a neutron poison.

Worldwide civilian reserves of tritium are less than 30kg [161] and the potential to make more is limited [68]. A more detailed study of worldwide tritium resources predicts that the operation of ITER will require approximately 2.2kg leaving between 14-28kg for proceeding DEMO reactors [136]. Breeder blankets are being designed so that future reactors can be self-sufficient in tritium, however no breeder blanket equipped fusion reactors currently exist. It is therefore necessary to create tritium in order to fuel fusion experiments that run DT fuel mixtures but have no breeder blankets. The ITER experiment will consume a large proportion of the world's tritium reserves. If fusion power is going to become a commercial reality the availability of start-up tritium inventories will also need consideration. The size of the start-up inventory required depends primarily on the device size, with typical 2.4GW (thermal) devices requiring 18.1kg [136]. One solution would be to overbreed tritium in

DEMO so that additional tritium can be generated for starting up subsequent reactors. The costs involved in overbreeding tritium are explored in Chapter 3. Another possible solution would be to breed tritium during the DD plasma phase and this is explored in Chapter 4. Ideally, a fusion reactor would produce its own T as it is expensive to produce via alternative methods. Tritium self-sufficiency can be achieved by using a lithium (Li) blanket that surrounds the reactor and breeds T from Li (see Equations 1.15 and 1.16).



To produce sufficient T, every neutron from a DT fusion event must generate at least one new T within the breeder blanket. The ratio of tritium atoms produced to the neutrons emitted by the DT reactions is known as the tritium breeding ratio (TBR), see Equation 1.17. The amount of T that can be returned into the plasma is less than the amount produced in the breeder blankets. This is because T readily adheres to the surfaces of the breeder blanket structural components, pipe work, the reactor walls and the uranium storage beds, also T decays with a 12 year half-life. El-Guebaly [44] estimates that a TBR of at least 1.1 will be required to account for these losses.

$$\text{TBR} = \frac{\text{Number of tritium atoms produced in the breeder blanket}}{\text{Number of tritium atoms fused by the plasma}} \quad (1.17)$$

Solid-type breeder blankets generate the majority of T via (n,alpha) reactions with ${}^6\text{Li}$. However FLiBe based blankets produce more T from (n,n't) reactions with ${}^7\text{Li}$. The likelihood of a tritium producing interaction within ${}^6\text{Li}$ or ${}^7\text{Li}$ is a strong function of neutron energy (see Figure 1.10). The reaction with ${}^7\text{Li}(n,n't){}^4\text{He}$ is more desirable as this liberates another neutron which could go on to create more T. The ${}^7\text{Li}$ reaction is more likely at high energy, however at neutron energies below the threshold energy of 2.47MeV the ${}^7\text{Li}$ reaction has zero likelihood. While the neutrons are initially emitted with 14.1MeV of energy

they are quickly moderated down to thermal energies. At lower neutron energies the ${}^6\text{Li}(n,t)$ cross-section increases by over five orders of magnitude and has a significantly larger likelihood of producing tritium compared to ${}^7\text{Li}$. Unfortunately natural lithium is only 7.6% ${}^6\text{Li}$ and 92.4% ${}^7\text{Li}$.

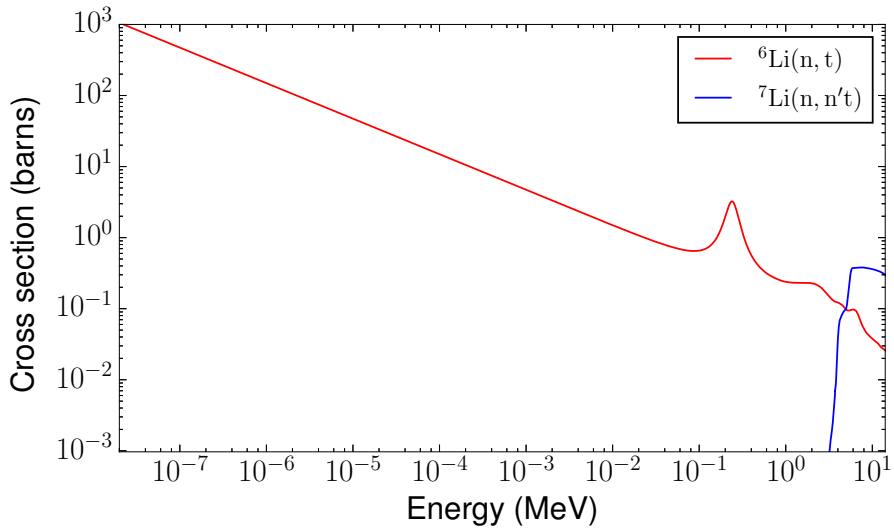


Fig. 1.10 Likelihood of a tritium producing reaction with lithium isotopes. Data from the ENDF/B-VII.1 library [22].

Neutron capture in structural and cooling components reduces the number of neutrons available for tritium breeding. Current breeder blanket designs rely on neutron multiplication and enriched ${}^6\text{Li}$ content to increase the TBR. Neutron multiplying materials such as beryllium and lead increase the number of neutrons through $(n,2n)$ and $(n,3n)$ reactions. The extra neutrons interact with lithium to create additional tritium atoms and this increases the TBR. Although lead and beryllium are the two most popular neutron multipliers for breeding blankets, fissionable isotopes such as ${}^{235}\text{U}$ also multiply neutrons. Naturally the use of fissionable isotopes would cause additional waste problems compared to Be and Pb; despite this there are several fission fusion hybrid designs considering such fissionable materials [113]. Figure 1.11 compares common neutron multipliers proposed for fusion reactors.

Creating sufficient tritium is only one of the tasks performed by the breeder blankets. They must also extract the energy from the DT reaction and shield the outer reactor from

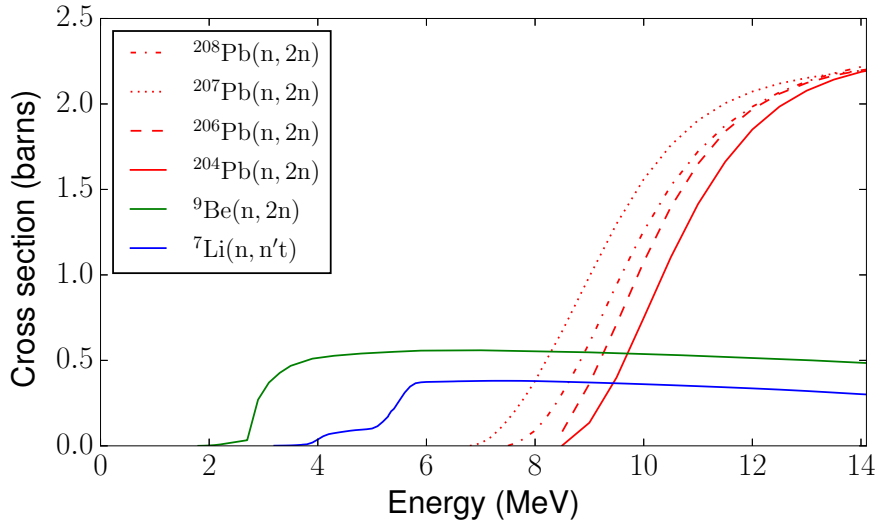


Fig. 1.11 Neutron multiplication reactions with Be, Li and Pb. Data from the ENDF/B-VII.1 library [22].

radiation. The majority (80%) of energy released by a DT reaction is carried away by the neutron (see Equation 1.4). The neutron is able to escape the magnetic field and deposit its kinetic energy in the breeder blanket material, as the neutrons interact; this causes the breeder blanket to heat up. The kinetic energy of the neutron is only part of the thermal energy produced in the breeder blankets. As energy is often liberated in exothermic nuclear reactions further energy is available. The Q value is used to describe the amount of energy released in a nuclear reaction and whether the reaction is exothermic or endothermic. Threshold reactions such as $^9\text{Be}(\text{n},2\text{n})$ and $^7\text{Li}(\text{n},\text{n}'\text{t})$ are both endothermic, while ^6Li is exothermic. The thermal energy present in the breeder blankets can then be extracted by a coolant such as water or helium. Another role of the blankets is to shield the outer reactor from neutrons; this is efficiently performed by the lithium content and steel is used to attenuate the gamma radiation. Although several novel designs for breeder blankets have been suggested [84], two main technologies have emerged. These are liquid lithium lead based blankets and lithium ceramic based blankets. Both technologies have their merits and disadvantages, therefore it is important to pursue these two parallel lines simply for the reason of risk mitigation. A comprehensive test called the Test Blanket Module (TBM)

program is currently being planned and agreed by all ITER parties. The TBM program involves six breeder blankets [66] that have been designed by various collaborations between ITER members. The ITER tritium breeding module (TBM) program is aiming to demonstrate that fusion reactors can be self-sufficient in tritium and extract high grade heat for electrical generation. Each of the six breeder blanket designs to be tested on ITER has a slightly different design and these are subject to change. Specific ITER TBM arrangements are currently being drawn up and these will clarify intellectual property, ownership of any radioactive waste produced and bring more certainty to the specifics of the TBM program. They all have to comply with the proposed ITER plasma regimes, H-H plasma is planned to start in 2020, followed by deuterium plasma with limited tritium content, then low duty DT finally followed by high duty DT plasmas [168]. Initial roadmaps have been produced for TBM being tested in ITER and longer term conceptual studies into developing breeder blankets suitable for DEMO have also started.

Breeder blanket research is critical for the development of commercial fusion [67] and DEMO reactors incorporating breeder blankets are also being designed. Mixed beds that contain pebbles of neutron multiplier and ceramic breeder are one option being considered. The mixed bed designs typically offer higher TBR values but require the use of beryllium intermetallic compounds (beryllides) instead of pure beryllium. The use of beryllides avoids tritium retention and swelling issues that occur with pure beryllium [93]. Mixed bed breeder blankets are being pursued by several research groups. The most progressed mixed bed designs are Japanese [172], Korean [145] and Chinese [24] [117] designs. All mixed bed breeder designs use Be_{12}Ti with lithium ceramic (Li_2TiO_3 or Li_4SiO_4).

Blanket	ITER partners involved	Breeder material and ${}^6\text{Li}$ enrichment	Multiplier material	Structural material	Coolant
HCLL-BB Helium Cooled Lead Lithium Breeder Blanket [16]	European Union	PbLi_{16} at 90% ${}^6\text{Li}$	PbLi_{16}	Eurofer	He
HCPB TBS Helium Cooled Pebble Bed Test Blanket System [16]	European Union	Li_4SiO_4 at 30% ${}^6\text{Li}$	Be	Eurofer	He
WCCB TBS Water Cooled Ceramic Breeder Test Blanket System [47]	Japan	Li_2TiO_3 at 30% ${}^6\text{Li}$	Be	F82H steel	H_2O
DCLL-BB Duel Cooled Lead Lithium Breeder Blanket [198]	United States and Korea	PbLi_{16} at 90% ${}^6\text{Li}$	PbLi_{16}	F82H steel	He
HCCB TBS Helium Cooled Ceramic Breeder Test Blanket System [53]	China	Li_4SiO_4	Be	RAFM steel	He
LLCB-BB Lead Lithium Ceramic Bed Breeder Blanket [23]	India and Russian Federation	Li_2TiO_3 at 30-60% ${}^6\text{Li}$ PbLi_{16} at 90% ${}^6\text{Li}$	PbLi_{16}	RAFM steel	He PbLi_{16}

Table 1.1 Summary table of ITER test blankets.

1.2.2 Requirements

The primary objective of breeder blankets will be to produce sufficient tritium to sustain the fusion reaction. Achieving this goal alone is critical to fusion reactors as no other practical source of tritium exists [136]. In addition to the primary objective, breeder blankets also have other responsibilities, these are:

- **Heat production and extraction.** The kinetic energy of incident neutrons should be converted into thermal energy and extracted by the coolant to facilitate the production of electricity. Breeder blankets are able to amplify the energy incident upon them by utilising exothermic reactions such as the ${}^6\text{Li}(\text{n},\text{t}){}^4\text{He}$ reaction which has a Q value of 4.79MeV. Typical energy amplification values are 120% for Helium Cooled Pebble Bed (HCPB) blankets; this will increase the economic feasibility of future fusion power plants.
- **Shield components and the exterior.** To avoid damage to sensitive devices such as diagnostics the breeder blanket must provide a degree of shielding. Shielding of cryogenically cooled component is of particular importance. In the case of superconducting magnets, excess heating can lead to quenching and damage to the magnet. In any cooled component, extra thermal energy deposition increases the amount of cooling required and associated costs. Due to the 2nd law of thermodynamics and inefficiencies in cooling technologies, every joule of heat deposited in the magnets requires approximately seven times as much energy to remove. Shielding the exterior of the reactor is also important to reduce the dose to personnel.
- **Avoid detrimental effects to plasma performance.** The innermost lining of the reactor vessel wall is often referred to as the first wall and is typically integrated into the breeder blanket design. Plasma properties are affected by the conductivity of the first wall material. The plasma temperature is affected by impurities introduced into the plasma from the first wall. The effects must be considered when deciding upon first wall materials.
- **Minimize radioactive waste.** The first wall and breeder blankets are likely to be the most intensely irradiated components in a fusion reactor. It is important to design these components with low activation materials to avoid the problems of long lived radioactive waste. During reactor shut downs, maintenance access to the reactor is required to inspect and ensure its safe operation. Naturally this can only be carried out if the activity of the reactor is sufficiently low to avoid harm to the personnel

or devices carrying out the maintenance. Reduced activation of blanket components would mean that maintenance can be carried out on the reactor and the machine can have a quick turn around between shutdowns; this directly affects the profitability of the device.

- **Avoid excessive costs.** To ensure fusion energy is as economically viable as possible it would be undesirable to have expensive breeder blankets, especially as the blankets are expected to be replaced every five years. Avoiding the use of unnecessarily expensive and unsustainable rare materials is therefore a requirement of any long term blanket solution.
- **Provide structural integrity.** To ensure stable operation the structural integrity of the blanket system is paramount. Failures in structural aspects of the blanket or loss of coolant accidents have the potential to cause large amounts of damage to the reactor. Currently no codes and standards are able to validate DEMO designs for their operational scenarios. Traditional nuclear codes such as ASME BPV and AFCEN RCC-MRx do not cover many aspects of a DEMO reactor's operation. The solution is to establish additional rules to cover previously neglected items and the ITER nuclear design code (ITER SDC-IC) is leading the way in this field. Designs will be validated against updated codes and standards before installation in the reactor. Remote maintenance will survey and inspect in-vessel components during their lifetime to ensure structural integrity.

Optimising the breeder blanket design to improve the performance in any singular function could inadvertently result in downgrading the blanket in other aspects. Often optimisation is a trade off and the end user will have to specify the relative importance of each requirement before the design can be optimised.

1.2.3 Breeding blanket materials

The requirements for breeder blankets combined with the intense operational environment require carefully selected materials. Many standard materials are ruled out due to their activation within intense neutron fields, others might not have sufficiently high melting temperatures. The exploration of materials suitable for fusion reactors is ongoing and new materials frequently emerge as contenders (although they are often later found to be incompatible). Breeder blankets have a need for a variety of materials to fulfill a wide range of functions. Particular functions include: tritium producing, neutron multiplier, coolant, tritium extraction and structural materials. Some criteria for ruling out a particular material or materials are:

- behaviour at high temperature
- neutron activation
- electromagnetic influences
- tritium retention
- irradiation induced embrittlement
- gas production
- chemical compatibility
- thermal conductivity
- mechanical properties

Decades of material testing, experimentation and simulations have homed in on a few selected materials that are suitable for use in fusion reactor breeder blankets.

In addition to the previously listed criteria, candidate tritium breeding materials should provide a high number density of lithium atoms. Other aspects such as: ease of manufacture and neutron scattering cross-section are also of importance. While pure lithium would be ideal in terms of the high lithium density it is highly reactive. Lithium compounds are currently used to avoid this problem. Candidates divide into two groups, solid and liquid. Liquid candidates include liquid molten salts (FLiBe and FLiNaBe) and liquid eutectic PbLi₁₆. Solid candidates take the form of lithium ceramics and include Li₂O, Li₄SiO₄, Li₂TiO₃,

Li_2Zr_3 , LiAlO_2 and LiF [27]. The only liquid option under consideration in ITER blankets is PbLi_{16} whereas two solid options are being considered (Li_4SiO_4 and Li_2TiO_3). Although both ceramics appear in blanket designs (see Table 1.1) they differ in terms of their tritium breeding potential. Typically Li_2TiO_3 requires higher levels of ${}^6\text{Li}$ enrichment to achieve the same TBR as Li_4SiO_4 . There are additional materials that show good potential but are relatively immature in terms of material testing and are therefore not yet considered as candidates. $\text{Li}_2\text{Be}_2\text{O}_3$ is a relatively recent suggestion that combines both neutron multiplier and lithium into one ceramic.

Neutron multipliers are required to increase the neutron flux; this compensates for parasitic neutron capture within the breeder blanket. Neutron multiplication is necessary when requiring a TBR above 1. Any isotope capable of $(n,2n)$, $(n,3n)$ or similar reactions is capable of neutron multiplication. For neutron multiplication in fusion breeder blankets the isotope must be shown to have a high probability of neutron multiplication with neutrons at 14.1MeV and lower energies. Possibly the best neutron multiplier available is beryllium; this has the lowest energy $(n,2n)$ reaction known at just 1.8MeV. Pure ${}^9\text{Be}$ has disadvantages such as irradiation induced swelling and tritium retention; in its pure form it may not be suitable for DEMO reactors [162]. Compounds of Be (beryllides) such as Be_{12}Ti and Be_{12}V have been shown to address these concerns and are being considered [93]. Lead is another option and has a higher $(n,2n)$ cross-section than ${}^9\text{Be}$ at higher neutron energies (see Figure 1.11). At present only Pb and Be are being considered for ITER blankets whereas Pb, Be and beryllides are being considered for DEMO reactors. Other materials that could be considered include zinc and fissionable isotopes which are effective neutron multipliers. Fissionable isotopes are not being widely considered due to the generation of actinides and inherent radiological hazards. Trace amounts of uranium may be present as an impurity in beryllium and steps are being taken to limit this. Lithium itself performs $(n,n't)$ reactions which are not strictly classed as neutron multiplication but perform a similar function for tritium breeding purposes. Figure 1.11 shows the neutron multiplication cross-sections for the main neutron multipliers present in current breeder blanket designs.

Coolants are necessary to remove the large amounts of thermal energy deposited in the breeder blankets. Candidates include water (heavy and regular) and helium. Helium is excellent in terms of its ability to endure high neutron fluxes without activation, however high pressures ($\sim 8\text{ MPa}$) and pumping speeds ($\sim 5\text{ m s}^{-1}$) are needed. The ability of helium to remove thermal energy at high temperatures results in higher efficiencies when generating electricity. Water has a higher specific heat capacity and is able to transport large quantities of heat with relatively slow pumping speeds. The temperature of the water coolant cannot go as high as helium which is perhaps the main disadvantage of water cooling. Heavy water (D_2O) and regular water (H_2O) differ in their moderating ability as well as parasitic neutron capture. Comparisons between the two coolants show that the TBR can be influenced [112] by changing the coolant. Use of D_2O instead of H_2O has been shown to influence the TBR by between 4.7% and -1.5%. The change in TBR depends on the volume of water used and the position of the coolant channels relative to the breeder zone. D_2O is known to absorb less neutrons than H_2O . However D_2O also moderates neutrons to a lesser extent compared to H_2O .

Structural materials are required to support the breeder blanket and provide structural integrity throughout the blanket's life. The material requirements were deemed too demanding for existing materials, so Reduced Activation Ferritic / Martensitic steels RAF/M and Oxide Dispersion Strengthening (ODS) have been specially developed for DEMO reactors. From the different RAF/M materials that have been developed, the leading candidate materials are from Europe (EUROFER), China (CLAM) and Japan (F82H) [75].

In solid-type breeder blankets it is necessary to extract the tritium from the lithium ceramic. Tritium is a highly mobile gas and diffuses out of lithium ceramics at fusion reactor relevant temperatures [4]. This can be encouraged by the addition of a purge gas such as helium. The pressure, temperature and flow rate of the purge gas can all be adjusted to optimise tritium release from the lithium ceramic into the purge gas. The tritium is then filtered from the purge gas and either sent directly to the plasma or stored for later use.

1.2.4 Homogenisation of materials

The homogenisation of materials has been carried out throughout this thesis. Representing different materials as discreet geometries is desirable as this accurately represents reality. However, this is not always practical or computationally achievable. In the case of solid-type breeder blankets the most appropriate materials for homogenisation are the pebble beds of lithium ceramic and neutron multiplier. These pebbles are typically 1mm in diameter and therefore modelling each pebble separately would result in large complex geometry definitions. Positioning each of these pebbles in the simulation geometry in a random nature is achievable using existing packing methods. However, tracking particle movements in and out of the separate volumes would be impractical and extremely computationally expensive. Homogenisation seeks to represent this pebble bed as a single volume that occupies the space filled by the pebbles and the voids between the pebbles. The pebbles are homogenised with the voids to create a single material which conserves the mass of individual constituents. This often involves a reduction in density of the homogenised material as voids (filled with purge gas) between the pebbles are assimilated. Homogenisation reduces the complex geometry of the randomly arranged pebbles and speeds up the simulation dramatically. Without this simplification the simulations of full blanket models would not be possible within current computational limits. Comparisons between homogenised and heterogeneous models for breeder blankets have been performed on small samples [111] and homogenisation typically underestimates TBR by 2%. Homogenisation of pebble beds therefore introduces a small safety margin and homogenisation has become standard practice for the simulation of breeder blankets containing pebbles. The materials homogenised during this thesis are mixed pebble beds containing Be_{12}Ti pebbles, Li_4SiO_4 pebbles, reduced activation steel (Eurofer) and helium which serves as both coolant and purge gas.

To accurately homogenise a material the material density and volume fraction must be known. The approach taken calculates the material density by first finding the volume of individual unit cells and then finding the mass of the unit cell. The volume fraction is then used to scale the resulting material density. Li_4SiO_4 and Li_2TiO_3 are both ceramics formed from monoclinic unit cells; their crystal structure has been examined in research studies

[187] and [91]. Knowing the lattice unit cell parameters (a, b, c), the non 90 degree angle (β) and number of formula units per unit cell (Z) allows the volume of the monoclinic to be calculated (see Equation 1.18).

$$\text{Volume of monoclinic} = abc \sin(\beta) \quad (1.18)$$

Combining this information with the atomic masses of the isotopes involved allows the theoretical density (TD) of the ceramic to be calculated. Importantly this approach to finding the TD density allows for different ${}^6\text{Li}$ enrichments to be accounted for. The molar mass of lithium ceramics such as Li_4SiO_4 varies from 120g/mol to 116g/mol depending on the amount of ${}^6\text{Li}$ enrichment.

Unit cell lattice parameters	Li_4SiO_4	Li_2TiO_3
a (Å)	11.546	5.0623
b (Å)	6.090	8.7876
c (Å)	16.645	9.7533
β	99.5°	100.212°
Z	14	8

Molar mass at natural abundance (g)	119.85	109.75
Volume (Å ³)	1154.3442	427.0068
Theoretical density (gcm ⁻³)	2.4129	3.4132

Table 1.2 Lattice parameters from [187] and [91]

It should be noted that the TD has not yet been achieved in the manufacturing of fusion relevant ceramic pebbles. Achieving the TD would be desirable as it would maximise the number density of lithium atoms. However, densities are typically over 90% TD [101] and up to 98% [149] has been achieved. The value of 98% of the TD was chosen as the ceramic pebble density for the simulations carried out in this thesis. Although this is at the higher end of currently achievable values it is assumed that techniques will improve before DEMO

is constructed.

The packing fraction of the near spherical pebbles also has to be accounted for. Pebble beds containing a single size of pebbles can theoretically achieve a packing fraction up to 0.7405. In practice, lower packing fractions are more commonly achieved due to effects such as lower density at the container's edge and the random ordering of pebbles. [64] suggests packing densities between 0.625 and 0.645 are acceptable; this was achieved by computer simulations and verified with experimental measurements. A value of 0.63 has been used for Li_4SiO_4 and Be_{12}Ti packing fractions throughout this thesis. One way of increasing the packing density would be to use binary mixtures where pebbles of two different sizes are used, however this is not yet being considered for European HCPB designs. One reason why increasing the packing density may not be desirable is that it makes tritium extraction using a purge gas more difficult. A calculation of the number of ${}^6\text{Li}$ atoms per unit volume can now be performed.

$${}^6\text{Li} \text{ atom density} = \frac{\text{packing fraction} \times \text{theoretic density fraction} \times \text{Li atoms per unit} \times \text{formula units per unit cell}}{\text{volume of monoclinic}} \quad (1.19)$$

This approach was used to find the atom density of all the isotopes present in Li_4SiO_4 . Be_{12}Ti pebbles also have specified atom ratios and can be combined into the mixture in a similar way. Structural steel can be combined into the mixture by once again knowing the volume fraction and the density required to achieve the resulting homogenised density. Helium coolant and purge gas can also be added to the homogenised mixture by knowing the atom density and the volume fraction. However, additional calculations must be made to account for density variations caused by pressure and temperature. Typical temperatures and pressures for the He coolant in HCPB designs are 500°C and 8MPa, while the purge gas is 400°C and 0.1MPa (atmospheric pressure) [202].

1.3 Sustainability of fusion energy

Fusion energy is often presented as a sustainable energy source with a virtually limitless supply of fuel. The fuel proposed for power producing reactors such as DEMO is a 50:50 mixture of deuterium and tritium. As previously discussed, it is necessary to use lithium to produce tritium. Worldwide supplies and availability of deuterium and lithium must therefore be investigated to ascertain the sustainability of the fuel source. Deuterium is a natural isotope of hydrogen and it accounts for 1 part in 6700 or 150ppm of all hydrogen atoms in the world [31]. The deuterium content of sea water has been shown to be uniformly distributed within ocean depths below 500m [54] [32] and therefore the amount of deuterium in the sea can be estimated at 1.1×10^{19} kg. Deuterium can be readily extracted from sea water using conventional methods such as isotope exchange in hydrogen sulphide [6]. Other plausible methods include gas chromatography, distillation and electrolysis [124]. Additionally, more advanced techniques are also being pursued (see e.g. [62]). Natural enrichment via selective evaporation occurs in closed bodies of water such as the Dead Sea and the Great Lakes in North America. The deuterium content of water is marginally higher in these reservoirs. Large scale extraction of heavy and semi heavy water has been carried out for a number of years to supply CANDU reactors and non-civilian needs. Deuterium supplies are extensive and accessible and will not be the limiting fuel in the case of fusion energy.

Lithium is not as abundant and consequently there has been more research into the availability of lithium for fusion power [41], [50] and [18]. The availability [107] and geographical distribution [76] of lithium mines are also key concerns for the rapidly growing electric vehicle industry. However, lithium batteries and fusion breeder blankets do not necessarily compete for the same lithium reserves, as lithium isotopes are chemically similar but differ in their nuclear properties. Current breeder blanket designs specify enriched ^6Li content because of its superior thermal cross-section. As natural lithium is 7.6% ^6Li and 92.4% ^7Li it would be possible to envisage lithium batteries made mainly from ^7Li and breeder blankets made mainly from ^6Li . The development of alternative battery technologies may result in reduced demand for lithium [114]. Current lithium is found in terrestrial reserves such as

salt brines under salars, typically in the form of lithium carbonate. Proven terrestrial lithium is concentrated in a few countries [76]. The majority of breeder blanket designs require lithium enriched in ${}^6\text{Li}$ content. FLiBe is an example of a breeder material that may be able to produce sufficient tritium without ${}^6\text{Li}$ enrichment [205]. However, FLiBe has technical difficulties such as low conductivity, high viscosity and corrosion issues.

Relatively little lithium prospecting has occurred to date and it is likely that further deposits will be found. There is a strong correlation between endorheic basins and salt lake brines which suggests plenty of additional lithium reserves are yet to be discovered [76]. Research carried out by [50] presents a pessimistic case by suggesting that there is only sufficient lithium in reserves and resources to supply fusion needs for 250 years. The report goes on to state that this estimate will naturally increase as additional fuel reserves become viable. Lithium is also found in sea water at 0.173mgL^{-1} which equates to a total of 2.4×10^{11} tonnes [165]. The feasibility of extracting lithium from sea water would increase the longevity of fusion fuel to approximately 14 million years [18]. Extraction of lithium from sea water has been investigated using manganese oxide absorbents [26], ion sieves [125] and a combination of solar evaporation with ion exchange [165]. Extraction of lithium from sea water appears viable using all of the previously mentioned methods. Once the natural lithium is obtained it is separated from the ore and enriched. During the 1950s and 1960s the COLEX method was used to create highly enriched ${}^6\text{Li}$, however this method has been ruled out due to environmental problems with the use of mercury [152]. More recent methods of lithium isotopes separation techniques have been developed that offer better separation coefficients and are environmentally acceptable [82]

Therefore the two fuels required for DT fusion can be characterised as sustainable due to the vast quantities available. In the longer term DD fusion does not require breeder blankets and therefore would not require lithium or tritium. The use of lithium in chemical reactions is more reversible than nuclear reactions. Following a chemical process it is possible to recover isotopes with sufficient energy input. However the lithium in breeder blankets is altered in a more permanent manner as the nucleus is changed.

Naturally fusion power stations will require materials for other parts of the reactor. Es-

ential components and the materials currently employed in these roles are listed below:

- First wall tungsten armour (tungsten).
- Superconducting magnets (niobium tin Nb₃Sn).
- Structural components (low activation steels).
- Coolant for the magnets (helium)
- Neutron multipliers (lead or beryllium).

According to the US geological survey [188] there is sufficient tin, iron ore, tungsten and niobium for the foreseeable future. These materials could also be recycled and used in several fusion power plants. There are complications involved when recycling first wall materials, as they become activated and remain too radioactive for ~ 100 years. [134] shows that recycling tungsten tiles from a first wall is possible.

The availability of neutron multipliers like beryllium and lead is more concerning. These two neutron multipliers are currently under consideration; although other neutron multipliers such as uranium, thorium and plutonium exist, their use in fusion reactors has been ruled out by many scientists. Using fissionable materials within the blanket would result in an increase in the level of nuclear waste produced, in addition to presenting proliferation opportunities. Using fissionable materials in the blanket could increase the neutron multiplication and negate the need for beryllium [118], however fusion would no longer be such an ideal energy source. The idea of a fission fusion hybrid reactor dates back to the 1950s when the first nuclear reactors were being designed. The hybrid gained popularity during the 1970's oil crisis when accomplished nuclear physicist Hans Bethe backed the concept [13]. There are several perceived advantages to such an approach as well as difficulties that would need solving [87]. Researchers in China have developed concept designs [199], however the majority of the fusion community is concentrating on pure fusion. Gernstner [65] published an article entitled "The hybrid returns" which presents the case for combining these two opposite but related technologies. However, the hybrid concept designs still require a fully functional fusion reactor. Proliferation issues are also a concern for hybrid reactors due to the potential to produce large quantities of plutonium [71].

The sustainability of likely multiplier materials beryllium and lead will now be considered. Reserves of beryllium are estimated to be from 80,000 tonnes [188] to 485,400 tonnes [102]. Due to the lack of economic demand the worldwide reserves have not yet been fully evaluated and the estimate of 485,400 tonnes excludes possible resources in Russia and China. DEMO plants incorporating a full solid-type breeder are expected to require in the order of 800 tonnes of beryllium. Assuming a simplistic situation with no recycled beryllium and no competing requirements for the element, then there are sufficient known reserves to construct 600 DEMO reactors. However, the shortage of beryllium has been noted by [18] “In particular beryllium, represents a major supply problem and requires that other, sustainable solutions be urgently sought”. [84] also highlights the problem of beryllium “An alternative high temperature compatible solid neutron multiplier option would be highly preferable in the very long term and therefore should be part of the research programs”. One solution suggested by [12] is efficient utilisation and recycling. A small portion of beryllium is used up during a breeder blanket’s life time, making it a consumable and therefore it cannot be recycled indefinitely. Annual burn-up of beryllium in a DEMO reactor equipped with HCPB blankets is estimated to be less than 0.2% of the beryllium installed [18].

Lead is another option as a neutron multiplier and is considerably more sustainable. Lead reserves and resources are estimated at 79Mt and 1.5Gt respectively [188]. The larger quantities of lead make it a more attractive neutron multiplier in the long term. However the neutron multiplying properties of lead are different to beryllium. For instance the $\text{Pb}(n,2n)$ reaction lead requires higher energy neutrons than the $\text{Be}(n,2n)$ reaction (see Figure 1.11). The lower melting point of lead means it will be in liquid form at breeder blanket temperatures. Lead is also burnt-up by the neutron multiplying reactions, at a rate of 0.1% per year in a DEMO reactor equipped with HCLL blankets and 4092 tonnes of lead.

Prior to beryllium and lead emerging as the neutron multipliers of choice, other materials such as zinc, bismuth and ^7Li were seriously considered [3] [183]. Vanadium, niobium, molybdenum and tungsten have neutron multiplication properties but were quickly ruled out due to compatibility problems, manufacturing problems and long term activation problems

[72]. Criteria for good neutron multiplier materials are not limited to neutronics reasons alone. The probability of the (n,2n) and (n,3n) cross-sections are the primary selection reason but cost, parasitic neutron interactions, availability, fabricability and compatibility with other blanket materials are all important. Bi was finally ruled out as a neutron multiplier due to its production of significant quantities of ^{210}Po which is an alpha emitter. Zn was found to have lower neutron multiplication than Be and Pb.

It is likely that the superconducting magnets used in future power producing fusion plants will require significant quantities of liquid helium as a coolant. Helium supply is a widely publicised dilemma (see e.g. [140], [139] and [29]) and particularly relevant to future fusion energy power plants. Although helium is the second most abundant element in the universe, its existence on Earth is scarce. The majority of terrestrial helium is generated by the decay of radioactive isotopes such as ^{238}U and ^{232}Th [18]. The emitted helium then escapes into the atmosphere and eventually space; only a small fraction is retained in the Earth's crust by impermeable rocks. Helium is therefore found in small concentrations (typically 1%) along with natural gases (methane & nitrogen) in impermeable geological strata. Helium extraction is a by-product of natural gas extraction and often vented to the atmosphere [139]. Helium reserves are in danger of being used up at the same rate as natural gas supplies [18]. Due to the dispersion of emission sources there is no possibility of accessing the helium as it is released from ^{238}U and ^{232}Th decay. Reclaiming helium from the air is economically viable [106] at an energy cost of between 2.3MWht^{-1} (ideal scenario) to 20GWht^{-1} (extrapolated results). The separation of helium from air has potential and it is reassuring to have options. Helium is produced via (n, ^4He) in many of the materials proposed for use in fusion reactors. Another source of helium is the DT fusion reaction itself. Significant sources of helium within the fusion reactor are:



The helium produced from a 1GW (electrical) DEMO like power plant is approximately 0.5 tonnes per year. This equates to less than 1% of the 60 tonnes inventory and around 30% of the annual helium leakage [18]. Unfortunately fusion reactors will not be fully self-sufficient in helium. One possible solution to this dependency would be a break through development in high temperature super conductors which would allow the use of liquid nitrogen as a coolant [55].

In summary, several aspects of the current fusion devices could be classified as unsustainable. Current knowledge of beryllium resources indicates that it is a rare element. Helium supplies are in great demand and running out. Elements such as lithium are only sustainable if new sea water extraction techniques are developed. In the long term promising alternatives and workarounds are possible. Helium can be replaced by nitrogen; beryllium could be phased out in favour of lead or other alternatives. Lithium would not be necessary if DD fusion could replace DT fusion.

Even more ambitious than DD fusion is the possibility of aneutronic fusion, which emits no neutrons. There are several possible reactions for aneutronic fusion all of which require formidable technical accomplishments such as higher temperatures, higher pressures and vastly improved confinement. However aneutronic fusion reactions such as the proton boron reaction are perhaps the very distant future of fusion energy [174]. Aneutronic fusion also offers the advantage of no neutron activated radioactive waste.



1.3.1 Conclusion

Fusion therefore has the potential to become a sustainable energy source. However, fusion reactor designs must eventually evolve to use different materials. Reference [18] shows that renewables such as wind and solar power suffer from similar sustainability issues. Rare earth-based permanent magnets for wind turbines, cadmium and tellurium used in solar panels are examples of non-sustainable materials currently in use.

Generally, definitions of sustainability centre on not being harmful to the environment and not depleting natural resources. Much of the research into the sustainability of fusion has gone into sizing up the various critical resources and assessing the feasibility of extraction. Little work has been done on assessing the environmental impacts of extracting sufficient raw materials. For example, attempting to extract sufficient helium from the air to meet current helium demands would require the filtering of over a hundred cubic kilometres of air [139], extracting lithium from sea water also requires huge volumes to be filtered. However, the assessment of the environmental sustainability of fusion power is perhaps best carried out once scientists have a better idea of the material requirements of future fusion power plants.

1.4 Nuclear simulations

To accurately simulate nuclear interactions within breeder blankets it is necessary to possess geometrical definitions of the reactor, material specifications, nuclear interaction cross-sections, neutron source characteristics and a method of transporting neutrons through matter.

The exact geometry of DEMO reactors is evolving and will not be finalised for some time. Research groups working on DEMO designs produce models that are the best available representations. Although several groups around the world are working on DEMO designs, access to their models is often restricted. Fortunately for the scope of this thesis, two EU designs have been made available. The details of the models, as well as the modifications made to them, are discussed in later chapters. Both of the models use Constructive Solid Geometry (CSG) to represent volumes occupied by a single material. CSG relies on geometric primitives such as spheres, cylinders, cones, etc that can be defined mathematically. Boolean operations such as unions and intersections are then used to define more complicated volumes; the MCNP manual contains more details [74]. CSG is well suited for modelling reactors which contain a large amount of symmetry and offers reduced memory consumption compared to other approaches such as mesh geometries.

1.4.1 Particle transport

The neutron transport equation which describes the movement of neutrons through space is essentially a balance statement that conserves the number of neutrons. Each term represents a source or sink of neutrons.

$$\frac{1}{v} \frac{\partial \varphi(r, E, \Omega, t)}{\partial t} + \Omega \bullet \nabla \varphi(r, E, \Omega, t) + \Sigma_t(r, E, t) \varphi(r, E, \Omega, t) = \int_{4\pi} \int_0^\infty dE' d\Omega' \Sigma_s(r, E' \rightarrow E, \Omega' \rightarrow \Omega, t) \varphi(r, E', \Omega', t) + S(r, E, \Omega, t) \quad (1.25)$$

as provided by [129] where v is the velocity, φ is the angular neutron flux, r is the position vector, E is the energy, Ω is the direction unit vector, t is time, Σ_t is the total macroscopic cross section and Σ_s is the double differential scattering macroscopic cross-section and S is the source term. See Equation 1.26 for a definition of macroscopic cross-section (Σ).

$$\Sigma = \sigma N_d \quad (1.26)$$

where the macroscopic cross section (Σ) has units of m^{-1} , the microscopic cross section (σ) has units of m^2 and the number density of atoms (N_d) has units of atoms per m^{-3} .

Two classes of methods exist for the simulation of particle transport through matter, these are deterministic and stochastic methods. The deterministic method is well suited to simple 1D or 2D geometry and solves simplified versions of the Boltzmann transport equation (equation 1.25) with high accuracy. However, this method is not well suited for the complex 3D geometries involved in fusion reactors. It is possible to simplify the geometry in many cases to obtain an exact answer to an approximation of the model, however this is rarely informative. Monte Carlo (MC) is an example of stochastic modelling technique that utilises a sequence of random numbers to produce an approximate answer even for complex geometry. Choosing between the two methods is a trade off between geometric complexity and accuracy of the answer.

A particular implementation of the stochastic MC method called Monte Carlo N-Particle

(MCNP)[74] is the current reference code for fusion neutronics calculations. Other popular MC transport codes exist such as Serpent, Geant, OpenMC and Fluka. These are continually being assessed in terms of their ability to replace MCNP, however MCNP remains prevalent within the fusion neutronics community [58]. MCNP originated from Los Alamos in the 1940s where it continues to be developed. The primary focus of MCNP is nuclear processes for fission reactions, but MCNP has branched out to other areas such as radiation shielding, detector design and dosimetry. MCNP has a long history of extensive benchmarking and testing to validate it for the needs of fusion and fission neutronics [156].

MCNP traditionally relies on Constructive Solid Geometry (CSG) to segment the 3D model into cells. Each cell has defined boundaries and can contain a different material. MCNP simulations start with the birth of a source particle. When simulating tritium production in fusion reactors the particles of interest are neutrons. Neutrons are liberated within the plasma in DT fusion events. They are emitted isotropically and with an average energy of 14.1MeV. The initial energy distribution of neutrons is a Gaussian distribution and described in more detail by [19]. Once the direction and velocity are decided upon, MCNP tracks particles from their creation to their termination. During the lifetime of a particle it will interact with the matter it passes through. Possible neutron interactions include elastic scattering (n,n), inelastic scattering (n,n'), neutron capture (n,g) and other reactions, some of which are included in Figure 1.12.

MCNP simulations involve three main processes; these are a physics step, geometry step, and tallying. In the physics step the distance from the particle location to the next interaction is found. To achieve this the material's macroscopic cross section (see Equation 1.26) is used to ascertain the probability of certain interactions. Probability density functions (pdfs) are then used together with random sampling to determine the outcome of interactions and the distance between the particle's initial position and the interaction site. In the geometry step the distance between the current particle location and the nearest intersecting boundary to the next cell is found. Uncharged particles such as neutrons and photons are assumed to travel in straight paths between collisions. This allows ray tracing techniques to be used to find the intersection between cell surfaces and the particle's trajec-

tory. The distances calculated in the geometry step and the physics step are then compared and the process with the shorter length is selected. Assuming the physics step is shorter then an interaction takes place. The next step depends on the interaction that takes place. For example in an (n,n') the direction and the velocity of the neutron are changed; while in an (n,g) reaction the particle type changes. Physics interactions require the particle location to be updated and the geometry step recalculating. If the particle's energy has changed then the probabilities of different interactions will also change and part of the physics step will need recalculating. Alternatively it is possible for the particle to cross a cell boundary before interacting. If the particle escapes the current material then new pdfs will need to be calculated that represent the new material that the particle has escaped into. This process is repeated until the particle is captured or killed by the simulation. Particles can be killed by the simulation if they fail to meet certain criteria such as user defined energy limit. This results in the simulated particle taking a random walk through the material.

Aspects of the individual particle's behaviour are then recorded during the simulation. This allows the average behaviour of the particle to be inferred using the central limit theorem. The user can request information (tallies) on certain aspects of the computation such as average tritium produced per source neutron (TBR). Two tallies used extensively throughout this thesis are F4 and F6 tallies. F4 refers to the average neutron flux for the cell and allows the number of particles at particular energies to be recorded. F4 tallies can be used to gain knowledge of the neutron spectra in difference cells as demonstrated by Figure 2.3. F6 tallies allow the energy deposited per cell to be recorded. The default units of F6 tallies are MeV per g. However, this can easily be converted to energy per cell by multiplying the tally result with the cell volume and density. F6 tallies used in this thesis include energy deposited by photons as well as neutrons. Photons are generated by neutrons in interactions such as neutron capture (n,g) and inelastic capture (n,n') . Recording energy deposited by both photons and neutrons requires coupled neutron photon simulations to be enabled in MCNP. An example of the type of information that can be gathered with the use of F6 tallies is demonstrated by Figure 5.6.

1.4.2 Nuclear interaction probabilities

The nuclear interaction probabilities (cross-sections) for various neutron induced interactions must be well characterised if the simulation results are to be acceptable. Reducing uncertainty in important interactions such as the tritium producing reactions is particularly important. Ideally, secondary interaction probabilities such as alpha and gamma induced reactions would also be well characterised. The nucleus can undergo changes as a result of the interaction and this often results in a new nucleus; common possibilities are shown in Figure 1.12. Different reactions have unique identification numbers assigned to them commonly referred to as MT numbers, e.g. the $(n,2n)$ reaction is MT number 16. The newly formed nuclei will have different cross-sections to their parent nuclei. The nuclear data for the new isotopes should also be included in the simulation when there is significant material evolution.

The probability of interaction can be experimentally obtained by colliding particles of different energies with targets. Experimental data corresponding to certain reactions are made available in the EXFOR database [206]. The EXFOR data base shows 37 data points for the important ${}^9\text{Be}(n,2n)$ reaction obtained from 8 experiments (see Figure 1.13). For comparison, the ${}^{235}\text{U}(n,f)$ cross-section is characterised by 179 experiments and contains several thousand datapoints. The physical data is then fitted using a combination of the experimental results, physics models and human judgment; the fitted result is referred to as an evaluation. Uncertainty in the evaluation is understandable due to the lack of experimental results to base the evaluation on. Evaluations are regularly carried out by several research groups; some examples are: Joint Evaluated Fission and Fusion File (JEFF [11]), Japanese Evaluated Nuclear Library (JENDL [167]) and Evaluated Nuclear Data File (ENDF [22]). All these evaluations have their different strengths and weaknesses but arguably the most mature is the U.S. evaluation ENDF VII.1. Special purpose libraries such as the Fusion Evaluated Nuclear Data Library (FENDL [61]) seek to create collections of cross-sections suitable for a particular purpose. This is achieved by extensive validation and selecting the most suitable existing cross-sections from a range of evaluations. Sophisticated tools have been developed to predict cross-sections where little or no nuclear data exists. TENDL [104]

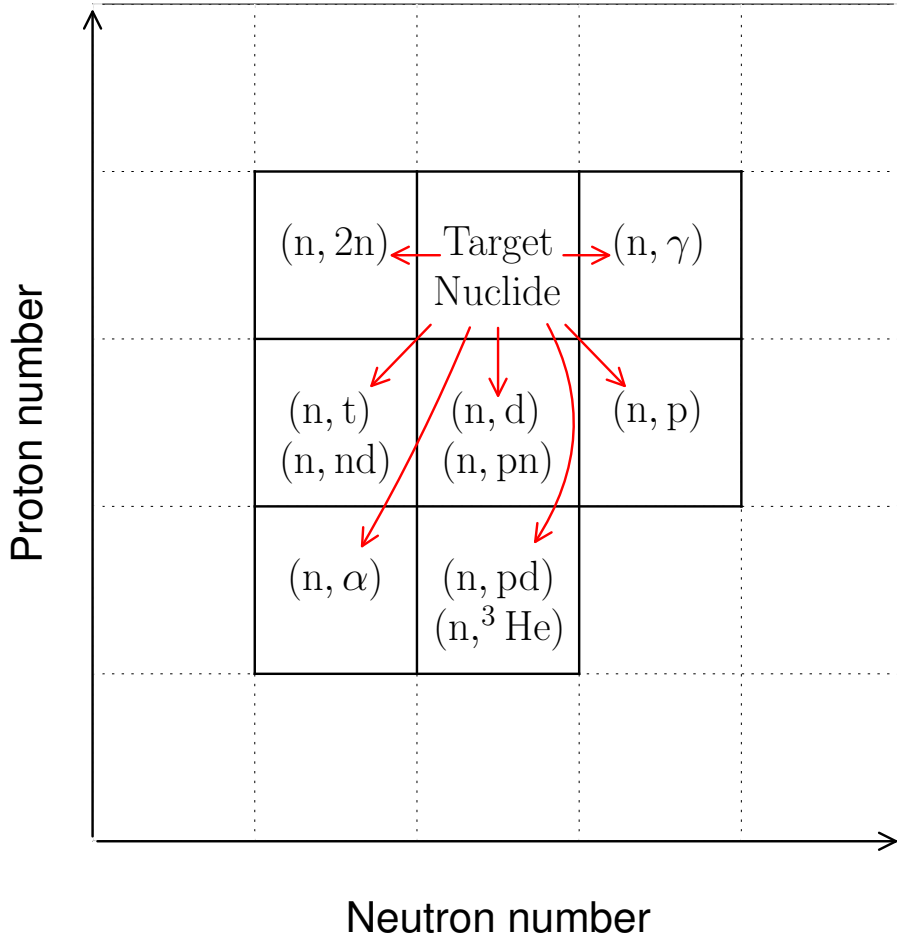


Fig. 1.12 The interaction cross-section of different fusion fuels.

is produced from a mixture of experimental results and nuclear physics models (e.g. the nuclear optical model [81]) and is arguably the most complete collection of cross-sections. The evaluations differ (see Figure 1.13) and each produces different simulation results. It is preferable to choose validated cross-sections when possible, such as FENDL. ENDF is considered the gold standard in many cases and much of FENDL data is reprocessed ENDF. For exotic isotopes produced when simulating activation and decay it is not always possible to find experimentally derived evaluations and in this case TENDL is the best choice.

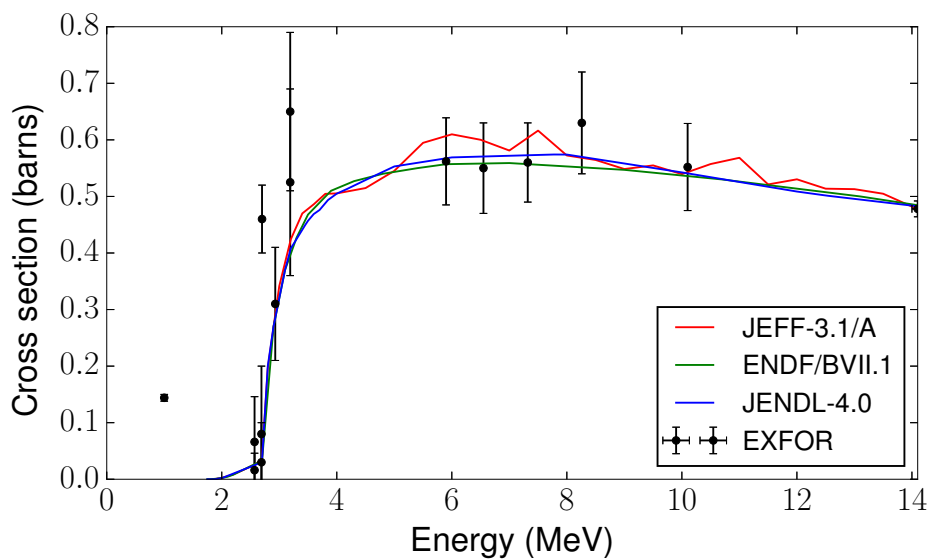


Fig. 1.13 Different evaluations of the EXFOR data for the ${}^9\text{Be}(n,2n)$ reaction.

1.4.3 Interface codes

The unprecedented neutron flux within fusion reactors will cause nuclear transmutations to occur. Isotopes with large capture cross-sections such as ${}^6\text{Li}$ will be gradually burnt up. Many of the isotopes created are unstable and will decay to form more stable isotopes. The material will evolve as isotopes are created, destroyed and change with respect to time. Subsequent particles will experience different interaction probabilities as the material contains different isotopes compared to the original material. These material changes are not accounted for in MCNP and another code is required to simulate this phenomenon. Inventory codes are a group of codes that attempt to utilise the Bateman equations [77] to keep track of the activation, decay and burn-up of nuclides. FISPACT is an activation code developed at CCFE [179] and made available for this thesis. Although FISPACT can model activation and decay, it is unable to perform particle transport. MCNP is able to perform particle transport but is unable to account for temporal changes to the materials. An interface or coupling code is required to combine these two separate functions. A fusion specific depletion interface code (FATI [131]) has been previously developed and successfully couples MCNP and FISPACT together. This interface code has been used extensively during Chapters 2 and 3 to study time varying tritium production in breeder blankets.

1.5 Summary and prelude

The thesis follows a general theme of varying material composition to better utilise the local neutron spectra within fusion breeder blankets. This includes breeder material, neutron multiplying material and structural material.

Chapter 1 introduced the reader to fusion energy, breeder blankets and relevant aspects relating to neutronics. The introductory chapter discussed the physics of fusion with a particular focus on magnetic confinement fusion. Specific challenges that must be successfully resolved if fusion energy is to become a reality were identified and the importance of breeder blankets is highlighted. The theory of breeder blankets and how they are designed to meet certain requirements through careful material choices were explored. Specific techniques applied throughout this thesis such as particle transport and material homogenisation were explained. The underlying nuclear physics that occurs within breeder blankets is covered in the final section of Chapter 1. The following chapters will concentrate on original research carried out as part of this thesis.

The long term performance of breeder blankets remains an area that has not been fully explored. The neutron flux experienced by breeder blankets is unprecedented and at these levels of neutron irradiation, effects such as nuclide burn-up become relevant. Previous neutronic simulations of breeder blankets have shown that their tritium producing capability decreases with time [9, 27, 143, 159]. The explanation for this decrease in tritium production is largely due to ${}^6\text{Li}$ burn-up. It is important to accurately predict time varying tritium production to avoid running out of tritium fuel. Chapter 2 investigates how the simulation of ageing breeder blankets can be performed more accurately and in particular avoid over-predicting the tritium production.

It is widely acknowledged that it is necessary to produce more tritium than the reactor fuses [59]; this is required to negate losses such as tritium leakage and retention in materials. The exact quantity of excess tritium required is not yet known [44] and it is likely that excess tritium could be required to start up subsequent reactors. It is therefore practical to ensure that blankets are capable of achieving increased tritium production to meet the new demand. Variation in the material composition of the blanket has a large effect on the

tritium producing performance and also on the rate at which tritium production decreases with time. Chapter 3 builds on work from the previous chapter to perform a parameter study where the composition and the geometry of breeder blankets are varied. The time varying tritium production is simulated and the results allow designers to understand how the tritium production is affected by compositional and geometrical changes. This clearly identifies compositions that are unable to produce sufficient tritium as well as the most economical solutions capable of producing a particular quantity of excess tritium. Compositions and geometries that are susceptible to large reductions in tritium production over time are also identified.

Producing excess tritium to start up subsequent reactors is shown to be viable but costly and resource intensive. There is potential to reduce the required start-up inventory by producing tritium using DD plasmas. Reactors typically operate with DD plasmas prior to DT plasmas in order to test the device. Relatively little energy is generated during this stage and it would be desirable to move to full DT operation quickly. The idea of using DD plasmas to generate tritium and hence reduce the start-up inventory has previously been investigated. Chapter 4 contributes to the work previously performed by optimising breeder blankets for tritium production with DD plasmas. The optimisation takes account of the lower energy neutrons emitted by DD plasmas compared to DT plasmas. It is shown how the tritium production in the blanket for DD plasmas can be increased. However, the time required to breed enough tritium for a DT plasma was only marginally reduced.

The sustainable aspects of fusion are one of the key reasons fusion is considered such a promising energy source. The abundance and availability of key fuels (deuterium and lithium) involved in fusion have been previously investigated and are considered sustainable, however, other materials involved in reactors are not. The most problematic dependency is the requirement for beryllium in solid-type breeder blankets. This element has a low abundance and large manufacturing costs. Chapter 3 identifies beryllium as the major cost for breeder blankets and therefore its reduction would be economically beneficial. There are a few possible solutions that have been previously investigated such as recycling and making use of alternative materials (e.g. lead). Chapter 5 takes a neutronics approach to

alleviating the problem and demonstrates a method of reducing the amount of beryllium required in breeder blankets. The neutronics study carried out also shows that beryllium usage can be reduced without detrimental effects on the performance of the blanket.

Mixed pebble bed breeder blankets currently employ a uniform mixture of lithium and beryllium. Enriched lithium is required to breed tritium via neutron interactions, while beryllium is required to multiply the neutron flux. Chapter 6 aims to improve the blanket performance by varying the lithium to beryllium ratio and the lithium enrichment as a function of blanket depth. This method utilises the difference in the interaction probabilities of the lithium and beryllium isotopes to maximise the tritium production. In addition to increasing tritium production the endothermic and exothermic nature of the dominant lithium and beryllium reactions allow them to beneficially affect the heat deposition within the blanket. This method of optimisation was also able to decrease the overall lithium enrichment and beryllium requirements.

The high neutron flux present within a fusion reactor requires the development of low activation materials. The selection of elements to exclude is typically decided by considering their nuclear properties. Enriching or depleting certain isotopes away from their natural abundance results in different nuclear properties for the element. The possibility of considering individual isotopes would allow materials to have a wider selection of elements as particular isotopes could be removed or depleted. This technique allows previously rejected elements to be reconsidered. Chapter 7 identifies isotopically enriched materials that offer reduced activity and lower gas production when compared to the materials with natural abundances. Preliminary costs benefit-analysis is also carried out.

Chapter 2

Time varying tritium production

2.1 Introduction

High energy neutrons produced in future fusion reactors will cause significant transmutation reactions in the breeder blanket, including the important tritium breeding reactions. The reaction rate per unit volume (R_r) for a given reaction type depends on the isotope number density (N_d), neutron flux (ϕ) and the microscopic cross section (σ) for the reaction.

$$R_r = \phi \sigma N_d \quad (2.1)$$

The overall tritium production of the solid-type blanket decreases as the ${}^6\text{Li}$, ${}^7\text{Li}$ and ${}^9\text{Be}$ are burnt up. Accounting for nuclide burn-up has consequences for time varying tritium production and tritium inventory estimations. Blankets such as the Helium Cooled Pebble Bed (HCPB) [15] have undergone neutronic design optimisation [57, 147] to ensure tritium self-sufficiency. This is particularly challenging when considering the burn-up of ${}^6\text{Li}$, ${}^7\text{Li}$ and ${}^9\text{Be}$.

Aside from ensuring tritium self-sufficiency, predictions of the surplus tritium inventory are of interest for subsequent fusion power plants requiring a start-up inventory. If the breeder blankets produce more tritium than the reactor requires (for fuel) then this tritium

can be stored for use in other reactors; this is referred to as a surplus tritium inventory. Predicting the maximum tritium storage requirements will be necessary for safety licensing. In this chapter simulations of the tritium breeding ratio (TBR) and surplus tritium inventory over the expected life time of the breeder blanket are presented.

The research builds on the work of [9, 27, 130, 143, 159] where simulations of time varying tritium production in solid-type breeder blankets have previously been carried out.

The burn-up of nuclides in fusion breeder blankets was first studied by Packer [143]. A 3D DEMO model with semi-heterogeneous breeder blankets was used together with a coupled FISPACT MCNP code. Two different ceramics, three different enrichments and two different blanket thicknesses were simulated. This preliminary study suggested that accounting for nuclide depletion influences the TBR and surplus tritium inventory calculations. The different variations showed differing impact and the topic was highlighted as necessary to ensure tritium self-sufficiency. Although [143] covered a broad range of thickness, ceramics and ^{6}Li enrichments, the results cannot be reliably extrapolated to designs that differ from the semi-heterogeneous configurations simulated. Research performed later by Sato [159] took a particular blanket design and carried out burn-up simulations. Although the blanket model was more detailed, the model as a whole was less realistic. The infinite slab model used does not accurately represent the shape of DEMO reactors. [27] expanded on the field by investigating burn-up with a wider range of liquid and solid type blanket materials. This was performed on a cylindrical geometry which is an improvement over the infinite slab model but is still far from DEMO designs. Subsequent studies [9] showed the inaccuracies of using simplified models by comparing the result of a simple spherical model with a more realistic 3D DEMO model. Another important contribution by [9] was a more sophisticated coupling code, the main improvement being recalculating the neutron spectra with each change to the material composition. This updating of the neutron spectra was later confirmed to be necessary by [130] who showed that the neutron spectra should be updated at least once a month (availability assumed to be 100%) to achieve less than 5% error. This chapter further contributes to the field by specifying a minimal spatial segmentation of the breeder blanket to avoid unnecessary errors.

The DEMO fusion reactor model used for my research contains 19 homogeneous breeder blanket modules made of Eurofer, helium, Be₁₂Ti and Li₄SiO₄, with enriched ⁶Li content. The computational advantages of homogenised models over more detailed heterogeneous models make them attractive for burn-up and parametric studies. My simulations use a DEMO 3D geometry containing homogenised breeder blankets that are segmented both radially and toroidally to examine the effects of spatial resolution of the breeder blanket on the surplus tritium inventory. The resolution of radial segmentation was varied from a single radial segment (as performed by previous studies) to 10 radial segments. Time-dependent tritium production was simulated with the use of the interface code, FATI, which couples radiation transport code MCNP 6 with the inventory code FISPACT-II. The radial segmentation performed allowed the time-dependent reaction rate as a function of depth to be analysed.

2.2 Material and methods

The reactor model was adapted from a tokamak DEMO model developed by KIT under an EFDA 3PT task [148]. The use of reflecting surfaces allows this $1/16$ sector model to adequately represent a complete reactor. This assumes the reactor has a repeating structure. The model includes first wall, homogenised breeder modules and a rear shielding layer. The breeder zones were split toroidally into 19 modules and up to 10 segments radially (see Figure 2.10). This resulted in up to 190 cells in which nuclide burn-up was simulated. The depth of the radial segmentation was found by calculating fractions of the module depth. As the outer modules are thicker, (130cm) compared to the inner modules (65cm), this results in segments of different depth.

The neutron source geometry was based on the plasma parameters: 9 m major radius; 2.25m minor radius; triangularity of 0.33; peaking factor of 1.3; and an elongation of 1.66. The major radius of the plasma is the distance from the centre of the tokamak to the centre of the plasma, while the minor radius is the horizontal width of the plasma. The triangularity of the plasma is the horizontal distance between the X point of the plasma and the major radius. The peaking factor is the volume average temperature divided by the pedestal temperature. The elongation is the height of the plasma divided by the minor radius. Future descriptions of these plasma physics parameters and others can be found in [191]. The monoenergetic (14.1 MeV) neutron source used birth locations based on the plasma density and temperature. The resulting neutron density profile is displayed visually in Figure 2.2 and is covered in depth by [51]. The neutrons are emitted isotropically.

The magnets were defined as Nb₃Sn and the vacuum vessel was assumed to be manufactured from 316 stainless steel. A 3mm layer of pure tungsten was defined as the plasma facing component (the first wall) [83]. The reduced activation steel Eurofer [115] with a helium coolant (3cm thick and homogenised) was selected as the material for the casing of the breeder blankets. Details of the materials used in the breeder zone can be found in Table 2.1. Eurofer was used as a structural material within the breeder blankets. Helium is both the coolant and purge gas. Be₁₂Ti was selected as the neutron multiplier instead of beryllium metal due to its performance capability at higher temperatures [39]. Li₄SiO₄ with a ⁶Li

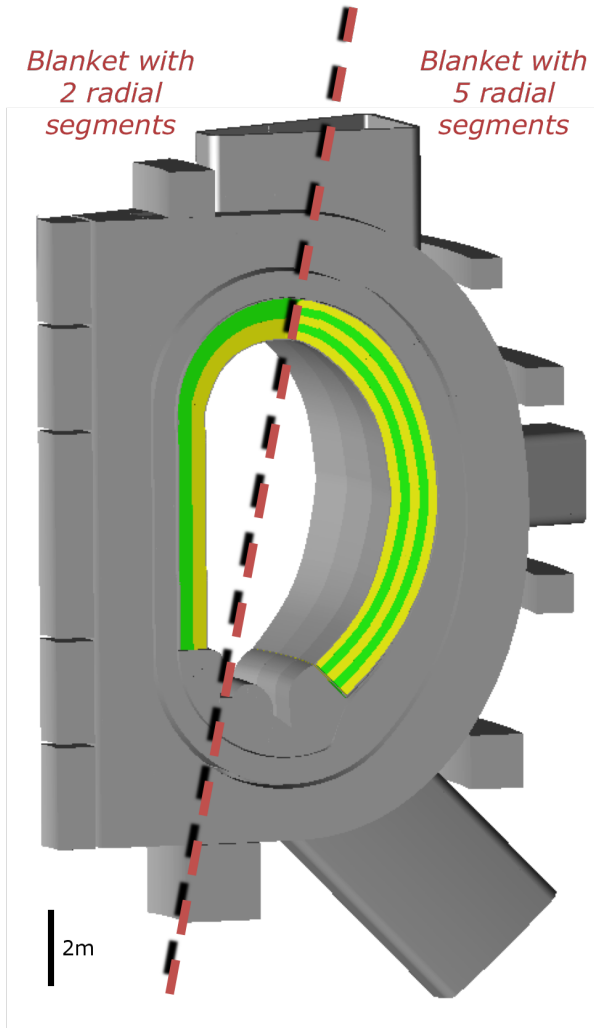


Fig. 2.1 Two differently segmented blankets are shown with alternate blanket layers coloured yellow and green .

enrichment of 40% was selected as the ceramic breeder material. Both the Be_{12}Ti and the Li_4SiO_4 were assumed to be in pellet form with a packing fraction of 0.63. The thickness of the inboard blankets was 0.75m and the outboard blankets was 1.30m.

Neutron transport was simulated using the Monte Carlo code MCNP 6 while the inventory code FISPACT-II [179] was used to model activation, transmutation and neutron induced burn-up. The interface code FATI [131] was used to couple MCNP 6 and FISPACT-II together. FENDL 3.0 [61] nuclear data was used preferentially for particle transport. TENDL 2014 [104] nuclear data with 315 energy group structure (TRIPOLI) was used by FISPACT-II to model activation, transmutation, neutron induced burn-up and also for par-

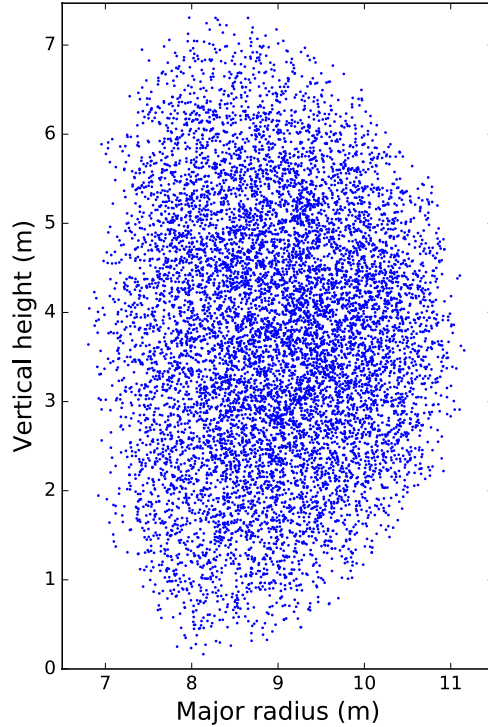


Fig. 2.2 Neutron source intensity map produced with 10,000 neutron birth locations.

Material	Component	Volume percent	Resultant density (g/cm ³)
Homogenised breeder material	Eurofer	9.705	1.816
	He coolant	5.295	
	Li ₄ SiO ₄	9.450	
	He purge gas	31.45	
	Be ₁₂ Ti	44.10	

Table 2.1 Material fractions for the homogeneous breeder blanket material.

ticle transport when FENDL data was not available. The energy values used in the 315 TRIPOLI group structure can be found in the appendix of [179]. Recent investigations into the effect of different sized time steps have been carried out and time steps of less than one month were recommended [130]. Burn-up was simulated in time steps of 15 days for a fusion reactor with 2.4GW of fusion power, operating 70% [185] of the time. The sur-

2.2 Material and methods

plus tritium inventory is the difference between production of tritium in the blanket and consumption in the plasma, accounting for tritium decay. Leakage, retention and isotope separation efficiencies of tritium were not accounted for in this simulation. H and He isotopes produced within the burn cells during irradiation were assumed to be removed from the breeder zones in the purge gas flow.

MCAM [200] and the MCNP Visual Editor [164] were used to visualise the geometry and find cell volumes. Breeder blanket cell volumes were checked using a stochastic method as MCNP 6 is unable to calculate volumes of asymmetric cells. This involves generating a larger cell of known volume that surrounds the cell of unknown volume, particles are then randomly created inside the volume encompassed by the larger cell. The ratio of particles created in the large cell to the asymmetric cell can then be used to find the relative volume.

2.3 Theory

Tritium is produced within a fusion breeder blanket, predominantly via the $^6\text{Li}(n,t)$ reaction; the $^7\text{Li}(n,n't)$ reaction also contributes via higher energy neutrons. Another key threshold reaction is $^9\text{Be}(n,2n)$ which is utilised by breeder blankets to increase the neutron flux. As the material is transmuted, the changing composition will result in a time-varying reaction rate, which results in a time-varying neutron spectrum. The neutron spectrum also varies spatially within the tokamak.

The rate of tritium production depends upon the neutron spectrum and regions which experience significantly different spectra should be modelled separately. Modelling regions with significantly different neutron spectra collectively causes a smearing effect as material transmutations occurring predominantly at one location are averaged across the cell. The energy loss per neutron travelling through materials is closely related to both the mass of the nuclei as well as the neutron's mean free path in the material. Ideally the segmentation size would therefore be on a similar scale to the mean free path, as this would allow even small changes in neutron energies or neutron flux to be accounted for. However such accuracy is computationally expensive and increased segmentation offers diminishing returns. The accuracy of particle transport simulations suffers from inherent errors in cross section data, geometry assumptions and statistical fluctuation which would become dominant at high segmentation resolutions [44]. The majority of lithium depletion occurs at the region of the breeder blanket nearest to the plasma due to the high neutron flux. The spatial resolution of the MCNP model must be sufficiently high to account for localised burn-up within the blanket, otherwise the simulation would effectively be replenishing lithium supplies at the inner surface of the breeder blanket and would overestimate tritium production.

Figure 2.3 shows how the neutron spectra vary with blanket depth. The neutron spectrum softens with respect to radial position in the breeder blanket; this is due to interactions with nuclei such as down scattering. Higher energy neutrons are also able to cause new neutron births through multiplication reactions. The newly liberated neutrons have lower energy than the neutron which liberated them; this is due to the endothermic nature of threshold reactions. The total neutron flux decreases roughly exponentially with blanket depth due to

capture events. However, more interestingly, different energy neutrons experience different attenuation factors. The part of the spectrum that decreases the most rapidly is the 14.1 MeV component. There are no neutrons available to down scatter into this energy bin and up-scattering is exceedingly unlikely in the blankets. Figure 2.3 shows that the neutron flux at lower energies is not attenuated as severely. This is due to neutrons down scattering and populating the lower energy bins. The creation of new neutrons through $(n,2n)$ reactions in ^9Be also increases the low energy neutron population.

Lethargy is defined by Equation 2.2 where E_0 is the energy of the upper bin limit and E is the energy of the lower bin limit.

$$\text{lethargy} = \ln \left(\frac{E_0}{E} \right) \quad (2.2)$$

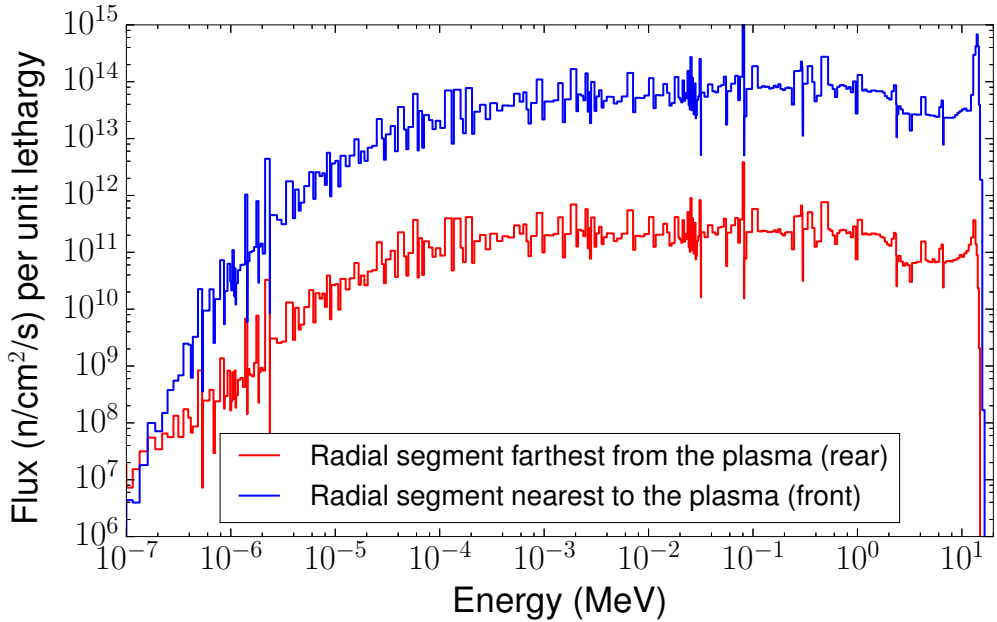


Fig. 2.3 Neutron spectra for different locations in the equatorial outboard blanket module at the first time step for a blanket with 5 radial splits.

Figure 2.4 shows both the uncollided neutron current (more commonly referred to as the neutron wall load) and the neutron flux. The blanket modules also receive different neutron fluxes (see Figure 2.4); this is largely due to the varying proximity of the breeder modules to

Time varying tritium production

the neutron source and the distribution of neutrons within the source geometry. The double peak neutron wall loading graph obtained is typical of Tokamak fusion reactor designs (see for example [143]) and neutron intensities tend to be higher on the inboard and outboard equatorial blanket modules. The neutron wall loading is a key parameter for designing reactors and is used by designers to quickly estimate the nuclear response. The graphs differ due to neutrons scattering between modules. Module 3 receives a high amount of scattered neutrons due to its prominent position within the reactor. Modules 8 and 9 receive far fewer scattered neutrons due to their withdrawn position at the top of the reactor. The moderated neutrons are more likely than unmoderated neutrons to cause ${}^6\text{Li}(n,t)$ reactions due to their lower energy (see Figure 1.10). The result of different modules receiving different fluxes is apparent in Figure 2.10 which shows slight variation in ${}^6\text{Li}$ burn-up around the inside of the reactor. The difference in neutron flux between modules reduces as neutrons move deeper into the blanket and undergo scattering interactions. The neutrons move between blanket modules and the neutron flux in the poloidal direction becomes more uniform deeper into the blanket.

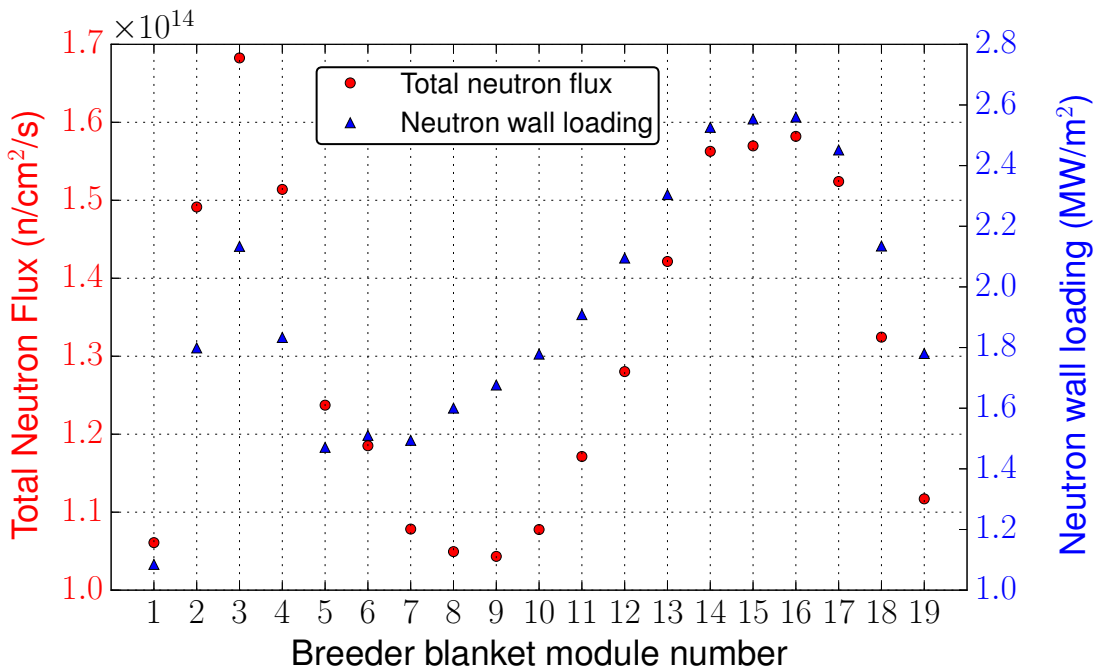


Fig. 2.4 Neutron flux incidence on the first wall of each breeder module. See Figure 2.10 for module numbers.

As materials are irradiated, transmutation and decay processes change the material composition, affecting the neutronic behaviour. The consequence of the changing material composition is a time-varying spectrum (see Figure 2.5). Nuclei with large capture cross sections are burnt-up more rapidly and therefore a slight increase in the flux at lower energies is observable over long irradiation periods. Due to the reduced capture probability of the highly burnt up regions of the blanket (e.g. the front nearest to the plasma), other parts of the blanket that were previously shielded (e.g. the rear furthest from the plasma) receive a gradually increasing flux. This increasing flux at the rear of the blanket can be sufficient to over-compensate for local ${}^6\text{Li}$ and ${}^7\text{Li}$ depletion and the TBR at the rear of breeder blankets has been shown to increase in some cases [159]. In other studies with longer irradiation times (20 years), increases in the thermal neutron flux (0.066eV at 500°C) have been observed [9].

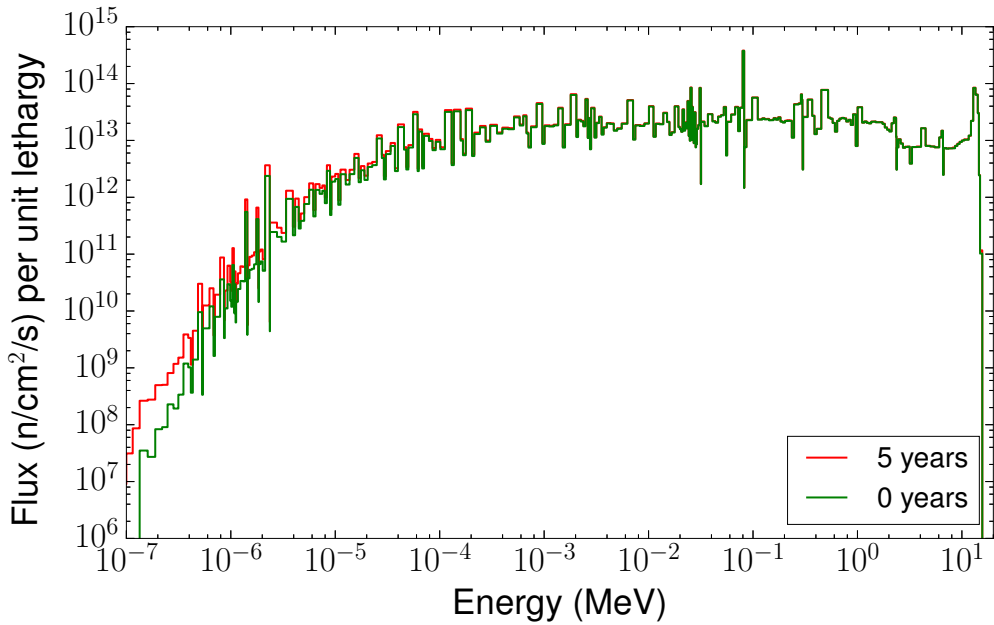


Fig. 2.5 Neutron spectra at two irradiation times for the equatorial outboard blanket module.

2.4 Results

The spatial segmentation of breeder blankets was investigated. FATI simulations were performed for the DEMO models, allowing the TBR and surplus tritium inventory as a function of radial segments to be investigated. The TBR of the system decreases as a function of time but remains above 1, as shown in Figure 2.6. The TBR of the breeder blanket with only 1 segment remained higher than the more finely segmented models for the five year irradiation time. The models with 5 or more radial segments converge to final TBR values that are within 0.005 of each other. Figure 2.7 suggests that modelling this particular breeder blanket as a single homogeneous segment overestimates the TBR at five years by 0.02.

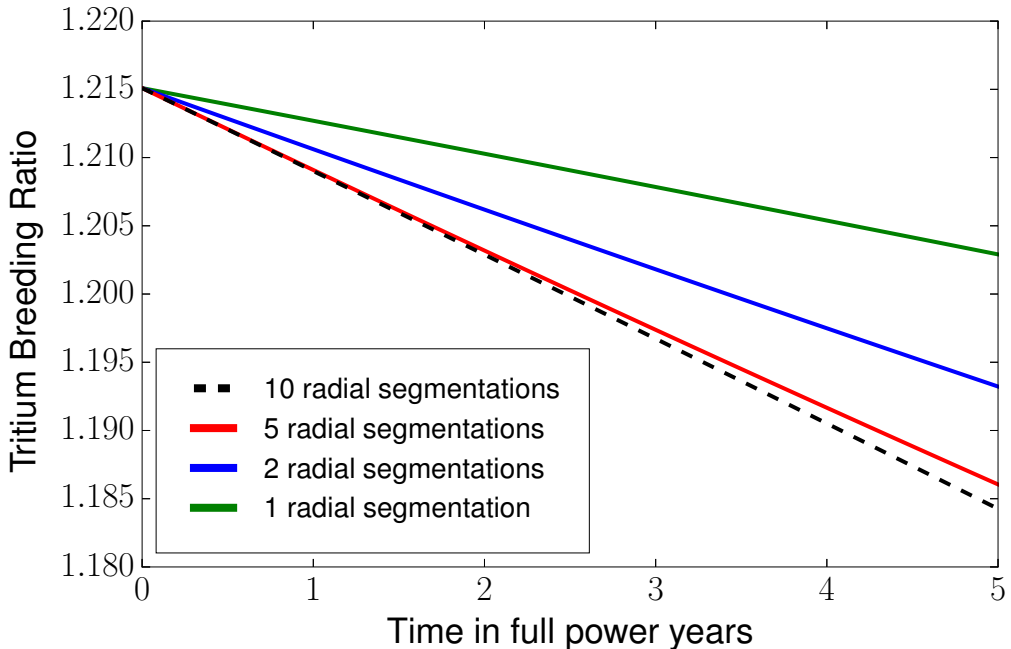


Fig. 2.6 TBR (fitted), only simulations with 1, 2, 5 and 10 segmentations are shown for clarity. Error bars are included in the plot but are too small to be visible. Errors were derived from MCNP tally uncertainties and represent a 1 sigma confidence.

The simulated surplus tritium inventory of the system increases as a function of time but approaches an apex. Surplus tritium inventory values typically approach an apex after a decade of irradiation [130]. The blankets in this simulation were assumed to be replaced after 5 years of irradiation and therefore the irradiation time is not long enough to reveal the apex of the surplus tritium inventory graph. The surplus tritium inventory will remain

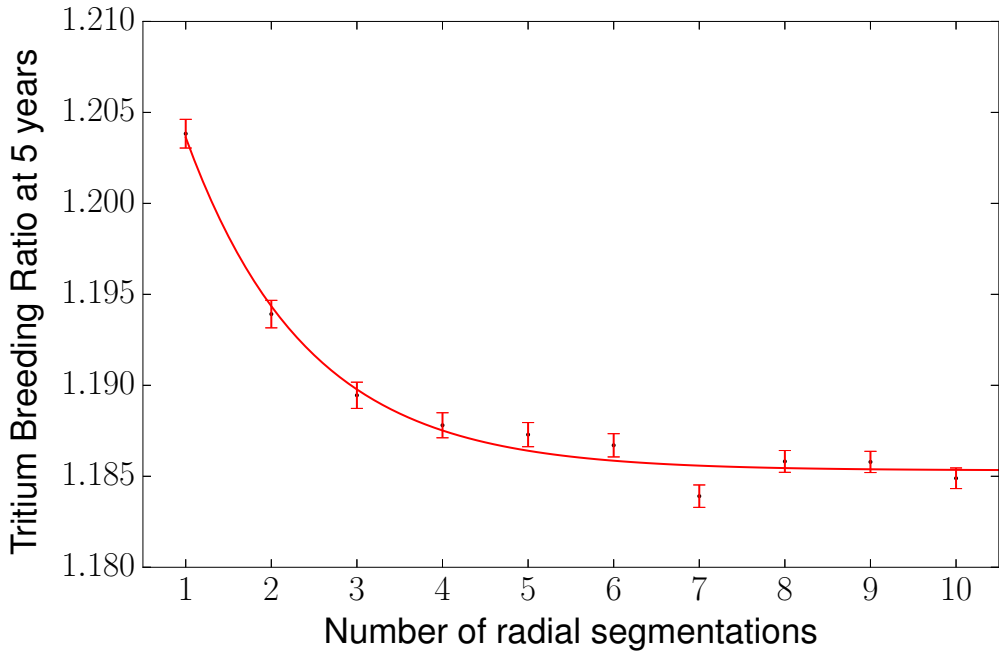


Fig. 2.7 TBR after five years for differently segmented blanket models. Error bars were derived from MCNP tally uncertainties and represent a 1 sigma confidence.

constant if the rate of tritium decay is equal to the rate of tritium production. This required combination of irradiation time or inventory size is not reached in the scenarios simulated. Figure 2.8 shows that the simulated surplus tritium inventory of the breeder blanket with only 1 segment remained higher than the more finely segmented models for the five year irradiation time. The surplus tritium inventory for models with 5 or more radial segments results in approximately the same value. Figure 2.9 suggests that modelling this particular breeder blanket as a single homogeneous segment overestimates the surplus tritium inventory at five years by 4kg (approximately 5% of the tritium).

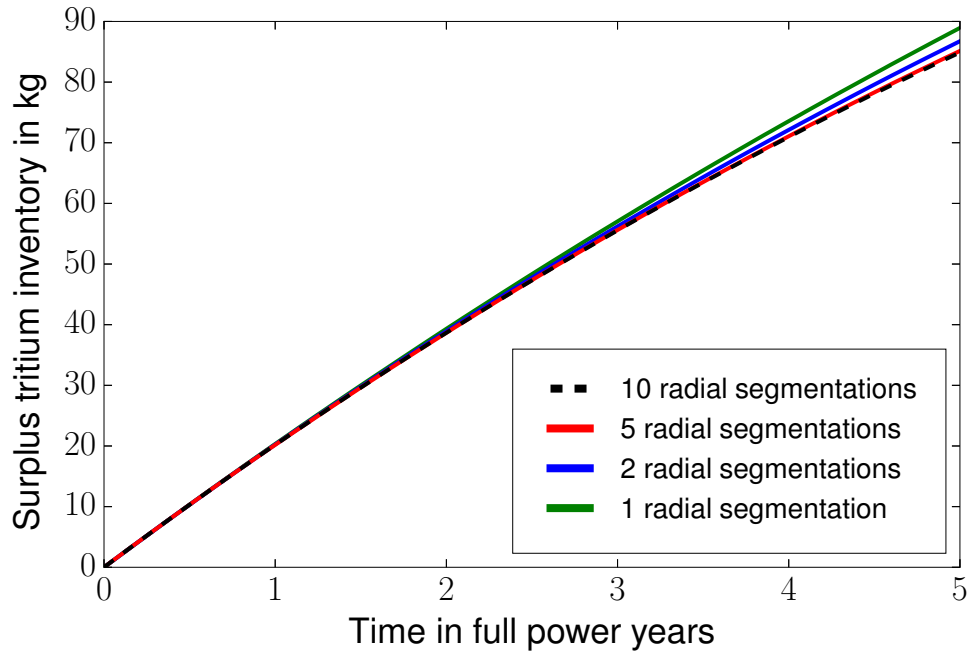


Fig. 2.8 Surplus tritium inventory, only simulations with 1, 2, 5 and 10 segmentations are shown for clarity. Error bars were derived from MCNP tally uncertainties and represent a 1 sigma confidence.

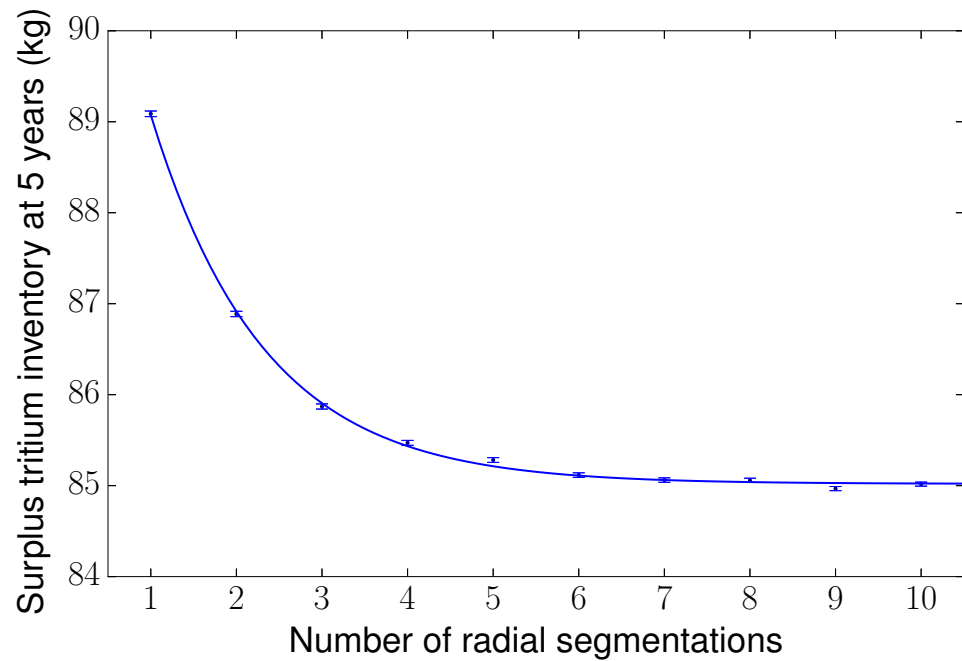


Fig. 2.9 Surplus tritium inventory after five years for differently segmented blanket models. Error bars were derived from MCNP tally uncertainties and represent a 1 sigma confidence.

${}^6\text{Li}$ burn-up is not uniform throughout the blanket, due to the different spectra experienced at different locations. Figure 2.10 shows the percentage of the original ${}^6\text{Li}$ remaining after 5 years. The ${}^6\text{Li}$ depletion is highest (81% remaining) at the inner segment of blanket module 3. Whereas the ${}^6\text{Li}$ burn-up in the outer segment of blanket module 19 is negligible (99.9% remaining). The modules are divided into segments with equal percentages of the overall module thickness. This results in outboard modules having thicker cells than the inboard modules. The ${}^6\text{Li}$ depletion shown in Figure 2.10 therefore compares cells of different thicknesses. The fraction of original ${}^6\text{Li}$ remaining is averaged over the entire cell but would typically be lower at the front of the blanket nearest to the plasma.

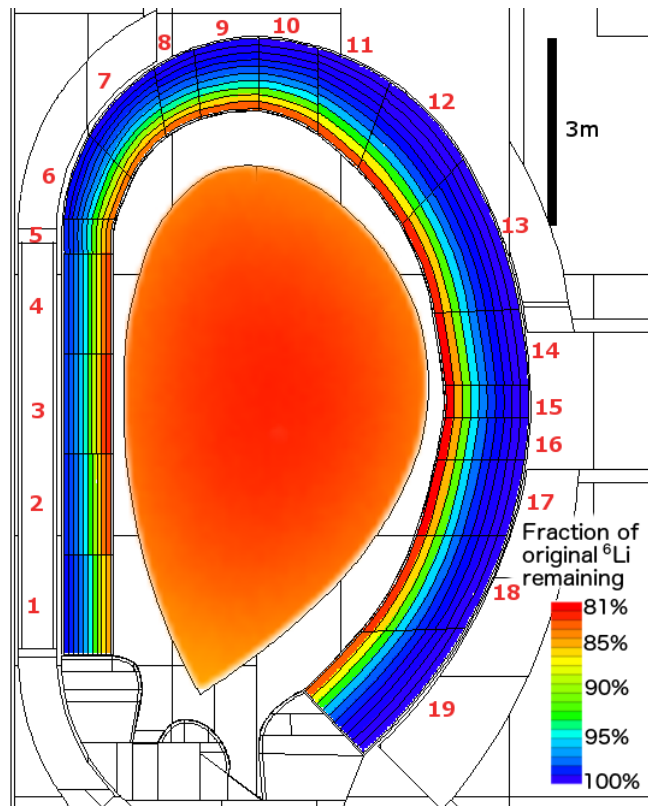


Fig. 2.10 ${}^6\text{Li}$ depletion throughout the breeder blanket after 5 years and neutron source intensity.
The breeder blanket modules numbered to aid the understanding of Figure 2.4.

2.5 Conclusion

TBR simulations have been carried out for breeder blankets with toroidal and radial segmentation. The simulations show that TBR declines more rapidly due to burn-up of lithium when blanket modules are radially segmented in the model. The increased geometrical complexity and computational time for segmenting the model beyond 5 segments only fractionally increased the accuracy of the TBR and surplus tritium inventory prediction. These results imply that some previous studies of tritium inventories in homogenised breeder blanket models may have overestimated tritium production over time due to lack of radial segmentation [27, 143].

Although 5 radial segmentations appears to be sufficient for this particular model, heterogeneous breeder blanket models are likely to require finer segmentation. This is because the lithium ceramic regions are often separated by structural materials or cooling components and the spectrum is likely to be different on either side of these components. This will be more noticeable with highly moderating materials such as water, which is a candidate coolant in several blanket designs.

The life-time of breeder blankets was assumed to be 5 full power years and this is in line with current estimates. It is currently determined by radiation damage in the ceramic breeder, beryllium and helium production in the steel [150]. However if material improvements are made then this life time could be increased. As Figure 2.6 shows the predicted TBR value for 5 and 10 segmentations are gradually diverging with respect to time. Therefore it would be necessary to increase the simulated spatial resolution if longer life time blankets become a possibility.

By performing these simulations it is clear that ${}^6\text{Li}$ burn-up varies throughout the blanket and some regions are under-utilised while other areas experience high ${}^6\text{Li}$ burn-up (see Figure 2.10). Locating regions of low ${}^6\text{Li}$ burn-up is of interest due to their increased recycling value when compared to regions with high ${}^6\text{Li}$ burn-up. Tailoring the blanket composition to suit the incident neutron spectra could improve the durability of the blanket while potentially reducing the material cost. This could be achieved by varying the ratio of neutron multiplier to lithium ceramic or the ${}^6\text{Li}$ enrichment.

From this research the following conclusions are made.

- A fine spatial resolution has been shown to be necessary for accurate predictions of the surplus tritium inventory when simulating time-dependent TBR in homogenised solid-type breeder blankets.
- Five radial segmentations were found to be sufficient when ${}^6\text{Li}$ burn-up is not more than 20% for this particular combination of neutron source strength, geometry, materials and time frame.
- Segmentation of the blanket cells allows the simulation to take account of the variation of neutron spectrum throughout the blanket.

Segmentation should be based on the gradient of neutron spectrum folded with the cross section of important reactions. The approach taken in this research has effectively found the appropriate level of segmentation by trying increasingly small divisions.

While cell based division is able to provide the required spatial resolution for this model, it may be less suitable for heterogeneous breeder blankets. The shape of regions experiencing similar spectra is likely to be more complex for detailed breeder blanket designs. A mesh-based approach to burn-up could be advantageous to facilitate more optimal geometric divisions.

Chapter 3

Breeder blanket parameter study

3.1 Introduction

The objective of this chapter is to report on a new neutronics module which links high fidelity neutronics parameters into the PROCESS code. Additionally this chapter makes recommendations for blanket design in terms of how the material composition of the blanket affects the tritium production.

Tritium production is of critical importance to prospective DT fusion power plants. Lithium ceramic and beryllium based solid-type breeder blankets are an option for supplying the tritium required to sustain the DT plasma. By changing the composition of breeder blankets, the tritium production can be varied significantly.

Previous neutronics parameter studies of blankets have focused on finding the minimal lithium enrichment required to achieve sufficient tritium production. This is typically performed by adjusting the blanket thickness or ${}^6\text{Li}$ level and simulating the resulting TBR (see e.g. [166]). Previous studies have also considered varying the breeder fraction (see e.g. [172]) to optimise the TBR. No parameter studies have been found that also include nuclide depletion. Accounting for nuclide depletion will have the general result of decreasing the TBR (as a function of time) of the breeder blanket, but some compositions will be affected more than others.

This chapter investigates the time-varying tritium production in solid-type breeder blan-

kets with different compositions. The ratio of Li_4SiO_4 to Be_{12}Ti was varied in conjunction with the ${}^6\text{Li}$ enrichment. The parameter study considered 198 different blanket compositions for three different blanket thicknesses. The cheapest configurations capable of meeting the tritium requirements were found. The cost of Li_4SiO_4 (including ${}^6\text{Li}$ enrichment) and Be_{12}Ti were considered. The time-varying tritium production of each blanket configuration was simulated using the interface code FATI that couples the radiation transport code MCNP 6 with the inventory code FISPACT-II. The blankets were segmented into five radial sections to comply with the suggestions made in Chapter 2.

For a breeder blanket with inboard and outboard blanket thicknesses of 0.75m and 1.3m respectively, the most economical composition based on the assumptions made and capable of tritium self-sufficiency, was a breeder fraction of 0.73 with a ${}^6\text{Li}$ enrichment of 18.9%. Economical blanket configurations capable of producing excess tritium for start-up inventories were also found. Fitting functions to predict the time-averaged tritium breeding ratio and the tritium inventory at five years were obtained for inclusion in the PROCESS systems code [105]. PROCESS is now able to consider different breeding blanket compositions and thicknesses when assessing the engineering, physics and economic feasibility of reactor designs.

Systems codes are designed to assess the engineering, physics and economic viability of future fusion reactors. Systems codes are often designed to run quickly through several iterations to find optimal solutions. This can be achieved by accessing preprocessed results and fitted functions from more computationally intense simulations. Several systems codes exist with differing approaches and objectives. PROCESS [105] is a systems code under development at CCFE with a particular focus on minimising a user chosen figure-of-merit (e.g. the cost of electricity). The PROCESS code has been utilised effectively in the Power Plant Conceptual Study [120] and in economic studies into the feasibility of fusion energy [30].

This chapter reports on a new neutronics module which links high fidelity neutronics parameters into the PROCESS code. Standard neutronics tools for fusion require enhancement via scripting and linking to an inventory code to allow for nuclei burn-up and transmutation

when predicting tritium production. The aim of this parameter study was to provide PROCESS with the time-averaged Tritium Breeding Ratio (TBR), the tritium inventory after 5 years of operation and material costs. Three different blanket thicknesses were considered. For each thickness different lithium enrichments and different breeder fractions were considered (see Equation 3.1). The lithium ceramic used was Li_4SiO_4 and the neutron multiplier used was Be_{12}Ti .

Fitted empirical functions allow PROCESS access to this data without having to perform the full neutronics simulations. Users will now be able to find the most economical blanket composition capable of tritium self-sufficiency or capable of providing a tritium surplus that could be used for subsequent reactors. The rate of fusion reactor deployment will be limited by the availability of tritium [68]; there are very limited worldwide reserves of this material. However, careful design and planning of tritium production will help to alleviate this risk. The ability to minimise the cost of breeder blankets, while still achieving the required target tritium production, is of particular importance, as currently the blankets are expected to be replaced several times during the reactor's lifetime and will form a large part of the capital cost.

3.2 Materials and methods

3.2.1 MCNP model

The reactor model used in this study was adapted from a European tokamak DEMO model [148] developed within the Power Plant Physics and Technology (PPPT) programme [52]. The model contains no blanket penetrations for heating or diagnostics and therefore overestimates global TBR as compared to a more detailed model incorporating such penetrations. Recent research [207] has suggested that each additional penetration results in a TBR reduction of 0.35% to 0.5% depending on the penetration size and the material present within the penetration. The neutron plasma source [51] utilised in the MCNP model was represented using primary plasma parameters. The model includes a first wall with a thin layer of armour, homogenised breeder modules, a rear shielding layer and a divertor with no breeding capability. Tungsten (3mm thick) was chosen for the first wall armour and Eurofer with helium coolant (3cm thick) was chosen for the first wall [83]. The breeder blanket was split radially into 5 layers and poloidally into 19 modules. The radial segmentation of the breeder zones was based on findings discussed in Chapter 2 and published [171] which shows radial segmentation to be necessary when simulating nuclide depletion.

3.2.2 Materials

The homogenised breeder blanket material used was based on the HCPB design and contained fixed volumes of Eurofer [115] (9.705%) and He coolant (5.295%). The homogenised volume fractions used are similar to previous studies [25]. The packing fraction of the Be_{12}Ti and Li_4SiO_4 pebbles was assumed to be 0.63 [69] which occupies 53.55% of the available volume. Helium purge gas was used to fill the remaining voids between pebbles (31.45%). The volume fractions of the Eurofer and helium were kept constant in all simulations. The assumption that volume fractions remain constant in different thicknesses of blankets may be oversimplifying the situation. It may be more realistic to increase the Eurofer and helium fraction with respect to blanket thickness. The breeder fraction (see Equation 3.1) was varied between 0 and 1 in 18 intervals and the ${}^6\text{Li}$ atomic fraction in the lithium

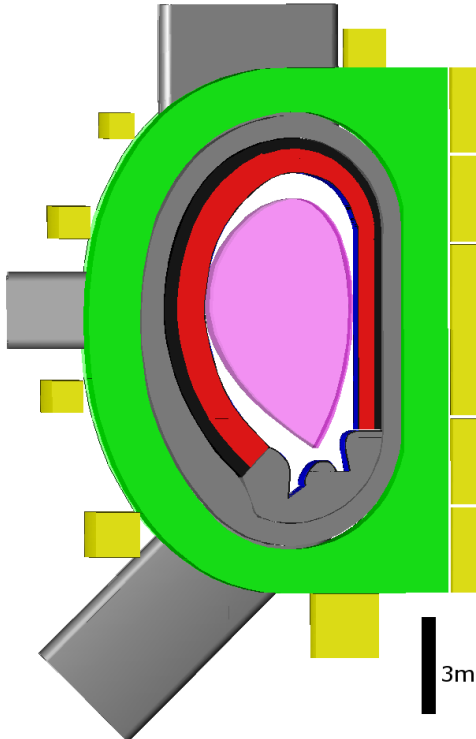


Fig. 3.1 The thin blanket tokamak model used. This model was adapted from a tokamak DEMO model developed within the PPPT programme [148]. The vacuum vessel and divertor (grey) ■, toroidal field coils (green) □, poloidal field coils (yellow) ▨, blanket (red) ▢, blanket casing (black) ▣, and tungsten armour (blue) ▤, are included. Image generated using [200].

was varied from 0 to 1 in 11 intervals. The breeder fraction is defined as:

$$\text{Breeder fraction} = \frac{\text{Volume of Li}_4\text{SiO}_4}{\text{Volume of Be}_{12}\text{Ti} + \text{Volume of Li}_4\text{SiO}_4} \quad (3.1)$$

This resulted in 198 different breeder blanket compositions for each of the 3 blanket thickness scenarios (see Table 3.1). In models with thin and medium blanket scenarios, the empty space left was filled with homogenised shielding material in the form of Eurofer (64.7% volume) and He coolant (35.3% volume).

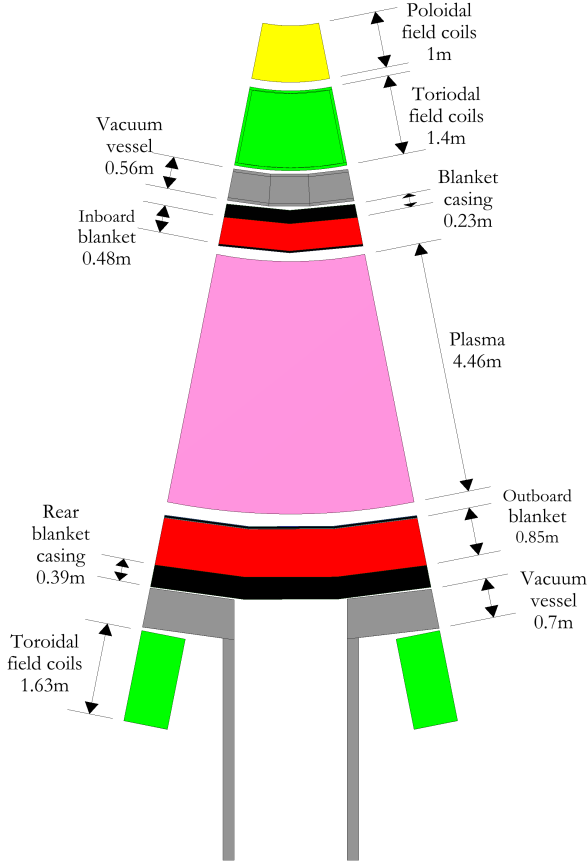


Fig. 3.2 Radial build of the thin blanket at equatorial level. This model was adapted from a tokamak DEMO model developed within the PPPT programme [148].

Blanket description	Maximum inboard blanket depth (m)	Maximum outboard blanket depth (m)	Volume (m^3)
thin	0.53	0.91	891.92
medium	0.64	1.11	1104.06
thick	0.75	1.30	1322.72

Table 3.1 The dimensions and volumes of the three different breeder blanket scenarios simulated.

3.2.3 Calculation method

To calculate the time-averaged TBR and final tritium inventories a Monte Carlo approach was used for each blanket composition. The interface code FATI [131] was used to couple the radiation transport code MCNP 6.0 [74] with the inventory code FISPACT-II [179]. FENDL 3.0 nuclear data [61] was used preferentially for particle transport and TENDL 2014 data [104] was used when FENDL data was not available for particular isotopes. TENDL

3.2 Materials and methods

data in 315 energy group format was also used for isotope burn-up calculations performed by FISPACT-II.

Burn-up was simulated in time steps of 15 days [130] for a fusion reactor with 2.4 GW of fusion power, operating at 70% [185] availability for 5 years. This resulted in 122 MCNP simulations for each blanket composition. The TBR for each module was found at each time step with MCNP F4 tallies combined with appropriate tally multipliers (reaction number 205 for tritium production). MCNP F4 tally obtains the average particle flux in the requested cell for the simulated particle (neutron in this case), further details can be found in the MCNP manual [201]. The final tritium inventory was taken as the difference between the cumulative tritium production and consumption while accounting for radioactive tritium decay. Tritium retention, leakage and isotope separation efficiencies were not accounted for. Tritium losses in the cycle were therefore dominated by tritium decay. Gases (H and He) produced through transmutations within the burn cells in the blanket during irradiation were assumed to be removed from the breeder zones in the purge gas flow.

3.2.4 Cost estimates

In order to compare breeder blanket configurations in terms of their costs it was necessary to make assumptions to quantify the cost of the variable components in each breeder blanket configuration. Other costs involved such as the cost of Eurofer, He coolant and manufacturing costs were assumed to be constant for all blanket compositions and therefore were not taken into account as a variable cost. The costs associated with shielding were also not included in this study. The shielding costs are likely to vary depending upon the blanket thickness. For instance, thicker blankets would offer increased attenuation of neutrons and photons but allow less space for shielding behind the blankets. The overall shielding effect of the different thickness blankets and corresponding shielding requirements is not investigated in this study but could be a major cost in a real reactor design. The cost of Be₁₂Ti was estimated to be \$4,500 per kg [38], the cost of Li₄SiO₄ (with natural Li) was estimated to be \$1000 per kg [100] and the cost of ⁶Li enrichment from [45] was used. The cost estimates used for Be₁₂Ti and Li₄SiO₄ were provided by experts in their respective fields (see [38] and [100]) and assume a cost reduction when compared to the current price for making small quantities for research purposes. Pure ⁹Be was estimated to be significantly cheaper than Be₁₂Ti at \$2000 per kg, however this was not considered as a suitable material for use in DEMO due to swelling under irradiation and tritium retention [93].

The costs of the different blanket compositions (see Figure 3.3) are best estimates of materials bought in bulk where no significant market currently exists. The inherent uncertainty in predicting the price of future commodities means these results should be updated when better price estimates are available. The recycling value of the breeder blankets was also not considered in this preliminary study; this may be substantial due to the large quantities of beryllium and enriched lithium present in the blanket at the end of life. The separation and sale of decay products (e.g. ³He from ³H decay has potential uses in neutron detectors) were also not taken into account.

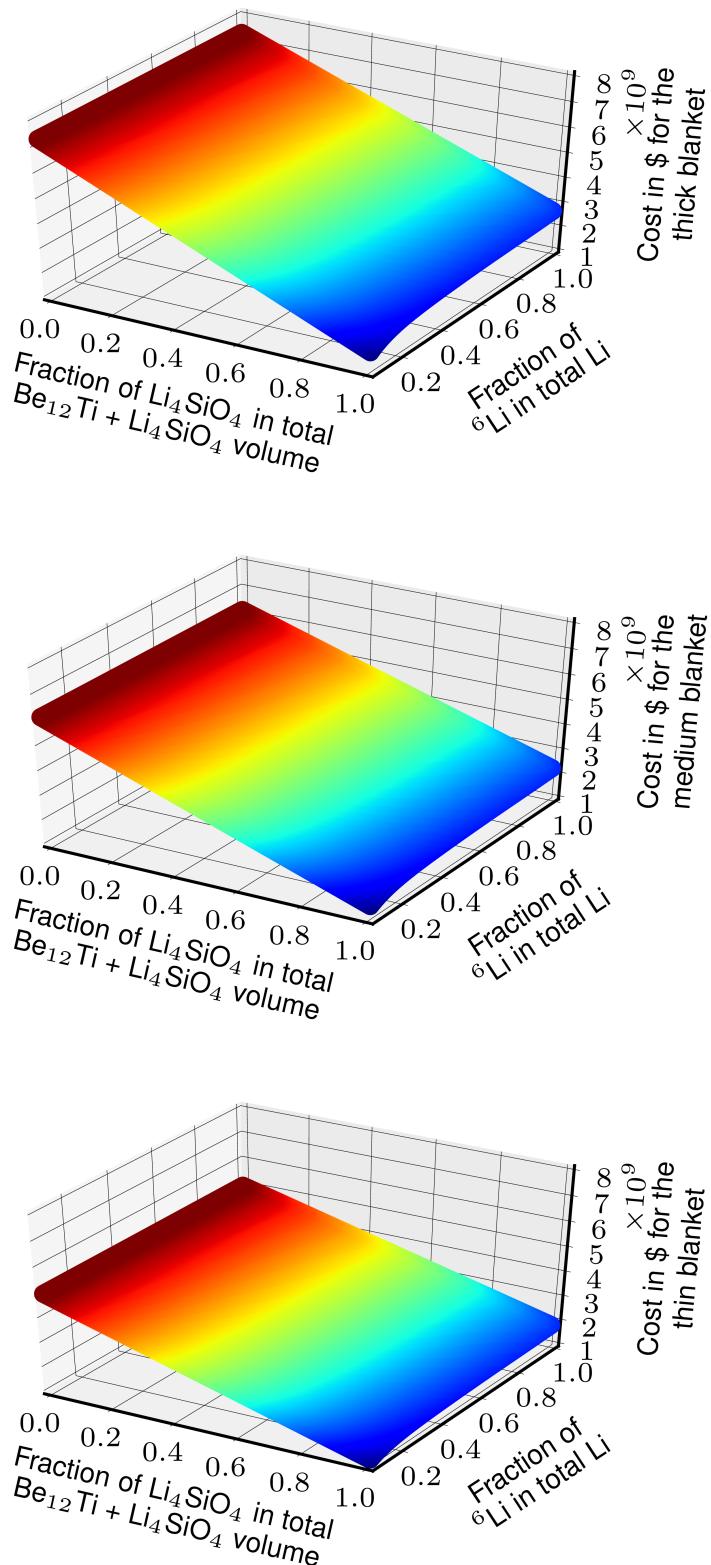


Fig. 3.3 The combined costs of Be₁₂Ti, Li₄SiO₄ and ⁶Li enrichment for different blanket compositions.

3.3 Theory

The breeder blanket composition affects tritium production, neutron multiplication, shielding, energy multiplication and activation. These different quantities are related, therefore changing the composition with the aim of increasing one aspect may negatively affect others. An optimal composition would take into account the relative importance of each neutronics quantity. While early fusion reactors might be more focused on producing excess tritium, later designs could be more interested in energy amplification to maximise electricity production. This chapter assumes excess tritium production is of primary importance and aims to optimise solid-type blanket compositions accordingly.

Tritium is produced predominantly via the ${}^6\text{Li}(n,t){}^4\text{He}$ reaction but it is also produced via the ${}^7\text{Li}(n,n't){}^4\text{He}$ threshold reaction. A small amount is produced via interactions in other nuclei (e.g. ${}^9\text{Be}(n,t){}^7\text{Li}$). Increasing the tritium production can be achieved by:

1. Increasing the number density of tritium producing isotopes.
2. Increasing the neutron population in the blanket region through neutron multiplication.
3. Decreasing the amount of parasitic neutron absorption.
4. Modifying the neutron spectra through scattering interactions, so that tritium producing reactions or neutron multiplication become more likely, or so that parasitic capture becomes less likely.

Enriching the lithium ceramic so that it has a higher ${}^6\text{Li}$ content increases the tritium production due to the large ${}^6\text{Li}$ thermal cross section. Increasing tritium production solely by ${}^6\text{Li}$ enrichment results in diminishing returns as higher enrichment values are reached. The corresponding reduction of ${}^7\text{Li}$ results in less ${}^7\text{Li}(n,nt){}^4\text{He}$ reactions and consequently a reduced neutron flux. The neutron flux is also diminished due to a reduction in neutron multiplying reactions in ${}^9\text{Be}$. The reduced neutron flux can be compensated by increasing the volume of neutron multiplier material. However, the volume not required for structural, cooling or gas extraction purposes is taken up by a combination of lithium ceramic and neutron multiplier. Therefore increasing the volume of neutron multiplier reduces the amount

of lithium ceramic and the amount of ^6Li and ^7Li .

Compositions containing large volumes of lithium ceramic at the expense of neutron multipliers show low levels of tritium production due to low neutron multiplication. These blanket compositions are located on the far right hand side of Figure 3.4. The opposite extreme is also possible, as compositions with an excessive neutron multiplier volume also produce low amounts of tritium due to the low number of Li atoms available for tritium production; these blanket compositions are located on the far left hand side of Figure 3.4. Compositions containing low levels of ^6Li enrichment were also not able to produce large quantities of tritium; these blanket compositions are located at the bottom of Figure 3.4. Finding the optimal ratio of neutron multiplier depends upon the relative benefit of increasing the neutron flux compared to increasing the lithium content and therefore different levels of ^6Li enrichment have different optimal neutron multiplier volumes. The ratio of lithium to beryllium also varies slightly with time, as ^6Li burns up more rapidly than ^9Be . For this reason it is important to take isotopic depletion into account when choosing a blanket composition to operate for sustained time periods. The task of predicting the time-varying tritium production while accounting for nuclei burn-up is well suited to a Monte Carlo approach that accounts for these neutronic effects.

3.4 Results

The TBR at each time step was found as a result of simulations, the average (mean) of these values was then calculated to produce a time averaged TBR value. The TBR was found to decrease slowly during the five year lifetime of the blanket, therefore a time averaged TBR value was used as a representative value of the changing TBR of the blanket. Achieving a TBR of at least 1.1 is deemed essential for DT fusion to become a commercial reality [44]. It was possible to achieve sufficiently high TBR values with all blanket thicknesses. However, as this simplified blanket does not contain all the necessary components of a blanket (such as a manifold and blanket attachments), a target TBR of 1.15 is suggested. The target TBR of 1.15 is identified on Figure 3.4. The number of compositions able to achieve a time averaged TBR of at least 1.15 was found to increase with blanket thickness.

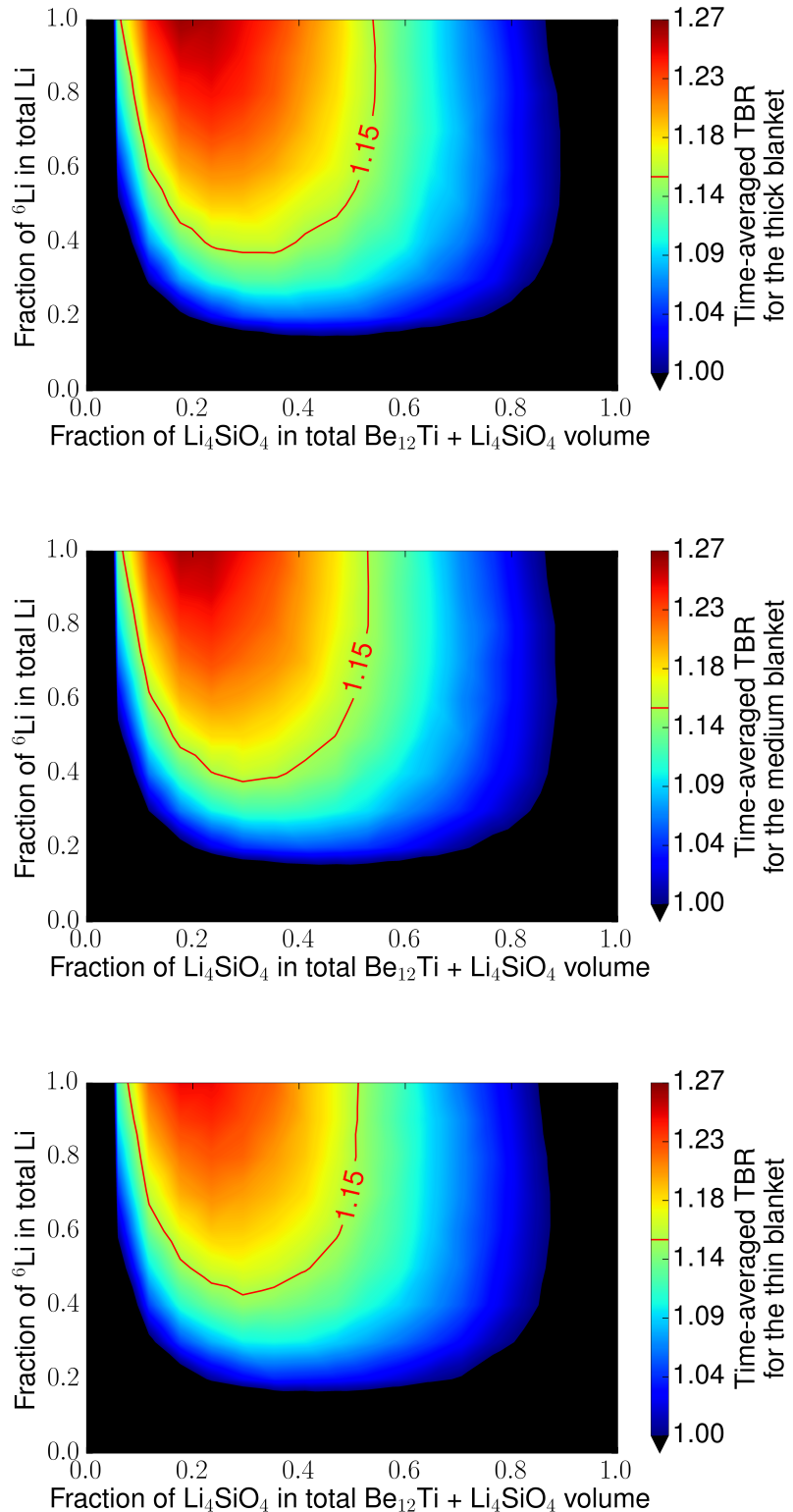


Fig. 3.4 The time-averaged TBR values for thick, medium and thin blanket thicknesses and different blanket compositions. A TBR of 1.15 is identified by the red contour line.

Tritium self-sufficiency was found to be achievable with numerous blanket configurations for all blanket thicknesses (see area within red self-sufficiency line on Figure 3.5). However, only blankets with high ${}^6\text{Li}$ enrichment levels and beryllium are capable of generating a useful excess of tritium, to allow for tritium losses and to fuel subsequent reactors. Figure 3.5 reveals that at low ${}^6\text{Li}$ enrichments the tritium production is less sensitive to breeder fraction compared to higher ${}^6\text{Li}$ enrichments when the tritium production is more sensitive to breeder fraction. When considering compositions with high ${}^6\text{Li}$ enrichment it is therefore particularly important to optimise the breeder fraction as this can make a significant difference to the tritium production. The shape of Figure 3.5 is similar to Figure 3.4 which shows time averaged TBR and this is largely because these results are derived from TBR values. The subtle differences in the surface shape of Figure 3.4 and 3.5 are mainly caused by tritium decay. Larger tritium inventories lose more tritium due to decay when compared to losses from small tritium inventories. At every level of ${}^6\text{Li}$ enrichment there is one optimal breeder fraction that maximises the tritium inventory. The optimal breeder fraction decreases as ${}^6\text{Li}$ increases. Decreasing the amount of lithium as the ${}^6\text{Li}$ increases allows sufficient neutron multiplication to occur. The three blanket thicknesses show only marginal differences in terms of their 5 year tritium inventory values. The thickest blanket produces the most tritium, followed by the medium blanket and then the thinnest blanket.

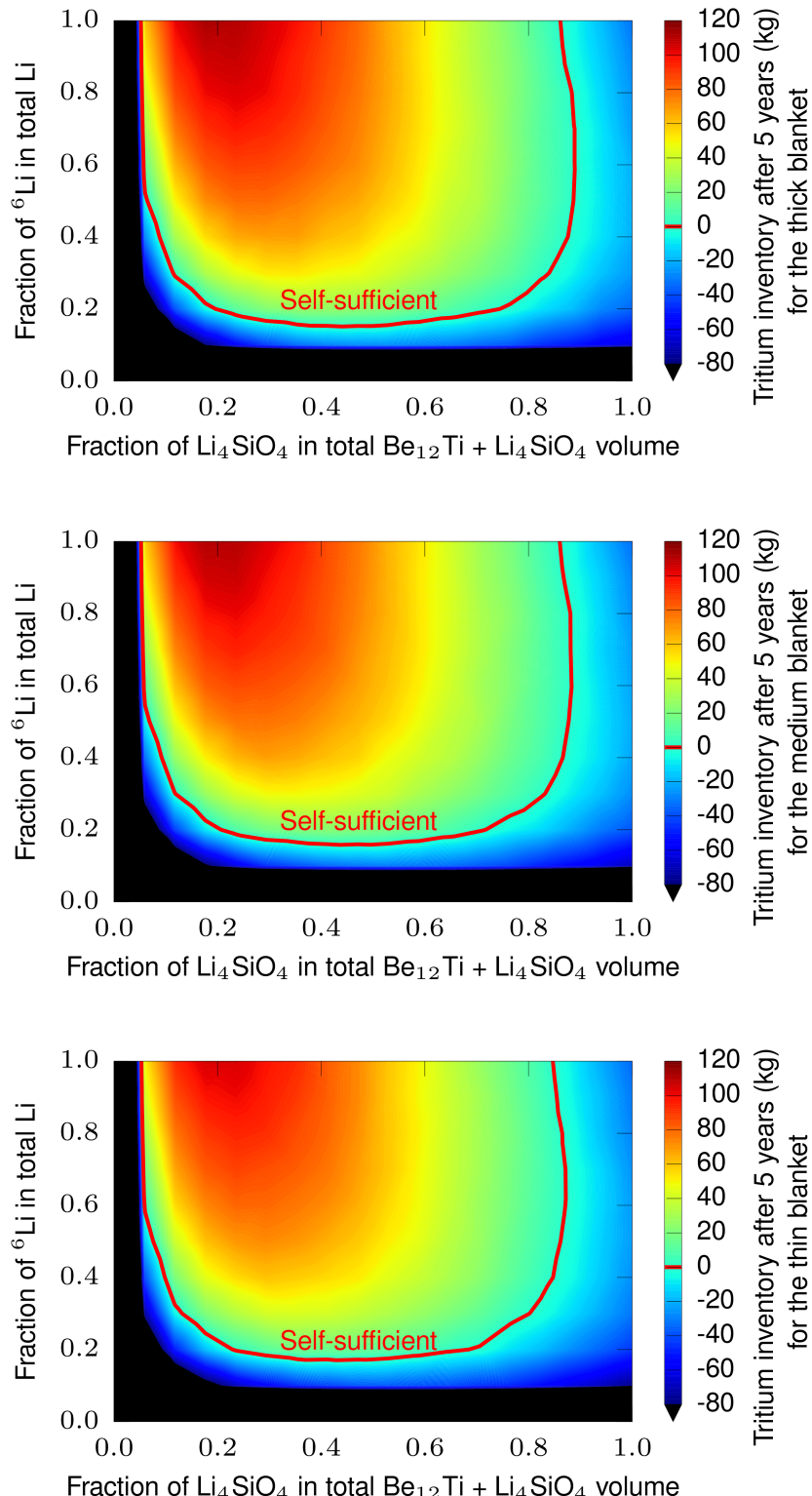


Fig. 3.5 The tritium inventory at five years for thick, medium and thin blanket thicknesses, with self-sufficient blanket compositions identified by the red contour line.

Time-averaged TBR and tritium inventory at 5 years were fitted by the same surface function (Equation 3.2). This allows both the TBR and tritium inventory at 5 years to be calculated for datapoints that were not simulated and optimisations to be carried out. The required output (either TBR or T inventory in kg) can be found by knowing the breeder fraction (x) where $0 < x \leq 1$, the fraction of ${}^6\text{Li}$ in total Li (y) where $0 < y \leq 1$, blanket thickness and the values of the 19 coefficients found in Tables 3.2 and 3.3. Tables 3.2 and 3.3 also include the average absolute difference between the simulated values and the fit. Coefficients for Equation 3.2 were obtained with a Python script that minimised the average difference between the simulated datapoints and the value of the fitting surface. For each of the blanket compositions simulated the difference between the simulated data and the value of the fit was found. The sum of these difference was then divided by the number of blanket compositions simulated to find the average difference. The averaged difference was minimised by the Python script without taking into account any error associated with individual datapoints; applying different weights to datapoints was also not considered. The Python script was programmed to accept different base equations. The script would then vary the values of the coefficients and optimise the fit. Several equations were fitted to the data prior to obtaining Equation 3.2. To start with several simple equations were investigated to see if they were able to roughly fit the datapoints. The first successful simple equation was $v_{18}\ln(x) + v_{19}\ln(y)$ as this equation was able to match the general shape of the simulated datapoints. Additional terms of increasing order were then added until the total number of terms reached 19; at this point additional terms no longer improved the fit.

Time average TBR or tritium inventory at 5 years =

$$\begin{aligned}
 & v_1 + v_2x + v_3y + v_4yx + v_5x^2 + v_6y^2 + v_7x^2y + v_8xy^2 + v_9x^2y^2 + v_{10}x^3 + v_{11}y^3 \\
 & + v_{12}yx^3 + v_{13}y^2x^3 + v_{14}xy^3 + v_{15}y^3x^2 + v_{16}y^3x^3 + v_{17}\ln(x) + v_{18}\ln(y) + v_{19}\ln(x)\ln(y)
 \end{aligned} \tag{3.2}$$

Coefficients	Tritium inventory after 5 years (kg)		
	Thick blanket	Medium blanket	Thin blanket
v ₁	484.511177687	489.818993739	486.789982299
v ₂	-415.892411688	-449.598253547	-498.345381625
v ₃	-98.391561281	-110.92454506	-145.93154029
v ₄	-255.859137886	-12.5050481028	159.811316367
v ₅	206.691260671	313.326084789	387.491648561
v ₆	30.9217399105	79.7823355573	101.954704874
v ₇	-360.734499132	-1051.11973928	-1196.56045034
v ₈	-134.851142496	-689.287533213	-767.97906346
v ₉	1133.48706945	2463.72332805	2423.27863764
v ₁₀	-96.0379800351	-169.028942532	-210.471309775
v ₁₁	-4.85999133468	-32.5360882734	-37.5882110014
v ₁₂	317.963200146	770.809305134	830.76354683
v ₁₃	-728.498952417	-1553.57818486	-1515.66927261
v ₁₄	132.262987525	428.301200541	441.537208381
v ₁₅	-618.192609936	-1306.04759015	-1267.67821617
v ₁₆	375.391947818	796.535412927	774.403281724
v ₁₇	110.780642107	115.6823286	111.94666004
v ₁₈	90.4340751694	94.8575663787	92.0566956802
v ₁₉	-20.1998328509	-17.425745771	-20.0367798637
Avg. diff.	0.694216163978	0.654043202356	0.704258216618

Table 3.2 Coefficients for use with Equation 3.2 to calculate tritium inventory after five years.

Coefficients	Time-averaged TBR		
	Thick blanket	Medium blanket	Thin blanket
v ₁	1.95893103797	1.96122608615	1.93920586301
v ₂	-0.809792727863	-0.860855681012	-0.948494854004
v ₃	0.016958778333	0.0193393390622	-0.0186700302911
v ₄	-0.120230857418	0.279977226537	0.483417432982
v ₅	0.461211316443	0.659918133027	0.785901227724
v ₆	-0.0478789050674	0.013070435947	-0.0120169189644
v ₇	-2.1978304461	-3.48450356973	-3.45723121388
v ₈	-1.38785787744	-2.3360647329	-2.05212472576
v ₉	4.93883798388	7.38314099334	6.45375263346
v ₁₀	-0.223668963335	-0.365511595682	-0.436421277881
v ₁₁	0.0178181886132	-0.0181287662329	0.0129809166177
v ₁₂	1.42583418972	2.30397890094	2.26116309299
v ₁₃	-2.80720698559	-4.37481611533	-3.87538808736
v ₁₄	0.814691647096	1.30804004777	1.05778783291
v ₁₅	-2.48568193656	-3.71450110227	-3.12644013943
v ₁₆	1.37932384899	2.1588023402	1.86242247177
v ₁₇	0.253355839249	0.263823845354	0.253324925437
v ₁₈	0.190845918447	0.198976219881	0.18795823903
v ₁₉	-0.0257699008284	-0.0192924115968	-0.0256707269253
Avg. diff.	0.00177414115123	0.00164963551716	0.00151024828175

Table 3.3 Coefficients for use with Equation 3.2 to calculate time-averaged TBR.

The maximum tritium production varied with blanket thickness and the thicker blankets were found to generate only marginally more tritium (see Table 3.4). The maximum tritium production assumed a lithium enrichment of 100% which is not practically feasible. The minimum level of ${}^6\text{Li}$ enrichment required to achieve self-sufficiency varied slightly with blanket thickness and thicker blankets were found to require marginally less ${}^6\text{Li}$ enrichment (see Table 3.4).

Blanket thickness	Maximum tritium surplus (kg)	Maximum TBR	Minimum ${}^6\text{Li}$ enrichment required for self-sufficiency
Thin	106.0	1.240	21.2
Medium	111.5	1.252	19.5
Thick	113.8	1.269	18.9

Table 3.4 The relative performance of the different blanket thicknesses.

Figure 3.6 shows how the optimal breeder to multiplier ratio required to achieve maximum tritium production varies with lithium enrichment. During the life of the breeder blanket ${}^6\text{Li}$ is burnt-up more rapidly than ${}^9\text{Be}$, this means the final breeder fraction ratio will be lower than the initial ratio. By modelling the blanket burn-up, it is possible to compensate for this and find the optimal breeder to multiplier ratio taking into consideration uneven burn-up. Figure 3.6 shows the compositions that maximise tritium production while minimising the amount of required lithium enrichment. Figure 3.6 also reveals that blanket thickness makes negligible difference to the optimal breeder fraction at different enrichment levels.

It is possible to achieve the same final tritium inventory with a variety of different compositions. It may be more desirable to select solutions that minimise other factors instead of minimising the lithium enrichment. For example, each blanket composition has different associated costs (see Figure 3.3). Inevitably from the competing blanket compositions some will offer a lower cost per kg of tritium. Figure 3.7 uses cost values from Figure 3.3 and tritium inventory values from Figure 3.5 to show the most economical blanket composition capable of producing certain amounts of surplus tritium. The quantities of surplus tritium

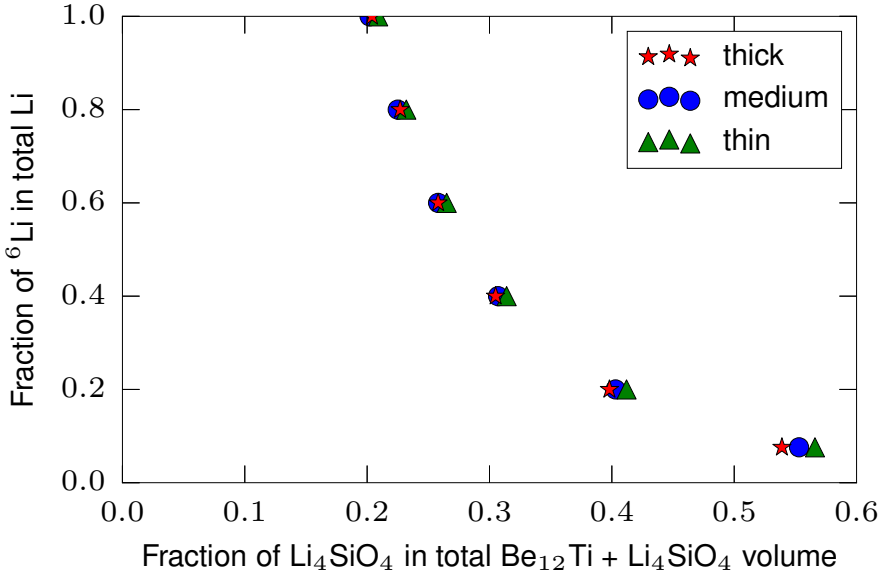


Fig. 3.6 Optimal ratio of breeder to multiplier in terms of maximising the TBR as a function of ${}^6\text{Li}$ enrichment.

considered are multiples of the tritium start-up inventory required (18.1kg) for a 2.5GW fusion reactor [136]. The most economical composition capable of producing a start-up inventory can be considerably cheaper than the most expensive composition that achieves the same surplus tritium. When considering that blankets are expected to be replaced every 5 years during a reactor's lifetime, the potential cost savings are substantial.

The requirements of the blanket will change with time. For instance the worldwide supply of tritium fluctuates and therefore the requirement of producing excess tritium could change from blanket to blanket. Upon changing the blankets it might be desirable to optimise the blankets differently and not place such emphasis on tritium production. However, if the objective is to produce excess tritium at the most affordable price then Figure 3.7 shows the compositions that should be considered.

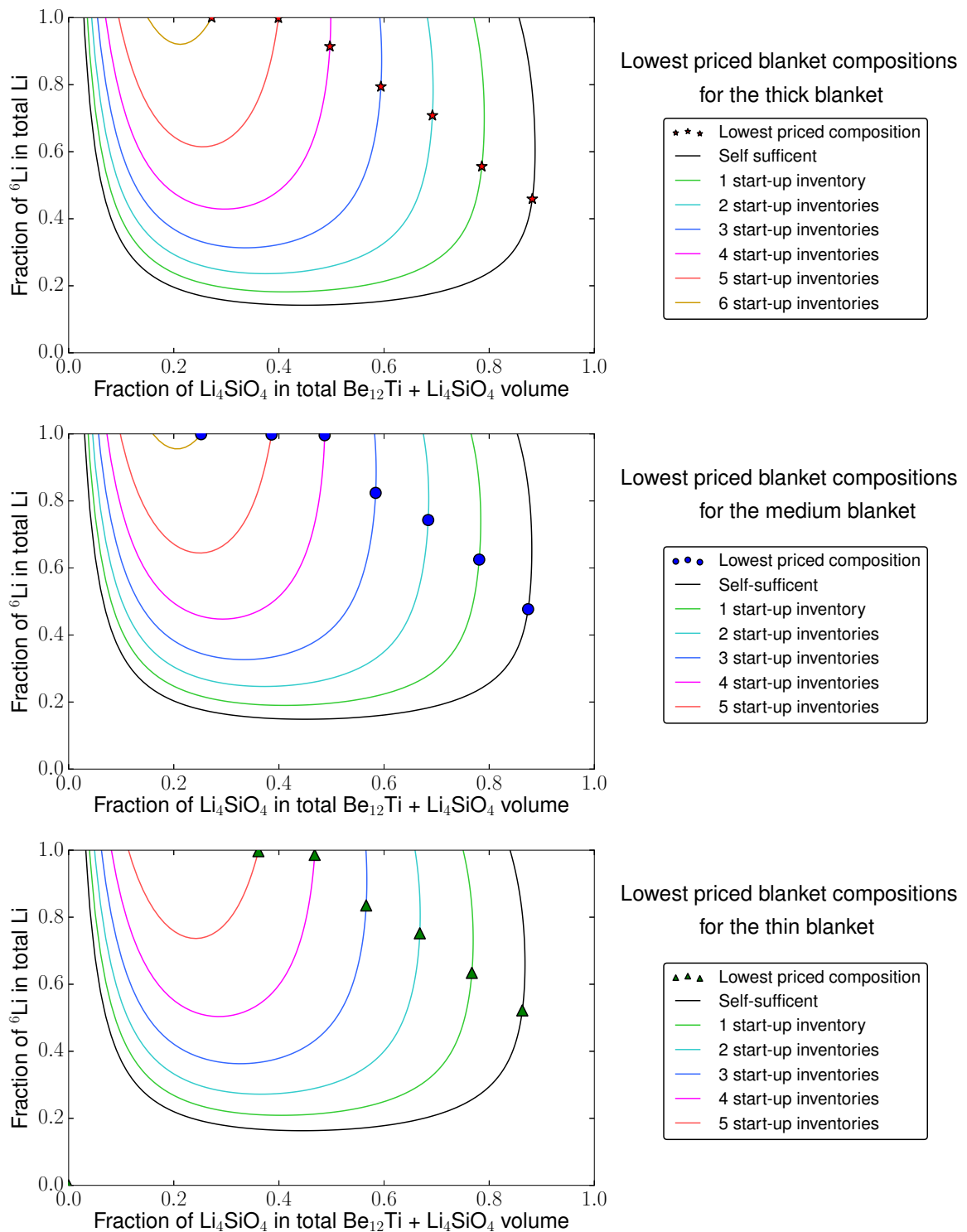


Fig. 3.7 Cost effective blanket compositions capable of producing different sized start up inventories.

The thickness of the blanket does not appear to make a significant impact on the total quantity of tritium produced over the five year irradiation time, however the thickness certainly affects the material costs (see Figure 3.8). The additional tritium production in the rear of the blanket is marginal compared to the tritium production at the front of the blanket. In terms of their tritium production, the additional costs inherent with thicker blankets make them economically unattractive. Figure 3.8 shows that it is often possible to produce the same quantities of tritium with the thin blanket at approximately $\frac{2}{3}$ of the cost of the thick blanket. However, thicker blanket designs may show greater merit if the irradiation time or fusion power were increased. The shielding of sensitive components such as the toroidal field (TF) coils should also be considered when deciding on blanket thickness. While thicker blankets would attenuate neutrons and gammas more effectively compared to thinner blankets, they would leave less space for shielding material. The resulting protection offered by different blankets is beyond the scope of this study.

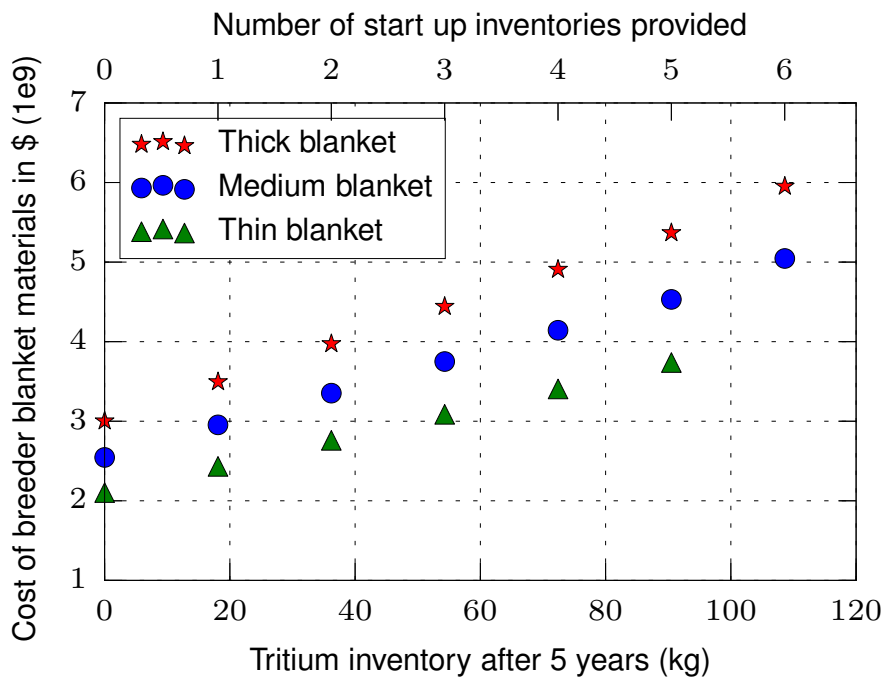


Fig. 3.8 A comparison between costs required for the three blanket thicknesses to produce different sized tritium inventories.

The cost per gram of producing excess tritium can be calculated by finding the additional costs incurred in the breeder blanket composition and dividing this by the quantity of tritium produced. This gives costs in the range of \$14,000 to \$28,000 per g depending on the quantity of tritium required and blanket thickness used. This is comparable to production from CANDU reactors (\$30,000 per g) [196] and cheaper than other proposed methods (\$84,000 to \$134,000 per g) of tritium production [136]. Proposed methods include Accelerator Driven Subcritical system (ADS), Accelerator Production of Tritium (APT) and tritium production in Commercial Light Water Reactor (CLWR).

Blanket compositions have been shown to vary in price but they also vary in the amount of thermal energy generated. The quantity of electricity produced and therefore the profitability of thermal power stations is directly related to the amount of thermal energy produced in breeder blankets. The monetary value of any additional thermal energy produced can be estimated by knowing the conversion efficiency, power plant availability and the sale price of electricity. The thermal efficiency depends on the design of the fusion reactor and in particular the temperature difference of the inlet and outlet coolant. However, for a HCPB design 40% is a reasonable approximation [120]. The UK price of wholesale electricity fluctuates, however £45 per MWh is a representative figure. The availability of future power plants is uncertain, however [185] suggested that a minimum of 70% is required for power plants to be feasible. This would result in a 2.4GW fusion power (1.9GW neutron power) reactor producing an average of £1.45 million worth of electricity every day. This figure is assuming there is no energy multiplication (see Equation 3.3) in the blanket, however if the energy multiplication was increased from 1 to 1.1 this would equate to an additional £145,000 per day or £265 million over the blanket's lifetime. Naturally this simple approximation does not account for all the complexities. More comprehensive studies of the economic viability of fusion energy have shown that the profitability relies heavily on external factors [193]. The figures serve only as an indication of the possible incentives for optimising the thermal energy deposition within the blanket.

It is possible to simulate the heat deposition in the breeder blanket using F6 tallies in MCNP which record the energy deposited. F6 tallies are a method within MCNP for mea-

suring the energy deposited per cell, further details are available in the MCNP manual [201]. The main contributors to the thermal energy in a breeder blanket are: the energy deposited by neutrons, the energy deposited by gamma rays and energy liberated by nuclear reactions. Neutrons deposit a large portion of their energy through inelastic scattering in the blanket; this process excites the nuclei that the neutrons interact with. Neutron induced reactions also contribute to the thermal energy within a blanket, for example each ${}^6\text{Li}(\text{n},\text{t})$ reaction liberates 4.79MeV. Excited nuclei are often produced as a result of inelastic scattering, decay and other interactions. Gammas are produced by nuclei as they undergo de-excitation, they then travel through matter and deposit their energy via interactions such as the photoelectric effect or Compton scattering.

$$\text{Energy multiplication} = \frac{\text{released energy}}{\text{incident energy}} \quad (3.3)$$

Figure 3.9 shows the energy multiplication from neutrons, gammas and the combined total energy multiplication of all the different blanket compositions. The results show that blankets with large quantities of beryllium or with low ${}^6\text{Li}$ enrichment are the best in terms of their energy multiplication. The reasoning behind this is due to neutron multiplication. In the case of large beryllium quantities there is increased opportunity for neutron multiplication. In the case of low ${}^6\text{Li}$ enrichment there are less competing interactions for the ${}^9\text{Be}(\text{n},2\text{n})$ reaction and therefore neutron multiplication becomes more likely. A single neutron entering the blanket and not undergoing neutron multiplication will typically deposit its own energy and liberate some energy in a ${}^6\text{Li}(\text{n},\text{t})$ reaction. The total energy deposited in this case would be $14.1 + 4.79 = 19.07\text{MeV}$. A single neutron that undergoes neutron multiplication will initially cool the blanket as ${}^9\text{Be}$ reactions are endothermic (-1.8MeV), however the total energy deposited would be larger, $14.1 - 1.8 + 4.79 + 4.79 = 21.88 \text{ MeV}$.

The increase in energy deposition resulting from neutron multiplication is limited to cases where the $(\text{n},2\text{n})$ reaction requires less energy than the energy released by the proceeding neutron capture. This is often the case for beryllium as the ${}^9\text{Be}(\text{n},2\text{n})$ reaction

requires only 1.8MeV and is the lowest energy ($n,2n$) reaction available. However, for other neutron multipliers such as Pb, the ($n,2n$) reaction requires more energy (8MeV). This is higher than the energy released by ${}^6\text{Li}(n,t)$ reactions (4.79MeV). Therefore, increasing the quantity of Pb in blankets results in lower temperatures while additional Be results in higher temperatures. This difference in the energy multiplication properties of Be and Pb has been previously commented on by [121].

Comparing the results of heating tallies from different time periods in the blankets' life revealed that the energy multiplication increased as the blankets aged. The increased energy multiplication over the 5 year period simulated was minimal (below 1% in all cases). The increased energy multiplication is also caused by increased neutron multiplication. As ${}^6\text{Li}$ and other isotopes burn-up more rapidly, the likelihood of ${}^9\text{Be}(n,2n)$ occurring increases due to less competition.

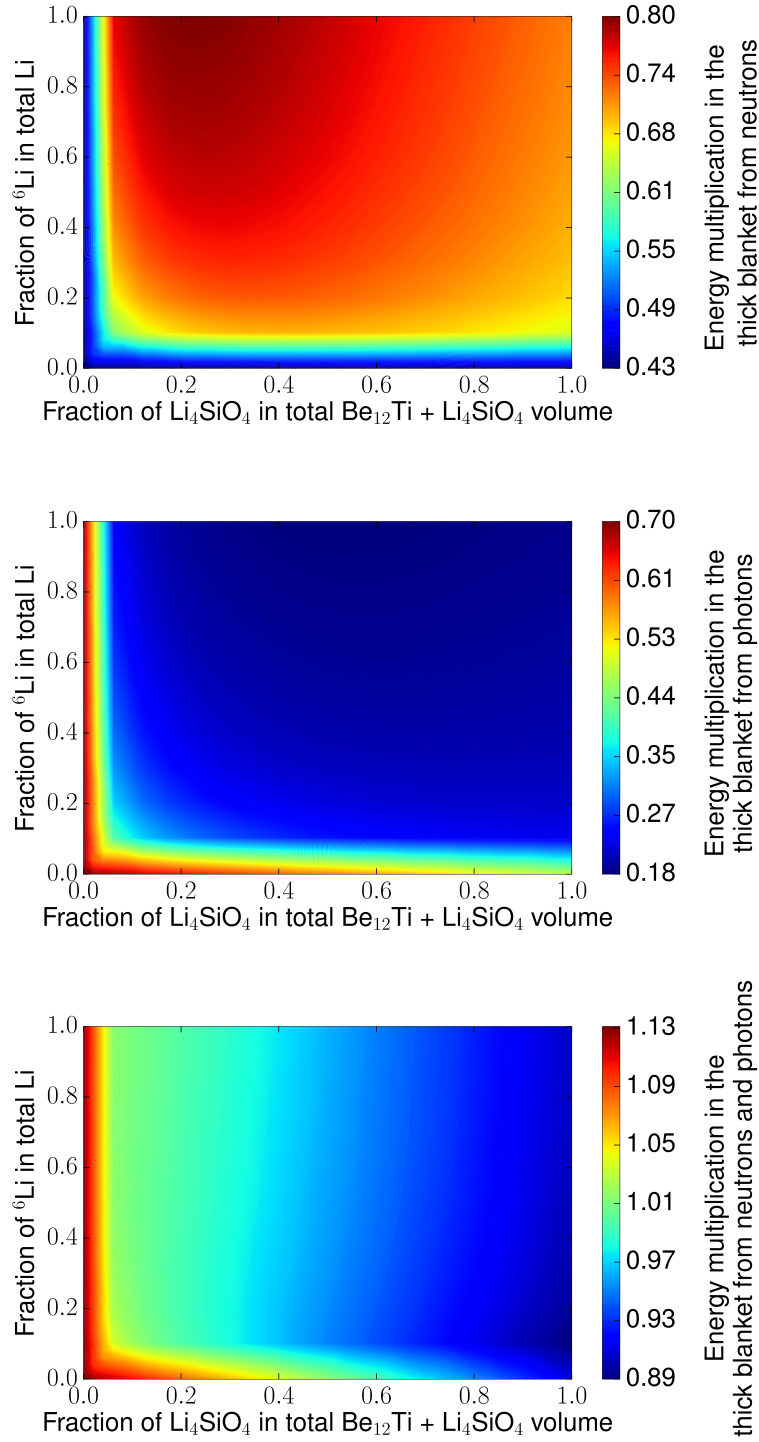


Fig. 3.9 The energy deposited by just neutrons, just photons and combined energy from neutrons and photons within the blanket

The parameter study accounted for nuclide burn-up and from the simulation outputs it is possible to identify blanket compositions that degrade significantly with respect to time. It could be desirable for blankets to maintain consistent tritium production throughout their lifetime. Blankets that initially overbreed and underbreed tritium towards the end of their life require a larger tritium surplus to be stored. Optimising the blanket so that it was able to achieve consistent tritium production would minimise the required storage. This would reduce the loss of tritium through decay and reduce the safety risks associated with storage of large quantities of tritium. This optimisation is not essential for the operation of DEMO and therefore will not heavily influence blanket designs. However, if the composition of blankets offering low TBR reduction coincides with compositions that are suitable in terms of heat, cost and sufficiently high TBR then it would be desirable to include.

All compositions that achieved a $TBR > 1$ were found to suffer from reduced tritium production with respect to time. The magnitude of reduction varied; blankets with low breeder fractions and low ${}^6\text{Li}$ enrichment showed the most rapid decrease in TBR over time.

The TBR of the solid-type breeder blanket was found to decrease over time as the tritium producing isotopes were depleted in nearly all cases. Blanket compositions with no lithium fraction are not capable of high TBR values but were included in the parameter study for completeness. Reaction products such as ${}^6\text{Li}$ built up in blankets containing high quantities of Be_{12}Ti . Production of ${}^6\text{Li}$ occurred via ${}^9\text{Be}(n, {}^3\text{H}){}^6\text{He}$ reactions and the subsequent decay of ${}^6\text{He}$ into ${}^6\text{Li}$. This caused a small increase in TBR for blankets with no initial lithium content, but the TBR still remained below 0.1. Time-averaged TBR values were calculated by taking the average (mean) value of the TBR from all 122 time-steps. TBR typically decreased by 1.4% for compositions capable of achieving tritium self-sufficiency over the 5 year duration. A 1.4% reduction in TBR of 1.115 to 1.099 equates to a 13.57% decrease in the margin of TBR over 1 and this would be sufficient to drop below the common target of $TBR>1.1$.

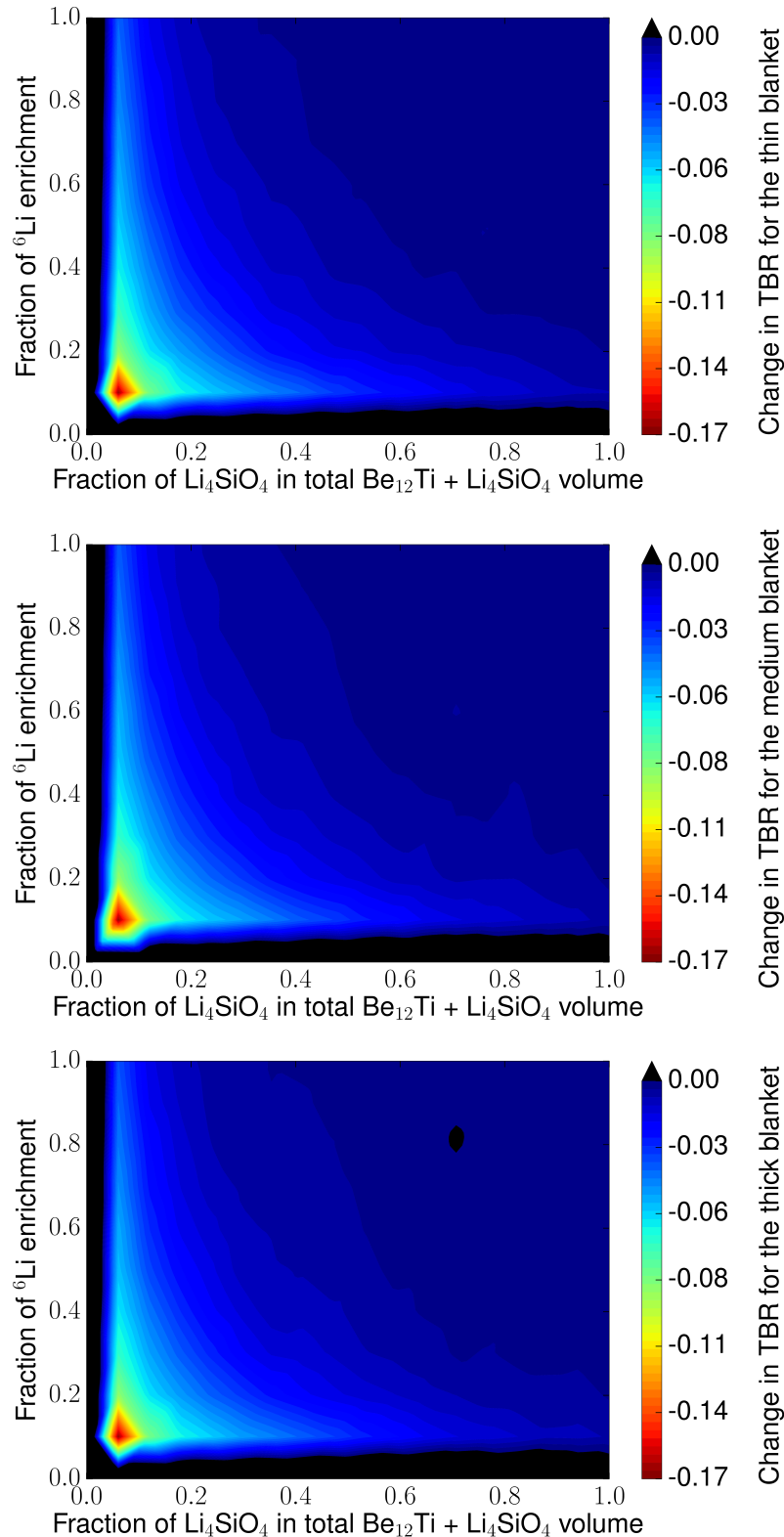


Fig. 3.10 The change in TBR over the blanket's five year lifetime.

The simulated breeder blanket performances presented in the chapter shows that it is possible to optimise the blanket for individual performance criteria. The blanket composition was optimised for TBR, tritium inventory, heat deposition and TBR reduction. There is no single uniform composition that is able to maximise all the desired performance criteria simultaneously. Designs are therefore likely to compromise on one or more of the desirable characteristics. There are clearly variables such as TBR which have minimum tolerable values ($TBR > 1.1$), whereas other variables such as heat deposition simply need to be maximised. Figure 3.11 shows compositions that are desirable in terms of high TBR values that do not reduce significantly with time and energy amplification. Unfortunately this region of compositions has high associated material costs due to the large quantity of $Be_{12}Ti$ required.

Methods of reducing the $Be_{12}Ti$ content are discussed in Chapter 5.

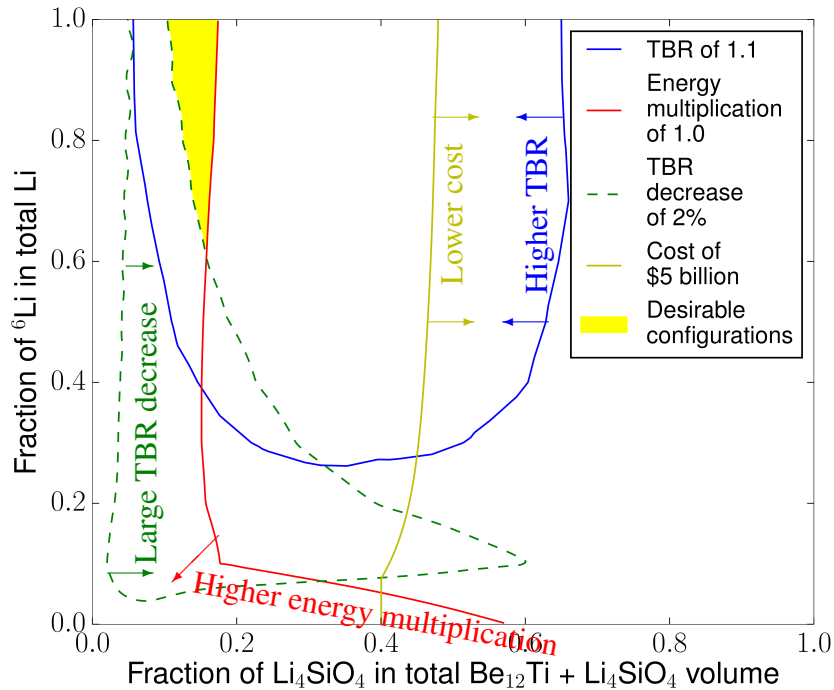


Fig. 3.11 Blanket compositions that meet specified TBR, heat and cost requirements.

3.5 Conclusion

It has been commonly assumed that the availability of tritium will be one of the limiting factors for future DT fusion reactor deployment. The findings of this study suggest that it is possible to optimise the production of tritium for solid-type breeder blankets by varying the breeder to multiplier ratio, the lithium enrichment and the blanket thickness. The calculated decrease in TBR values over time shows that it is desirable to take account of nuclide depletion when accurately studying time-varying tritium production in solid-type breeder blankets. The additional computational time (122 MCNP runs instead of 1) and complexity required to simulate nuclide burn-up can be avoided in cases where burn-up is negligible (high breeder fraction and high ${}^6\text{Li}$ enrichment). This study shows there is scope to reduce the cost of breeder blankets by changing the composition and thickness of the blankets. Thinner blankets were found to be capable of achieving the same amount of tritium production for reduced costs. For example the thin blanket is capable of producing up to 106 kg of excess tritium and is typically $\$1.5 \times 10^9$ cheaper than the thick blanket. Excess tritium can be produced at an additional cost of \$14,000 to \$28,000 per g depending on the quantity required. This production price is comparable to limited production from CANDU reactors (\$30,000 per g) and cheaper than proposed methods (\$84,000 to \$134,000 per g) [136]. The cost analysis focuses on the costs of breeder and multiplier materials and does not take into account all the associated costs in breeder blanket construction, operation and decommissioning. The cost of the solid-type breeder blankets in this study is dominated by the cost of Be_{12}Ti which is estimated to be \$4,500 per kg. Reducing the cost of Be_{12}Ti would have a substantial impact on the cost predictions made in this study. A further study will look at the possibility of reducing the quantity of Be_{12}Ti used in the blanket by varying the breeder fraction with blanket depth. There is no single composition that maximises heat deposition, TBR and tritium inventory while also minimising the cost and TBR reduction. A single composition of breeder material for the entire blanket is not likely to be the most optimal solution in terms of tritium production. It would be advantageous to optimise separate blanket modules for their position within the reactor, however this would incur additional design and manufacturing costs. Blankets with different layers

comprising of different compositions is proposed as a potential method of achieving multiple variable optimisation. The approach used in this study makes several assumptions in order to achieve the goal of demonstrating a methodology for producing parameterised neutronic inputs into the PROCESS systems codes. Ideally the study would be carried out on a more refined breeder blanket design and less homogenised blanket structure. This would allow more realistic volume fractions for Eurofer and helium to be found for blankets with different thicknesses. Accounting for burn-up as well as multiple dimensions resulted in large computational expense and this is perhaps the main limitation of the study. Before incorporating further dimensions or realism into such a study, further development of the coupling code FATI that links FISPACT II and MCNP 6 should be carried out. Upgrading the coupling code so that it is able to use the new unstructured mesh geometry available in MCNP 6.1 would allow more complex heterogeneous designs of breeder blankets to be studied. Further studies involving optimisation of multiple criteria (e.g. shielding ability) would also be of interest to reactor designers.

Chapter 4

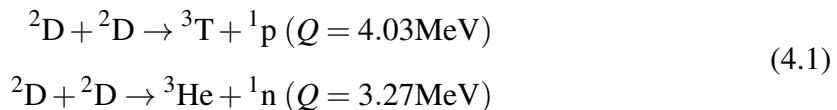
Breeder blankets for DD plasmas

4.1 Introduction

Providing tritium start-up inventories for DT fusion reactors is currently achieved using existing reserves. Civil tritium reserves are largely accumulated from CANDU fission reactors [136]. There have been several studies into tritium reserves available for fusion research ([68] and [195]). More recently [136] predicts the worldwide civil tritium reserves available after ITER to be between 14 and 28kg and the anticipated required start-up inventory for a DEMO reactor is 18.1kg. It is uncertain whether sufficient tritium will be available to start-up a DEMO reactor and in the event of several DEMO reactors this would almost certainly exhaust the tritium reserves. Research that mitigates against any potential shortage of tritium is therefore important for the future of fusion. One potential solution would be to increase the tritium supply and dedicated tritium production facilities have been proposed [196]. Another method of increasing the tritium supply would be to design breeder blankets to produce surplus tritium. This could provide start-up inventories for succeeding reactors but would not provide tritium for the first DEMO reactor. Surplus tritium production is not ideal as the storage of tritium is also problematic due to its affinity to diffuse through barriers and the natural decay of tritium (12.3 years half-life) means stocks will decrease with time. Creating surplus tritium with breeder blankets also requires additional expenditure on lithium enrichment and beryllium (see Figure 3.8).

Another option would be to reduce demand for tritium by decreasing the amount of tritium required to start-up a fusion reactor. Achieving DT operation with a diminished start-up inventory would dramatically reduce the demand. Ideally fusion reactors would be able to provide their own start-up inventory. Reactors capable of operating without external supplies of tritium would also be more resilient against any unforeseen outages. Additionally, removing the need to store or transport tritium would decrease the proliferation risk that fusion reactors pose.

The use of DD fuel as an energy source in conventional Tokamak devices presents particular challenges compared to DT fuel. The primary difficulty is that DD fusion has a smaller reaction rate at low temperatures compared to DT fusion (see Figure 1.3). Higher temperatures are required in DD fusion when compared to DT fusion in order to successfully achieve an energy break-even situation [176]. However, the use of DD fuel as a neutron source for breeding tritium is more feasible and has been previously considered [160], [203], [153], [109] and [90]. DD fusion occurs via two reactions which are approximately equal in probability (see Equation 4.1).



The production of tritium from DD plasmas occurs predominantly via the three routes shown in Figure 4.1 and listed below. Other reactions such as TT reactions result in neutrons and can lead to the production of tritium in the blanket, however the relative number of TT reactions is negligible.

- 2.45MeV Neutrons are created by DD reactions and these can interact in the breeder blanket to create tritium (see Equation 4.1).
- Tritium is produced by 50% of DD reactions and this can be extracted from the plasma (see Equation 4.1).
- Tritium produced by DD reactions within the plasma, reacts with deuterium; this creates 14.1MeV neutrons that can breed tritium in the blanket.

Previous research in this area has considered using DD plasmas to generate small quan-

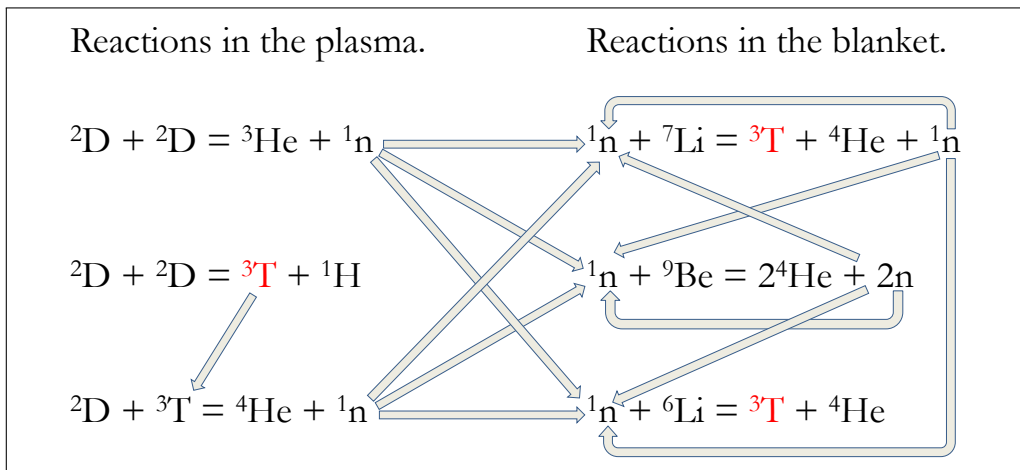


Fig. 4.1 Nuclear interactions that result in the production of tritium.

tities of tritium which is used to fuel the plasma. The DT ratio gradually builds up towards a 50:50 mix at which point the reactor has reached the target tritium concentration without the need of an external tritium start-up inventory. The time required to reach 50:50 DT operation varies but the most comprehensive studies suggest that ≈ 50 days would be sufficient [90].

Another option would be to operate a DD plasma and store all the accessible tritium without feeding it back into the plasma. Once the storage tank reaches the required start-up inventory the reactor could be shut down and refueled with a 50:50 mix of DT. The two scenarios described are not mutually exclusive and could certainly complement each other. The accumulated tritium could also be used as a seed inventory, as suggested by [203], who shows that a seed inventory can significantly reduce the amount of time required to obtain a 50:50 DT plasma when feeding the tritium back into the plasma. A typical seed inventory could be as small as 50g and would halve the time to full DT [203]. DD plasmas are used routinely prior to operating with a DT plasma to test diagnostics, fueling and other aspects of the reactor operation. ITER currently plans to perform several months of low capacity rate DD fusion prior to DT [168].

In both cases the breeder blankets are expected to provide a significant proportion of the tritium. Previous studies have used existing blanket concepts that have been optimised for tritium production from DT (14.1MeV) neutrons. There is scope to improve this process

by considering the neutronics of breeding tritium from 2.54MeV in addition to 14.1MeV neutrons.

Further discussion on this topic requires an adaption of the familiar concept of TBR (see Equation 1.17). A Tritium Production Rate (TPR) is a more suitable term as DD plasmas do not necessarily involve the consumption of tritium to produce tritium.

$$\text{Tritium Production Rate (TPR)} = \frac{\text{Number of tritium atoms produced}}{\text{Number of DD neutrons produced}} \quad (4.2)$$

Neutrons from DD fusion are lower in energy (2.45MeV) compared to DT neutrons (14.1MeV) and therefore interact differently with materials. The important nuclear reactions within the breeder blanket also vary with energy. Threshold reactions such as neutron multiplication via n,2n reactions (e.g. $^9\text{Be}(n,2n)^2\text{He}$) are particularly sensitive to neutron energy (see Figure 1.11). The high volumes of neutron multiplier material used in DT breeder blankets are therefore not effectively utilised by the DD neutrons. Lower energy DD neutrons also have little likelihood of breeding tritium via $^7\text{Li}(n,n't)^4\text{He}$ reactions (see Figure 1.10) and TPR will therefore be particularly sensitive to ^6Li enrichment. Using breeder blankets optimised for tritium production with a DT plasma is therefore unlikely to be optimal for DD plasmas.

As tritium is created in the plasma by DD reactions (see Equation 4.1) there will also be DT reactions occurring in plasmas that are only fueled with deuterium. The fraction of tritium atoms created in a DD plasma that fuse before exiting the torus is referred to as the burn-up fraction. The higher the burn-up fraction the less opportunity for tritium to be lost (via absorption, leakage or decay) and consequently tritium production requirements can be relaxed a little [44]. While a higher burn-up fraction is desirable a value of over 10% is challenging to achieve [88]. For the purpose of this study the burn-up fraction was assumed to be 10%. It was also necessary to choose an appropriate DD reaction rate. A typical DEMO reactor producing 2.8GW of thermal power would require DT reactions at a rate of $1 \times 10^{21} \text{n s}^{-1}$. The DD reaction cross-section at 15KeV is approximately 100 times smaller

Reference	Time required until full DT operation (days)	TPR value used	TBR values used
Satoshi [160]	100	Not stated	1.1
Asaoka [203]	55	0.67	1.1
Hiwatari [153]	107	Not stated	1.05
Kwon [109]	89	0.84	1.2
Kasada [90]	50	0.67	1.1

Table 4.1 Summary of TBR and TPR values used by previous research.

than the DT reactions at 15KeV, therefore this would correspond to a DD rate of $1 \times 10^{19} \text{ n s}^{-1}$.

Previous research into this topic has established that it is theoretically possible to start with a DD plasma and achieve a 50:50 DT plasma within a reasonable time period (see Table 4.1 for a summary of previous research). Research methodology varies but one important factor is the probability of producing a tritium atom when neutrons are generated in the plasma. High TBR and TPR values will increase the rate of tritium production and shorten the time until full DT operation.

The blankets used in previous studies have been designed for use in DT neutron facilities. This research explores the idea of optimising the blanket for the mixed DT DD neutron flux that it receives. By optimising the blanket for this mixed neutron field it is possible to reduce the time required to produce sufficient tritium for a 50:50 DT plasma.

4.2 Materials and methods

Optimising breeder blankets in terms of tritium production from DD neutrons was carried out for two scenarios:

- Tritium created is returned to the plasma and as additional tritium is generated the tritium fraction in the plasma gradually increases to 50%
- A DD plasma is operated continually and any tritium created is stored. Once sufficient tritium has been achieved for the production of a small seed inventory or a full start-up inventory the reactor stops and restarts with 50:50 DT fuel.

The first scenario follows on from previous research ([160], [203], [153], [109] and [90]). Different breeder blanket compositions are compared; the different compositions result in different values of TPRs and TBRs. This extends previous research which has considered a single value for TPR and another value for TBR. The aim is to find the optimal breeder blanket composition for the mixed DT DD neutron field. The duration of time required to reach 50:50 DT operation is the parameter that was optimised.

The second scenario initiates a new line of research by considering using breeder blankets for DD plasmas and storing the tritium produced. By varying the blanket composition it is possible to increase the TPR from previously reported values (see Table 4.1). The aim of this research was to find the optimal breeder blanket composition for neutrons generated by DD plasmas.

The DEMO model used for these investigations was based on a DEMO reactor model provided by KIT [148]. The model includes individual blanket modules and is based on the HCPB bed design [57]. Standard fusion materials consistent with previous chapters have been used. The breeder zones were made of homogenised material (Be_{12}Ti , Li_4SiO_4 , Eurofer and helium) and more details can be found in Table 2.1.

Different material compositions were constructed with a range of ${}^6\text{Li}$ enrichment fractions (0-1) and multiplier fractions (0-1). In total 11 different enrichments and 16 different multiplier fractions were simulated, this resulted in 176 different blanket compositions. Each composition was then simulated twice using MCNP 6.0. The source energy was varied

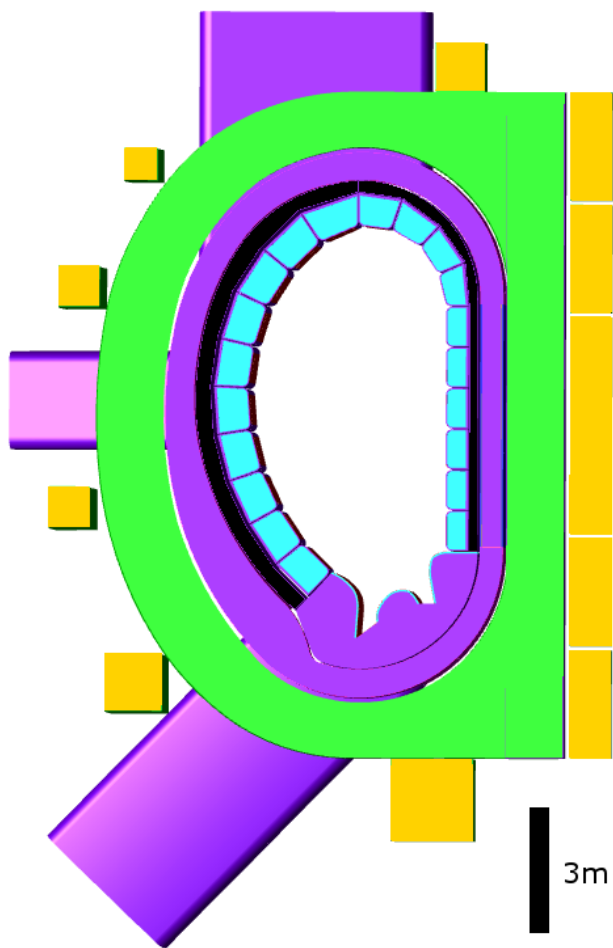


Fig. 4.2 HCPB DEMO model used. The vacuum vessel, divertor and blanket casing (purple) ■, toroidal field coils (green) □, poloidal field coils (yellow) □, blanket (light blue) □ and the rear casing for the blanket (black) ■.

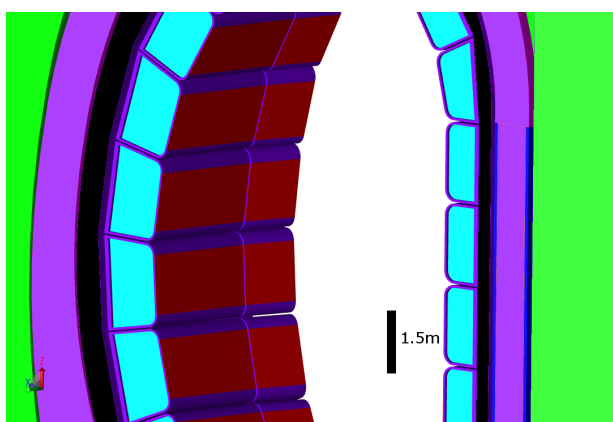


Fig. 4.3 View of HCPB DEMO model showing individual blanket modules. The tungsten first wall armour is also shown (red) ■.

so that the blankets' response to DT and DD neutrons could be found separately. FENDL 3.0 [61] nuclear data was used for particle transport and particle interactions. The same parametric plasma source was used in both cases to represent the neutron emissions from the plasma. The outputs of the simulations revealed how TPR and TBR vary as a function of ${}^6\text{Li}$ enrichment fraction and multiplier fraction.

Additional factors were considered to improve the realism of the simulation. The radioactive decay of tritium was accounted for. Tritium absorption and diffusion in the various systems were estimated. A previously developed system dynamics model was used to simulate the flow of tritium through the system. Details of the system dynamics model are published by [90] and information on the saturation levels, sinks and various pathways are described in detail. A simplified model is shown in Figure 4.4 to show the fundamental flow of tritium around the system.

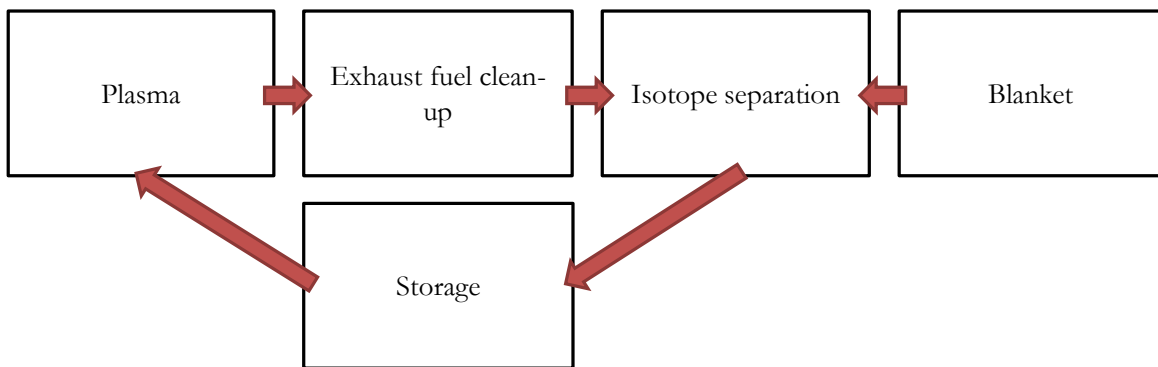


Fig. 4.4 A simplified diagram of the system dynamics model used; this diagram only shows the main tritium pathways.

4.3 Results

The TPR and TBR of the different breeder materials were found (see Figures 4.5 and 4.6). The maximum TBR of 1.124 was found to be achievable with a ${}^6\text{Li}$ enrichment of 100% and a breeder fraction of 0.31. Operating this blanket with a DD plasma would result in a TPR of 0.794. However, the maximum TPR was found to be 0.884 and required a ${}^6\text{Li}$ enrichment of 100% and a breeder fraction of 1. By optimising the blanket for the different neutron energies it has been possible to increase the tritium production in the blanket with a DD plasma by over 10%.

${}^6\text{Li}$ enrichment of 100% is not practical to achieve. To represent more realistic scenarios, the maximum TPR and TBR achievable with ${}^6\text{Li}$ enrichment limited to 70% were also found. The difference between Figures 4.5 and 4.6 highlights the need to consider neutron energy when optimising the blanket material. Blankets optimised for tritium breeding from a DT plasma require a different material composition to blankets optimised for tritium breeding from DD plasmas. The optimal composition is summarised in Table 4.2. The TBR and TPR values of blankets optimised for tritium production from DD and DT neutrons are also summarised in Table 4.2.

Blanket description	${}^6\text{Li}$ enrichment (%)	Breeder fraction (%)	TBR	TPR
Blanket optimised for TBR	100	0.31	1.124	0.794
Blanket optimised for TPR	100	1	0.952	0.884
Blanket optimised for TBR with ${}^6\text{Li}$ enrichment limit	70	0.50	1.092	0.770
Blanket optimised for TPR with ${}^6\text{Li}$ enrichment limit	70	1	0.956	0.867

Table 4.2 A summary of the different compositions required to optimise the blanket for different neutron energies.

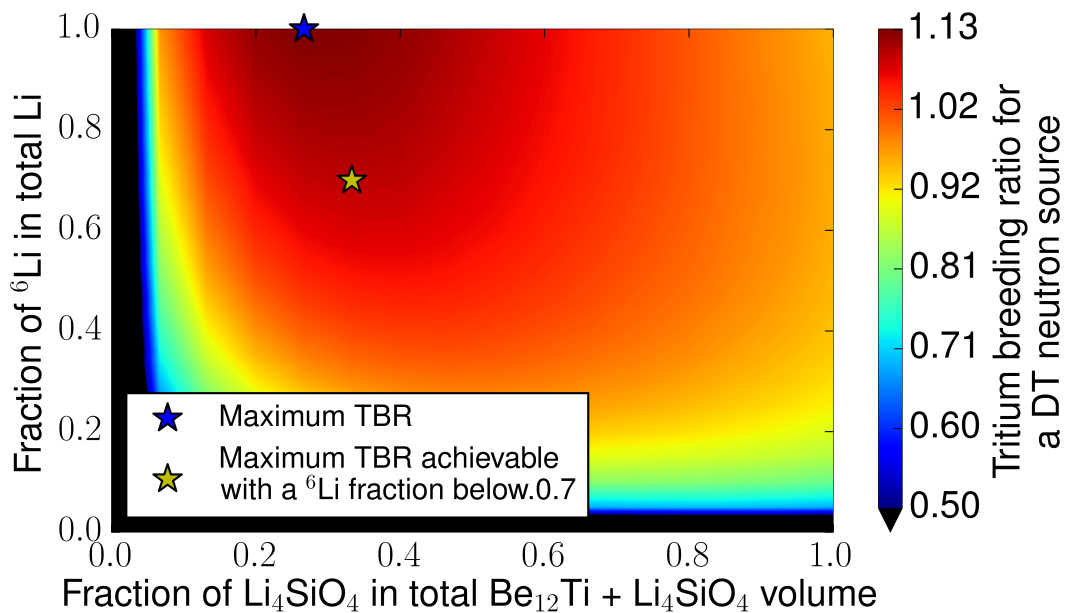


Fig. 4.5 TBR values for different blanket compositions.

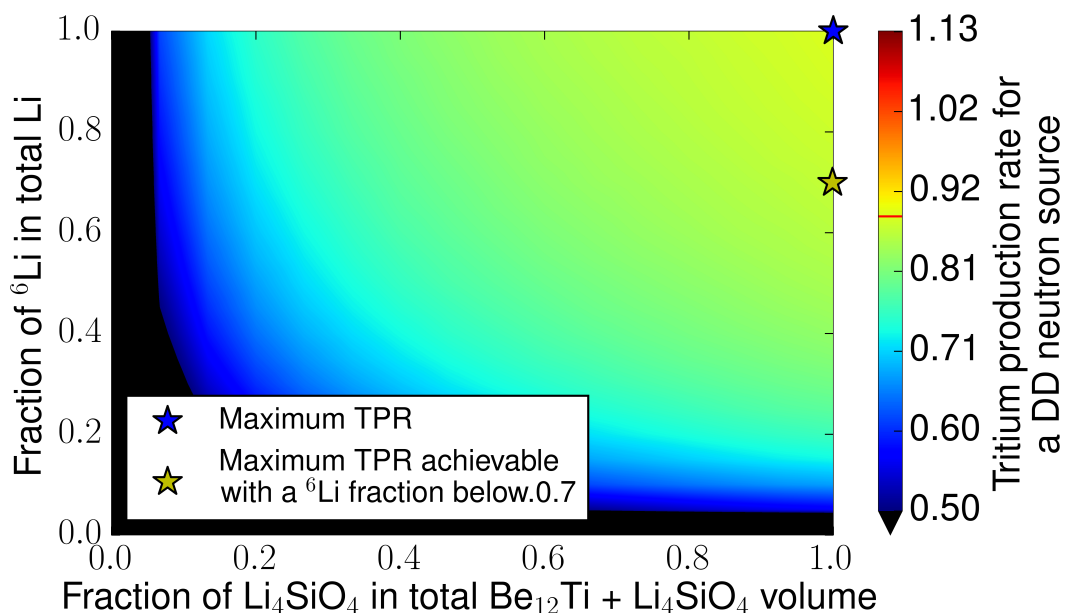


Fig. 4.6 TPR values for different blanket compositions.

4.3.1 Storing the tritium produced

Tritium produced within the blanket and the plasma can be stored for later use as a start-up or seed inventory. The rate at which tritium is accrued is influenced by the material composition of the blanket. Figure 4.7 shows how the tritium build-up differs when the blanket is optimised for DT or DD neutrons. The blanket optimised for TPR is significantly better at producing tritium in a DD neutron field compared to the blanket optimised for TBR. However, the tritium produced in the blanket is only part of the tritium created in a fusion reactor operating a DD plasma. Additional tritium is produced in the plasma and can be extracted from the exhaust if it does not burn-up in the plasma. Tritium that is burnt-up in the plasma (10% for this study) produces 14.1MeV neutrons which interact in the blanket to produce tritium. A value of 10% was chosen for the tritium burn-up as this is stated as an essential requirement for achieving tritium self-sufficiency (see [44]). However, the 14.1MeV neutrons naturally produce more tritium in blankets optimised for TBR instead of TPR. The overall result is that the blanket optimised for TPR only marginally out performs the blanket optimised for TBR.

This simulation based approach suggests that accumulating 18.1kg with either blanket would require an excessive amount of time (over 30 years) and is therefore not practical for this particular model. It becomes increasingly difficult to accumulate tritium as the rate of loss through decay approaches the rate of production, this occurs after 4 / 5 half-lives. However providing a small (50-100g) start-up inventory appears to be more feasible. 100g could be accumulated in approximately 30 full power days. Again the blanket optimised for TPR production only marginally out performs the blanket optimised for TBR (produces 100g of tritium 2 days quicker).

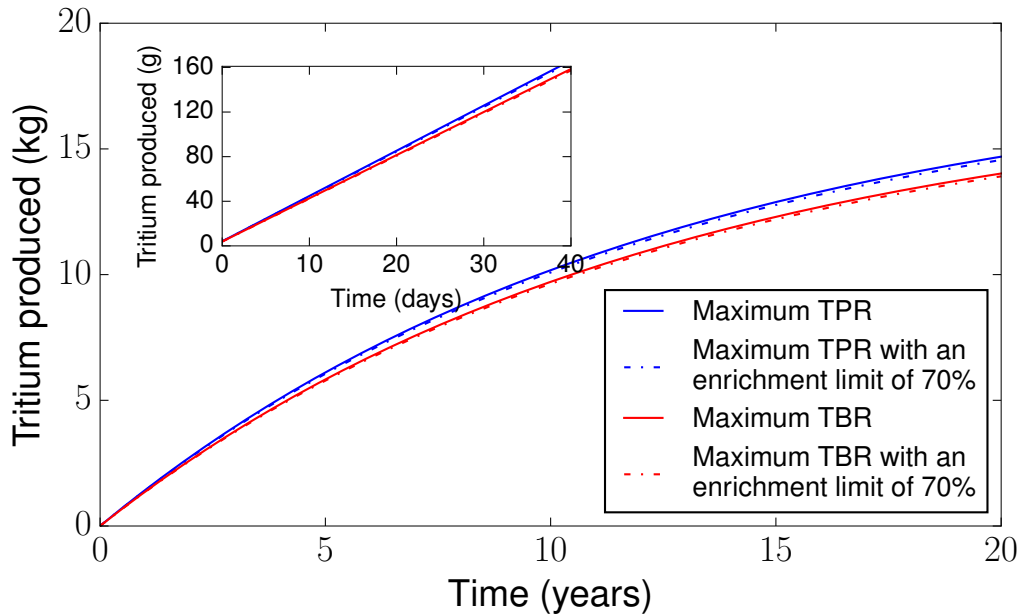


Fig. 4.7 Time required by each blanket composition to reach a 50:50 DT plasma.

4.3.2 Refueling the plasma with the tritium produced

Obtaining a 50:50 DT plasma by refueling the DD plasma with tritium created in the breeder blankets and tritium extracted from the plasma was investigated. Different breeder blanket compositions result in different TPR and TBR values. As the tritium content of the plasma gradually increases from 0% to 50% the energy of the emitted neutrons changes from 2.45 to 14.1 MeV. Blankets optimised for tritium production in either pure DT or pure DD plasmas are therefore suboptimal for this scenario. Figures 4.8 and 4.9 identify an optimal composition, in terms of the time taken to reach 50:50 DT operation and TBR. The composition that achieves 50:50 DT in the least time was found to have a breeder fraction of 0.31 and a ${}^6\text{Li}$ enrichment of 100%. When limiting the enrichment to 70% ${}^6\text{Li}$, the composition that achieved a 50:50 DT plasma the most quickly was found to have a breeder fraction of 0.31. These are also the same compositions for achieving maximum TBR as shown in Table 4.2. No noticeable improvement in reducing the time required to achieve a 50:50 DT plasma was achieved. The optimal composition in terms of tritium production from 14.1MeV neutrons

was also found to be the optimal when the varying (2.45 and 14.1MeV) neutron field was used.

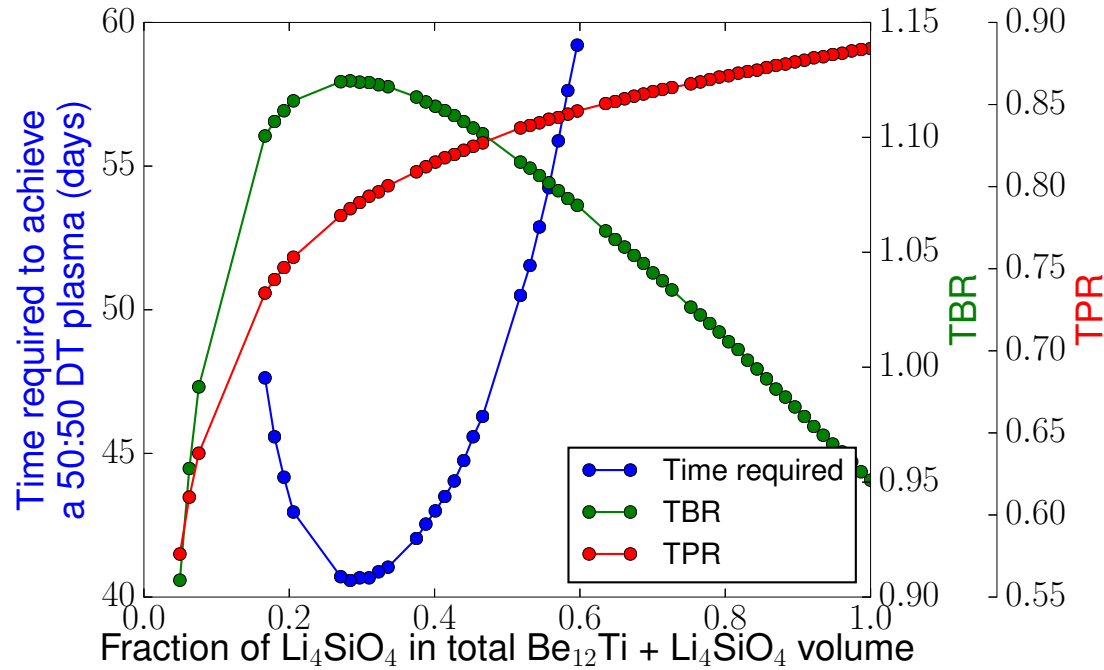


Fig. 4.8 The time required to reach a 50:50 DT plasma with different breeder fractions and 100% ${}^6\text{Li}$ enrichment. TPR and TBR of the compositions are also shown.

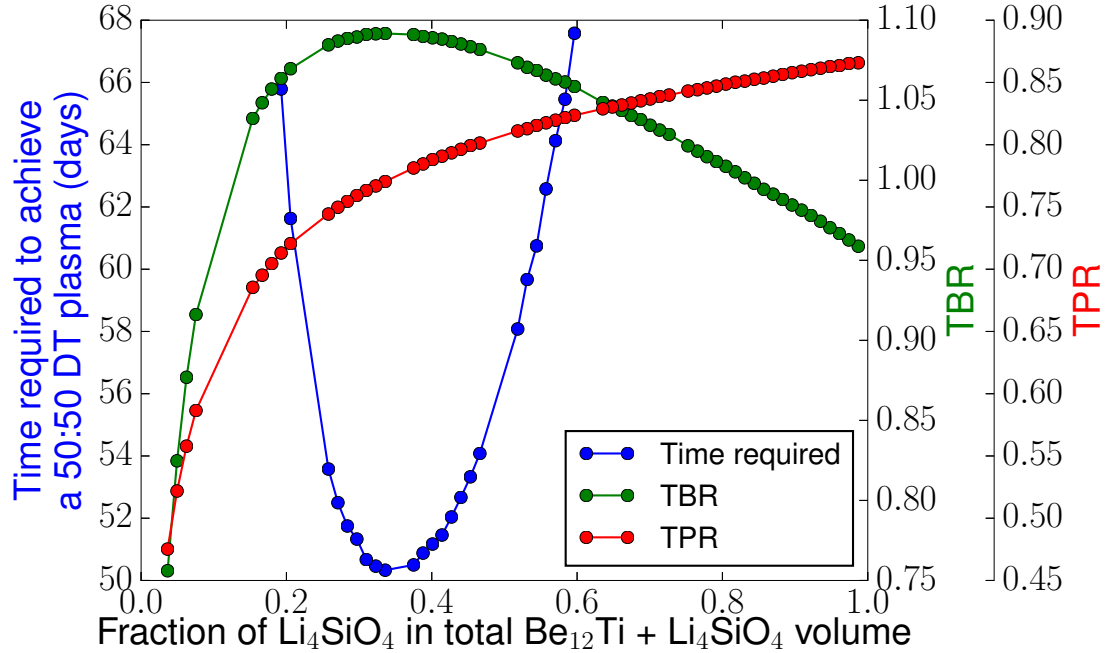


Fig. 4.9 The time required to reach a 50:50 DT plasma with different breeder fractions and 70% ${}^6\text{Li}$ enrichment. TPR and TBR of the compositions are also shown.

4.4 Conclusion

As shown in the results section, by varying the composition of the blanket to better suit neutrons from DD it is possible to increase the tritium production per source neutron. The tritium production per DD source neutron was increased from 0.794 to 0.884 when the blanket was optimised for TPR instead of TBR. Optimising the blanket composition for DD neutrons involves replacing neutron multiplier material (Be_{12}Ti) with lithium ceramic (Li_4SiO_4). Although increasing the TPR was found to be possible, this resulted in little or no resulting benefit for the two scenarios considered.

Two scenarios that could potentially benefit from breeder blankets optimised for TPR were investigated. Storing the tritium produced in the blanket and the tritium extracted from the exhaust was the first scenario considered. It was shown to be possible to create sufficient tritium for a small seed inventory; 100g of tritium was accumulated in 30 full power days of operation. However, it would not be practical to use a DD plasma to provide a complete

start-up inventory (18.1kg) due to the large time requirements (over 30 years). In both cases optimising the blanket for TPR resulted in only marginal improvements in the rate of tritium accumulation.

Refueling the plasma with tritium that has been generated and gradually building up to a 50:50 DT operation were both investigated. Optimising the blanket so that DD neutrons are more likely to produce tritium resulted in negligible reduction in the time required to achieve DT operation.

The observed improvements in terms of TPR appear reasonable, however, the resulting impact on the rate of tritium accumulation was not significant in the first scenario and no benefit was found in the second scenario. This is due to multiple sources of tritium production; when operating a DD plasma the tritium production in the blanket is only part of the equation. Reactors with lower burn-up fractions may benefit more from the optimisation carried out on blankets. High burn-up fractions result in additional 14.1MeV neutrons which are well suited to blankets optimised for TBR.

A potential use of blankets optimised for mixed DD and DT neutrons is in reactors that operate with tritium-poor fuel [128]. The blankets are not required to achieve a TBR of greater than 1.1 in order for the reactor to continue operation. Tritium-poor DT fuel for ICF devices (see e.g. [95] [151]) has been studied more extensively than MCF and goes beyond the scope of this research.

Chapter 5

Reducing beryllium content in mixed bed solid-type breeder blankets

5.1 Introduction

Beryllium (^9Be) is a precious resource with many high value uses; the low energy threshold ($n,2n$) reaction makes ^9Be an excellent neutron multiplier for use in fusion breeder blankets. Estimates of ^9Be requirements and available resources suggest that this could represent a major supply difficulty for solid-type blanket concepts. Reducing the quantity of ^9Be required by breeder blankets would help to alleviate the problem to some extent. In addition, it is important that the reduction in the ^9Be quantity does not diminish the performance of the blanket in key aspects such as: the tritium breeding ratio (TBR), energy multiplication and peak nuclear heating.

Mixed pebble bed designs allow the multiplier fraction to be varied throughout the blanket. This neutronics study used MCNP 6 to investigate linear variations of the multiplier fraction in relation to blanket depth, in order to better utilise the important multiplying $^9\text{Be}(n,2n)$ and breeding reactions. Blankets with a uniform multiplier fraction showed little scope for reduction in ^9Be mass. Blankets with varying multiplier fractions were able to simultaneously use 10% less ^9Be , increase the energy multiplication by 1%, reduce the peak heating by 7% and maintain a sufficient TBR when compared to the performance achievable

using a uniform composition.

The sustainability of resources required for deuterium-tritium fusion have been previously considered [37] [18]. Reported availability of ^9Be resources is particularly concerning, although further successful prospecting could alleviate the situation. The usage of ^9Be in fusion devices is common and is demonstrated by ^9Be being the reference material for solid-type breeder blankets in ITER [66] and beryllides such as Be_{12}Ti are considered a promising neutron multiplier for DEMO [93] [173]. Recycling of irradiated beryllium [40] is one option that could reduce the amount of ^9Be usage over a reactor's lifetime. Another approach that could be carried out in tandem is to reduce the amount of ^9Be specified in breeder blanket designs. This chapter aims to explore the possibility of decreasing the amount of ^9Be required in mixed bed breeder blanket designs.

Mixed bed breeder blankets are being pursued by several research groups [24], [145], [173] and [172]. They utilise a mixture of breeder ceramic and neutron multiplier pebbles. Using pure ^9Be as the neutron multiplier has been ruled out in mixed beds due to tritium retention in the beryllium [162] and incompatible chemistry [97]. The development of advanced beryllide neutron multipliers such as Be_{12}Ti has shown them to be suitable for mixed bed blankets [92]. Studies into the chemical compatibility, tritium retention and fabrication have been carried out. Studies have also shown that mixed pebble beds offer higher tritium breeding ratio (TBR) than separated bed breeder blankets [93]. Consequently mixed pebble bed breeder blankets are being considered for future fusion reactors [24], [145], [173] and [172]. Neutronic optimisation studies have been carried out to ascertain the optimal multiplier fraction (see Eq. 5.1) in terms of maximising TBR in mixed pebble beds [172] [166]. Studies aiming to reduce the amount of beryllium in blankets with separated breeder and multiplier blanket designs have also been carried out [56]. The traditional approach has been to find a single optimal multiplier fraction for the entire blanket. By varying the ratio of neutron multiplier and lithium ceramic the TBR can optimised (see Figure 5.3). The TBR values obtained by simulation throughout this study refer to the local TBR of the DEMO model used. The DEMO model used in this study contains no penetrations (gaps) for heating or diagnostics; the assumed coverage of the breeder blankets is 85%.

Other aspects to consider are the energy multiplication and peak heating. The heat energy produced in a blanket can be more than the sum of the neutron energies entering the blanket, due to the release of binding energy, as disturbed nuclei rearrange themselves into stable configurations. The ability of the blanket to multiply the incident energy will be of interest when maximising the electricity generated. The peak heat refers to the maximum heat deposition per cm³ in the blanket and is a criterion that may require minimising to prevent material damage.

Mixed bed blankets have the potential to offer different multiplier fractions throughout the blanket (see Equation 5.1). This might be achievable through careful control of the pebble mixture when filling the blanket. The objective of this work is to highlight the potential benefits of using a varying multiplier fraction in mixed pebble bed breeder blankets. This allows further optimisation of the identified performance criteria as well as a reduction in the quantity of beryllium usage. Investigations have previously been carried out with the aim of reducing beryllium content in homogeneous blanket designs. [57] considered replacing the solid ⁹Be slabs at the back of the blanket with more efficient moderator materials (ZrH), however, at that time mixed bed blankets were not considered viable and were not the focus of the paper. There is a lack of published research into the reduction of beryllium usage within mixed bed breeder blankets. This study aims to optimise the beryllium usage in a bed of equally sized Be₁₂Ti and Li₄SiO₄ pebbles by simulating linear variations in multiplier fraction throughout the blanket.

5.2 Theory

Neutron induced reactions in beryllium and lithium make them desirable materials to use in fusion breeder blankets. The cross sections of $^9\text{Be}(n,2n)$, and $^6\text{Li}(n,t)$ respond to different energy neutrons. The $^9\text{Be}(n,2n)$ reaction is a threshold reaction requiring neutrons of at least 1.75MeV. The $^6\text{Li}(n,t)$ reaction is increasingly likely to occur as neutron energy decreases. A combination of both reactions is required to ensure a TBR of at least 1.1.

The neutron spectrum varies throughout the breeder blanket mainly due to scattering and capture interactions. Due to the softer spectrum and the threshold nature of the $^9\text{Be}(n,2n)$ there will be a lower proportion of neutrons capable of $^9\text{Be}(n,2n)$ reactions at the rear of the blanket. The degree of spectral variation depends largely on the material composition of the blanket material and the first wall.

When discussing positions within the blanket the region of the blanket nearest the plasma is referred to as the front. The back of the blanket where the blanket is attached to the rest of the tokamak is referred to as the rear.

The two reactions of interest also differ in their Q values (energy release per reaction). The $^9\text{Be}(n,2n)$ reaction is endothermic with a Q value of -1.57MeV whereas the $^6\text{Li}(n,t)$ reaction is exothermic with a Q value of 4.78MeV. Peak heating tends to occur at the front of the breeder blankets nearest to the plasma where the neutron flux is highest. The endothermic nature of the $^9\text{Be}(n,2n)$ could allow the local heating to be reduced compared to the exothermic nature of the $^6\text{Li}(n,t)$ which would cause additional local heating.

The variation in spectrum, the difference in cross section and the different Q values suggest that a uniform mixture of the two materials is not optimal. Preliminary calculations suggest that the quantity of beryllium at the front of the blanket is expected to be higher than the optimal quantity at the rear of the blanket. As a first approximation, a linear variation in multiplier fraction, with respect to depth within the breeder blanket was decided upon.

5.3 Materials and methods

The MCNP model used in this study was adapted from a tokamak DEMO model developed at KIT [148]. The geometry was modified to incorporate a breeder blanket with a uniform blanket thickness of 68cm (see Figure 5.1). The model includes a first wall with a thin layer of armour, homogenised breeder modules, a rear shielding layer and a divertor with no breeding capability. Tungsten (3mm thick) was chosen for the first wall armour and Eurofer with helium coolant (3cm thick) was chosen for the first wall [83].

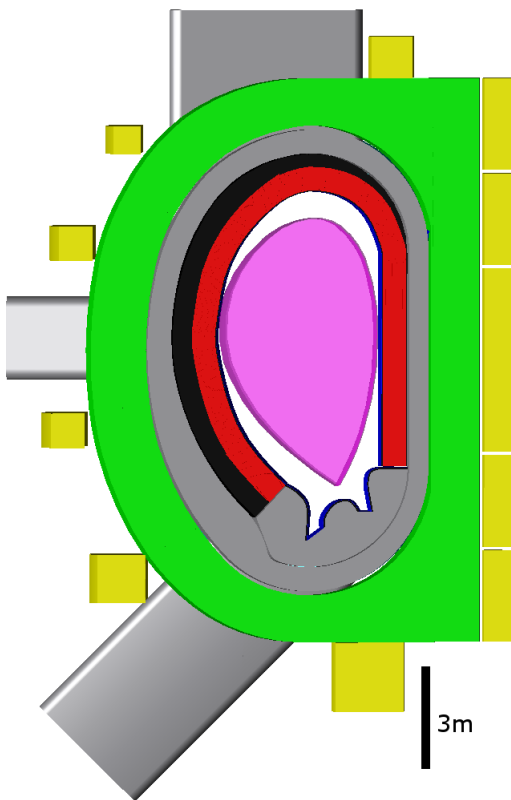


Fig. 5.1 The tokamak model used. The vacuum vessel and divertor (grey), toroidal field coils (green), poloidal field coils (yellow), blanket (red), blanket casing (black) and tungsten armour (blue) are included. Image generated using [200].

The blanket breeder zones contain a homogenised mixture of Eurofer, helium (as coolant and purge gas), Be_{12}Ti and Li_4SiO_4 enriched to 40% ${}^6\text{Li}$. Further details of the material composition are contained in Table 5.1.

The breeder zone was segmented into 40 layers of equal radial depth (1.7cm). The study aimed to vary the multiplier fraction throughout the blanket and observe the results.

Material	Component	Volume percent	Density (g/cm ³)
Homogenised breeder material	Eurofer	9.705	1.770 to 2.032
	He coolant	5.295	
	Li_4SiO_4	0 to 53.55	
	He purge gas	31.45	
	Be_{12}Ti	0 to 53.55	

Table 5.1 Material specifications for the homogenised breeder blanket material.

Multiplier fractions were chosen for the first layer; these ranged from 0 to 1 in increments of 0.0588. Multiplier fractions were chosen for the rear layer, these also ranged from 0 to 1 in increments of 0.0588. Every permutation of the 18 first layer and 18 rear layer compositions were considered and this resulted in 324 different MCNP models. Linear interpolation between the multiplier fraction in the front layer and the rear layer was used to find multiplier fractions for the remaining 38 layers in the middle. For example an initial multiplier fraction of 0.6 decreasing to 0.2 would involve decreasing the multiplier fraction by 0.01 with each layer (see Figure 5.2 for a diagrammatic representation).

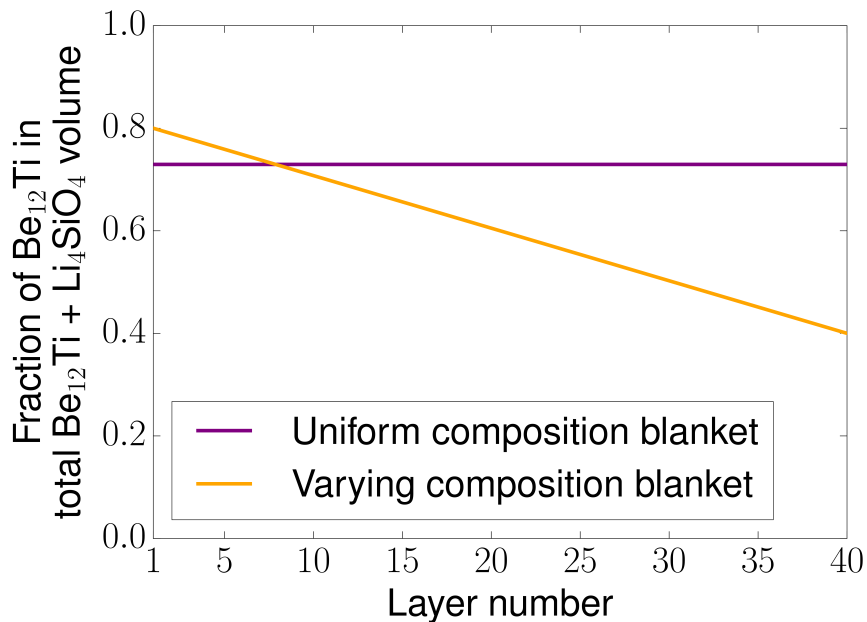


Fig. 5.2 Examples of how multiplier fraction varies with blanket depth.

$$\text{Multiplier fraction} = \frac{\text{Volume of Be}_{12}\text{Ti}}{\text{Volume of Be}_{12}\text{Ti} + \text{Volume of Li}_4\text{SiO}_4} \quad (5.1)$$

Once the material definitions of the breeder blanket were decided upon individual MCNP 6.0 [74] simulations for each of the 324 blanket permutations were carried out. FENDL 3.0 nuclear data [61] was used for particle transport. MCNP F6 tallies were set up to ascertain the energy deposition within the individual breeder blanket and casing cells. MCNP F4 tallies were used to find the TBR. The neutron plasma source utilised in the MCNP model [51] was represented using primary plasma parameters. The DEMO reactor simulated was 2.7GW fusion power.

5.4 Results

5.4.1 Performance of uniform multiplier fraction blankets.

Figure 5.3 shows the performance of breeder blankets with constant multiplier fractions throughout. Selecting the optimal composition depends on the relative importance of energy multiplication, peak heat, ^9Be usage and TBR. The parameter which is most commonly optimised is TBR and it is widely accepted that a TBR of at least 1.1 is required [44]. The maximum achievable TBR with a uniform multiplier fraction was found to be 1.21 for this model. This TBR optimised composition results in a ^9Be mass of 487.7 tonnes, peak heating of 9.65Wcm^{-3} and energy multiplication of 1.13. The uniform multiplier fraction blanket offers no scope to improve the overall performance while reducing the ^9Be usage. Reducing the ^9Be usage results in higher peak heat, lower energy multiplication and lower TBR values (see Figure 5.3). The results shown later in this chapter show that by varying the breeder fraction throughout the blanket it is possible to reduce the ^9Be without negatively impacting on the performance.

The results show that as the multiplier fraction is increased then peak heat in the blanket decreases. The neutron flux is attenuated by the blanket and this results in an exponential decrease in the neutron flux throughout the blanket. For this reason the peak heat tends to occur towards the front of the blanket and typically the first layer is the hottest. As the multiplier fraction increases, the energy deposited in the first layer decreases, due to the endothermic nature of the $^9\text{Be}(n,2n)$ reaction. At the same time the energy multiplication of the blanket increases as additional neutrons result in additional high Q value reactions, such as $^6\text{Li}(n,t)$ reactions where the Q value is 4.79MeV. At very high multiplier fractions, there is very little ^6Li available and other reactions with higher Q become increasingly probable. This results in a rapid rise in energy multiplication at high multiplier fractions.

To demonstrate the possible advantages of varying the multiplier fraction with blanket depth it is necessary to compare the performance of uniform composition blankets with non uniform blankets. The performance of the TBR optimised uniform blanket has been compared with the performance of varying multiplier fraction blankets (see Figure 5.8).

Figures 5.4 - 5.7 show the performance of both uniform and varying multiplier fraction blankets on the same diagram. The uniform blanket designs are included in Figures 5.4 - 5.7 but restricted to a relatively small section of the parameter space.

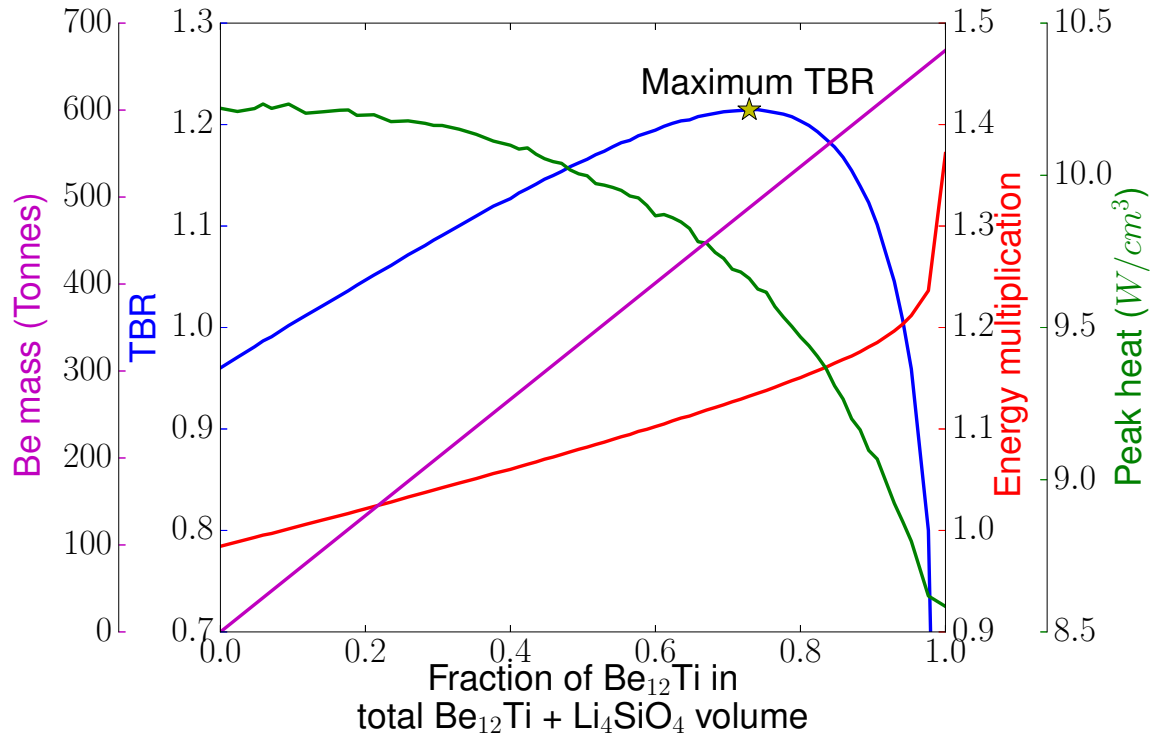


Fig. 5.3 Key performance criteria for different multiplier fractions in a mixed pebble bed breeder blanket utilising uniform multiplier fractions.

5.4.2 Decrease quantity of beryllium

Figure 5.4 shows the ${}^9\text{Be}$ required for each of the blankets simulated. As expected, blankets with high multiplier fractions at both the front and the rear of the blanket require the most ${}^9\text{Be}$. The dashed black line identified compositions that are achievable with a uniform multiplier fraction (designs with equal front and rear multiplier fractions). The location of the optimal TBR uniform multiplier fraction blanket is located on this line and requires a multiplier fraction of 0.74 at the front and rear which results in 487.73 tonnes of ${}^9\text{Be}$. The diagram includes a single contour line to identify varying multiplier fractions that also require 487.73 tonnes of ${}^9\text{Be}$. This contour line features again on Figure 5.8 where it helps to identify undesirable parameter space (i.e. blanket designs which require more Be_{12}Ti than 487.73 tonnes). Layers near the front of the breeder blanket have smaller volumes than the rear layers, this is revealed by Figure 5.4.

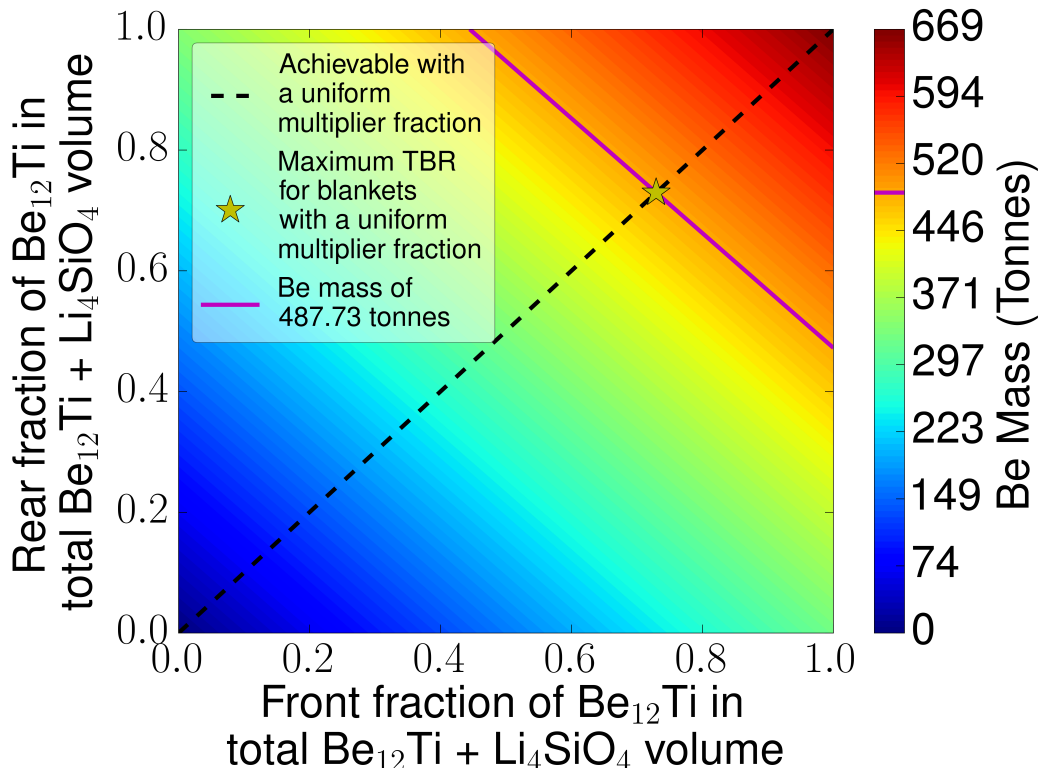


Fig. 5.4 Total ${}^9\text{Be}$ requirements for each blanket composition simulated.

5.4.3 Maintain sufficient tritium breeding ratio.

The TBR is dependant on the profile of the multiplier fraction throughout the blanket. Figure 5.5 shows that TBR is very sensitive to changes in the multiplier fraction at the front of the blanket. However, the TBR is relatively insensitive to variation in multiplier fraction at the rear of the blanket. The maximum TBR achievable using a uniform multiplier fraction blanket was found to be 1.2147; this was achieved with a multiplier fraction of 0.741 throughout the blanket. A marginal increase in TBR is achievable ($TBR = 1.2150$) if a varying multiplier fraction is used. The maximum TBR achievable with a varying multiplier fraction requires a front breeder fraction of 0.765 and a rear breeder fraction of 0.647. This composition is not achievable with a uniform multiplier fraction. Increasing TBR is often desirable, however it is more desirable to demonstrate improvement in multiple performance criteria simultaneously. To identify parameter space that offers a high TBR a single contour line showing a TBR of 1.2 has been included; this contour line also features in Figure 5.8.

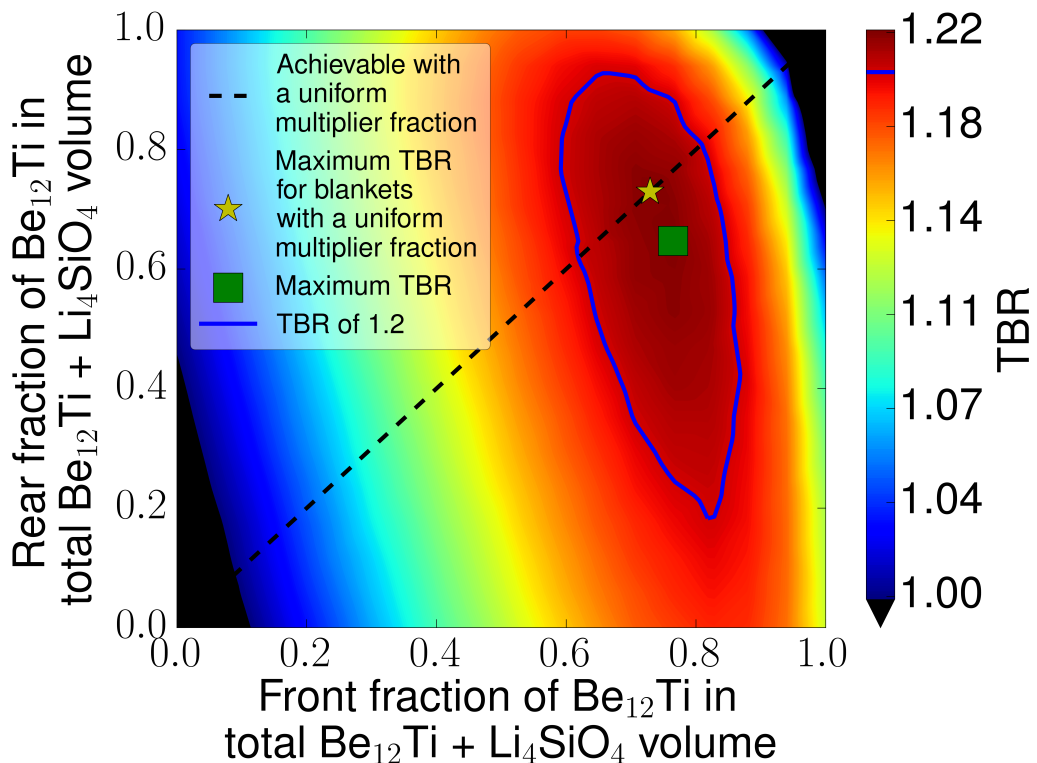


Fig. 5.5 The simulated TBR results for different blanket configurations.

5.4.4 Increase energy multiplication

Increasing the energy multiplication is desirable as it increases the quantity of electricity that can be generated by the reactor. Blankets with large quantities of ${}^9\text{Be}$ and in particular large multiplier fractions at the front, were found to produce the highest energy multiplication (see Figure 5.6). A single contour line representing an energy multiplication of 1.13 is included to show the performance of the TBR optimised uniform multiplier fraction blanket. The energy extraction for generating electricity is assumed to be exclusively from the breeder blanket. Although it is theoretically feasible to extract power from the divertor, this would result in additional complexities. Simply cooling the divertor is already considered a substantial challenge. Ultimately cost benefit analysis will be performed and the economical feasibility of extracting power from the divertor will be analysed. The contribution to the energy multiplication from the divertor is not likely to be largely influenced by blanket composition and has not been considered in this study.

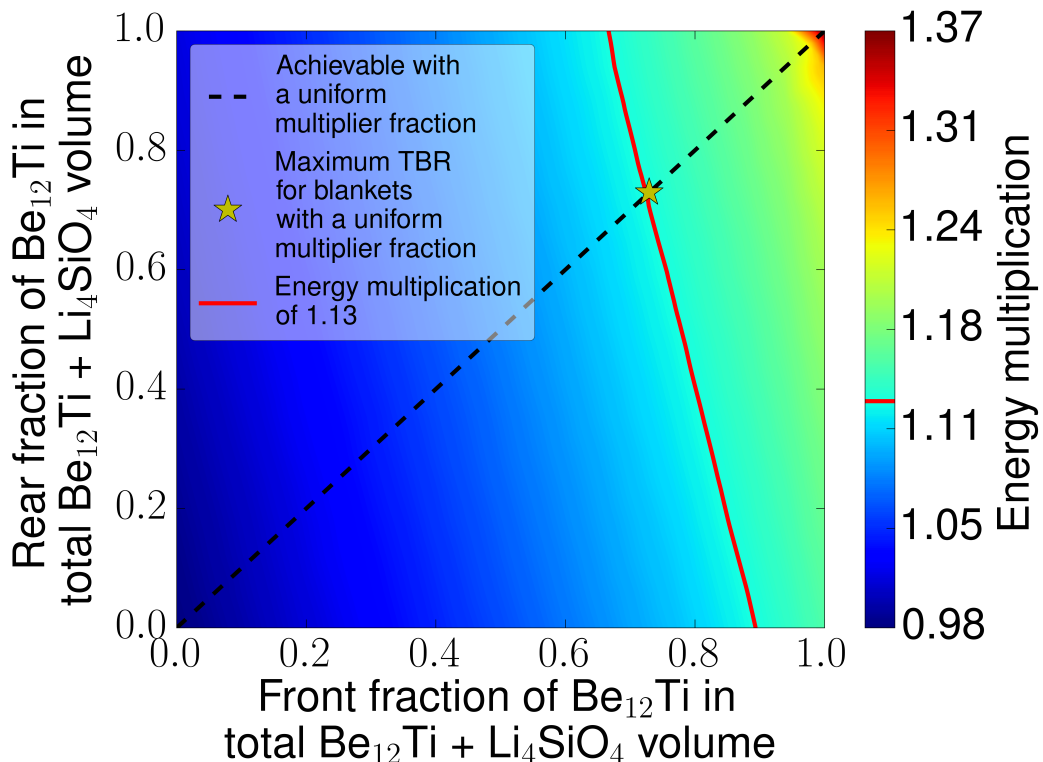


Fig. 5.6 Energy multiplication in the breeder blanket by neutrons and photons.

5.4.5 Reduced peak heating

The maximum neutronic and photonic energy deposited in any one region should be kept low to minimise the chance of material failure. As the ${}^9\text{Be}(n,2n)$ reaction is a threshold reaction and therefore endothermic, this results in lower temperatures in regions where the reaction occurs. Therefore use of ${}^9\text{Be}$ at the front of the blanket can reduce the peak heating in the blanket. Lower peak heating could result in a reduction of cooling requirements, this could leave more space for breeding materials and subsequently increase the TBR. Large multiplier fractions at the rear of the blanket do not help to reduce the peak heat. In this case ${}^9\text{Be}$ acts increasingly as a neutron reflector. The worst performing blanket in terms of peak heat has large quantities of Be_{12}Ti at the rear of the blanket and large quantities of Li at the front.

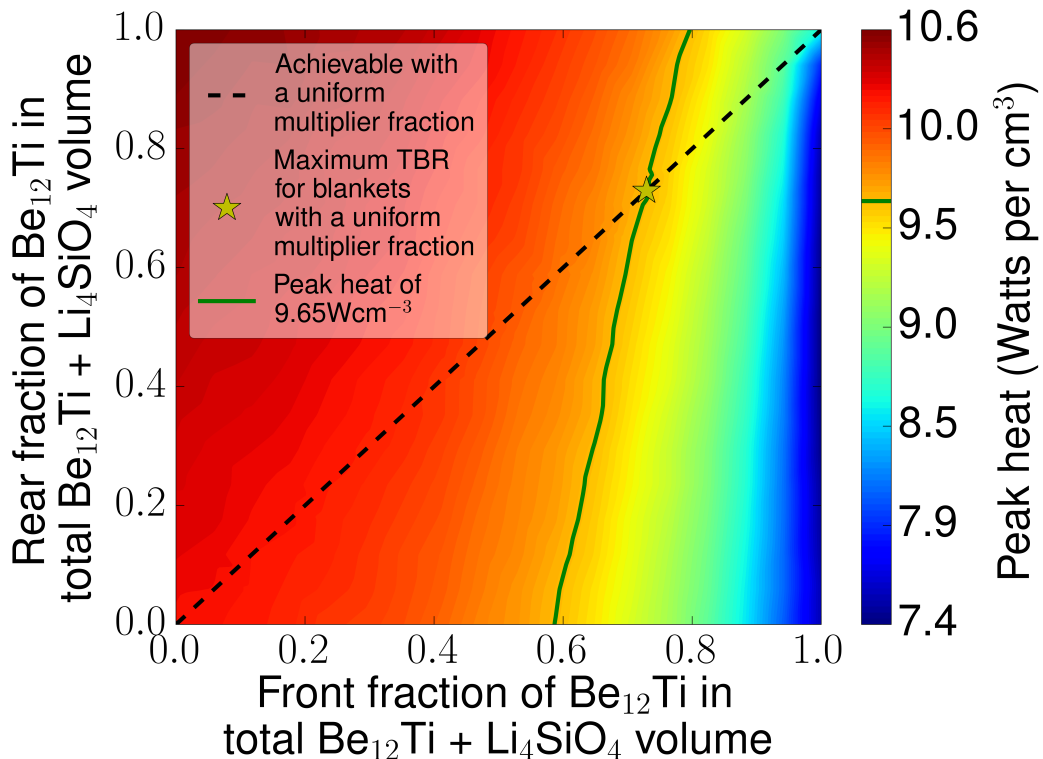


Fig. 5.7 Peak nuclear heating (photon and neutron) in the variable multiplier fraction blankets.

5.4.6 Improved performance

Comparing the performance of blanket designs with uniform and varying multiplier fractions shows the additional flexibility allowed by varying the multiplier fraction. Figure 5.3 shows that reduction in the ${}^9\text{Be}$ mass for uniform multiplier fraction blankets results in detrimental performance, as energy multiplication reduces and peak nuclear heating increases.

Blanket designs using a varying multiplier fraction can offer reductions in ${}^9\text{Be}$ mass without these disadvantages. Moving away from the optimal TBR configuration to improve energy multiplication and peak heating naturally involves some reduction of TBR for both blanket designs. Figure 5.5 reveals that variable multiplier fraction blankets are capable of reducing the rear multiplier fraction with only minimal reduction in TBR. Figure 5.8 identifies blanket configurations (yellow region) that offer higher energy multiplication, lower peak heat, less ${}^9\text{Be}$ usage and minimal reduction to TBR when compared to the uniform multiplier fraction blanket optimised for TBR.

Figure 5.8 also shows one example blanket configuration which could be considered an improvement. This blanket configuration simultaneously uses 10% less ${}^9\text{Be}$, increasing the energy multiplication by 1%, reducing the peak heating by 7% and maintaining a sufficiently high TBR (1.2) when compared to the performance achievable using a single uniform composition. This reduction in ${}^9\text{Be}$ usage and subsequent improvement in energy multiplication and reduction of peak heating is not accessible with a uniform multiplier fraction blanket. The best composition depends upon the preference placed on optimising each of the performance criteria. However, a far wider range of values is accessible when using varying multiplier fractions compared to a uniform multiplier fraction.

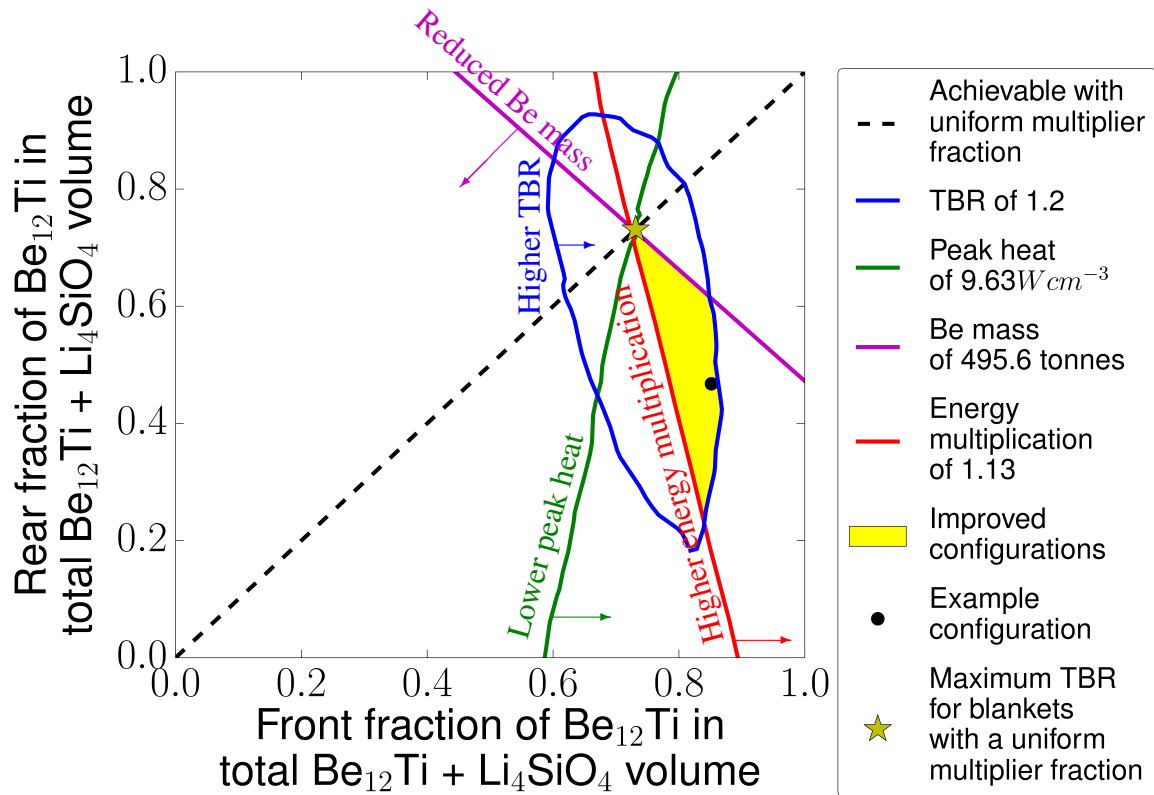


Fig. 5.8 The diagram shows the region of blanket configurations that offer higher energy multiplication, lower peak heat, less ${}^9\text{Be}$ usage than the uniform multiplier fraction blanket (optimised for TBR).

5.5 Conclusion

Linear variations in multiplier fraction are one way to better utilise the different nuclear properties (cross section and Q value) of ^9Be and ^6Li . Blankets employing a varying multiplier fraction were shown to achieve higher TBR values than blankets with uniform multiplier fractions (see Figure 5.5). The performance of the blanket in key areas such as peak heating and energy multiplication were improved, whilst achieving a reduction in the quantity of ^9Be . This was not possible with a uniform multiplier fraction blanket. A reduction of 10% in the ^9Be mass of blankets was found to be achievable when using varying multiplier fractions. In addition to reducing the use of a precious resource there are potential financial advantages of using less Be_{12}Ti , as it is likely to be more expensive than Li_4SiO_4 . The cost of Be_{12}Ti was estimated to be \$4,500 per kg [38], the cost of Li_4SiO_4 (with natural Li) was estimated to be \$1000 per kg [100] and the cost of enriching ^6Li to 40% was estimated as \$1,700 per kg[45]. The cost estimates used were provided by experts in their respective fields and assume a cost reduction when compared to the current price which is based on a smaller scale of production for research purposes. Using these cost estimates the reduction of Be_{12}Ti by 10% would reduce the material costs of the blanket by \$120M. Although the linear variation in multiplier fraction improves upon current mixed ceramic blanket designs, using a uniform multiplier fraction is likely to be suboptimal. Nonlinear variations in multiplier fraction in the poloidal and toroidal directions should be considered and could potentially further improve the performance of the blanket.

Chapter 6

Layered breeder blanket

6.1 Introduction

The primary requirement of the blanket is to breed sufficient tritium to sustain the reactor. This is particularly challenging for reactor designs that have reduced space available for breeder blankets. Reduction in blanket volume could occur due to use of upper and lower diverters (also known as double null) [96], blanket penetrations for diagnostics or heating [207] and designs that do not include breeder blankets around the inner solenoid [123]. There is a renewed emphasis on ensuring the reactor has a sufficiently high TBR to accommodate potential reductions in blanket volume.

The research carried out in this chapter seeks to increase the tritium production within breeder blankets so that potential reductions in blanket coverage can be mitigated against. This is achieved by segmenting the blanket into layers and varying the material composition of individual layers within the blanket. Previous chapters have looked at varying the bulk breeder material (Chapter 3) and making linear variations in material composition with depth (Chapter 5). This chapter extends the work previously carried out by allowing more flexible variation in blanket composition with depth. This more flexible approach is potentially able to better utilise the different material cross sections involved and maximise tritium production.

Material	Material description	Volume fraction
Be	Neutron multiplier	0 to 0.6075584
Li	Tritium breeder	0 to 0.6075584
He	Helium coolant	0.01789357
He	Purge gas	0.3417516
Eurofer	Structural material	0.03279643

Table 6.1 Volume fractions of the materials used in the homogenised breeder zone.

6.2 Method

The approach taken involved adapting an existing EU HPCB DEMO design developed by KIT under an EFDA 3PT task [148]. The breeder zones within the model were segmented into eight layers of equal depth (4.9cm). Section dividers (0.9cm thick) have been added between the layers to represent structural cooling plates. The combined thickness of the breeder zones and the inter-layer cooling plates was 45.5cm. Figure 6.1 shows the DEMO model used and detailed views of the layered blanket design. Dimensions of the blanket components were based on existing mixed bed blanket designs [117].

Layers were filled with a homogenised mixture of Be_{12}Ti , Li_4SiO_4 , Eurofer and helium gas (used for purge gas and coolant). More details on the additional materials are given in Table 6.1, the composition is similar to previous chapters. The homogenised material used in these breeder zones contains less structural steel (5%) compared to previous chapters (9.705%). However, this model contains additional Eurofer in the inter layer dividers and the total Eurofer volume is equivalent.

The aim is to show that by varying the material composition as a function of blanket depth, it is possible to improve the tritium production of a breeder blanket. For this preliminary study a uniform blanket thickness was incorporated into the model. This ensured that similar neutron spectra were experienced by corresponding layers in different breeder modules and reduced the complexity of the study but allowed the principle to be demonstrated. However, it is likely that in more realistic reactor designs the outboard blanket would be thicker than the inboard. This inaccuracy in the model is not important in terms of proving the idea of non uniform breeder blankets. However, if this was to be incorporated into more

realistic reactor designs then optimisation for different thickness blankets would need to be carried out. Naturally this would be far more computationally expensive and is not required to demonstrate the principle.

There are engineering difficulties in making mixed pebble beds. For instance, it may be challenging to create single pebbled beds with multiple different pebble ratios. Pebbles may move from their planned location during the filling process and the resulting mixture might not represent the intended composition. By dividing the bed into discreet sections each part could be filled separately with pebbles premixed to the desired ratio. The dividers would prohibit any unwanted mixing between layers.

The approach taken to illustrate that non uniform blanket compositions can breed more tritium than uniform blanket compositions involved two stages. Firstly the maximum TBR achievable using uniform breeder blankets at two different ${}^6\text{Li}$ enrichments was found. MCNP 6.0 simulations were carried out involving a wide range of material compositions in the breeder zones in order to find the maximum TBR achievable with a uniform blanket. In each separate simulation the material composition was kept constant in all eight layers of the breeder blanket. The breeder fraction was varied from (0 to 1), while ${}^6\text{Li}$ enrichments of 70% and 100% were used. The result of these simulations is shown in Figure 6.2.

The second stage was to find non uniform compositions capable of achieving higher TBR values than the uniform blankets, while keeping below the ${}^6\text{Li}$ enrichments already established. An exhaustive search involving every combination of beryllium fraction and ${}^6\text{Li}$ enrichment possible in the eight layer breeder blanket would provide the maximum TBR for non uniform blankets. However, it would be prohibitively computationally expensive. An exhaustive search of all the compositions was not required to show that layered blankets with different compositions can produce more tritium than uniform blankets . The approach taken was to use the best uniform composition as a starting design and try variations in this design to see if the TBR could be increased. Compositional variations to individual layers were made to make variants of the starting design. The material composition of individual layers was changed in one of the following ways:

- Increase the ${}^6\text{Li}$ enrichment by 2%.

- Decrease the ${}^6\text{Li}$ enrichment by 2%.
- Increase the breeder fraction by 2%.
- Decrease the breeder fraction by 2%.

Varying each of the eight layers in four different ways would result in 32 different variants of the starting design. However, ${}^6\text{Li}$ enrichment limits of 70% and 100% were set for the two cases investigated. In practise when the enrichment limits were applied, the number of variations simulated was reduced from 32 to 24 configurations. It is important to allow both increasing and decreasing the enrichment to be explored by the simulation as it is not known which composition will lead to the highest TBR. However, reducing the ${}^6\text{Li}$ enrichment from the initial values of 70% and 100% was never found to increase the TBR for this model. The winning composition from the previous round was always present in the compositions simulated in the following round. Once all the variations of the starting design had been constructed, simulations were performed of each variant and the TBR was found. The TBR values of all the variants were compared (see Figure 6.3) and the variant with the highest achieving TBR was chosen as the next starting composition from which future variants would be made. This process was repeated \sim 50 times and each time the highest performing TBR value was found (see Figure 6.6).

It is possible for MCNP simulations to result in TBR values that are over predictions of the TBR of the model. This is due to the statistical nature of the simulation technique. However, the winning blanket design is simulated again in the following round. When the winning blanket design was simulated a second time a different random seed value was used. This avoided obtaining the same TBR value and performing exactly the same simulation. By incorporating this into the system it decreases the chances of anomalous over predictions being misinterpreted.

Although the code was programmed to allow any step size in enrichment and breeder fraction, 2% was found to provide sufficiently different TBR values within the computation limits. Although smaller changes (less than 1%) would be desirable in order to obtain a better optimal value, this would require extended simulation time to obtain a noticeable difference between the different variants and to establish the best design of the round.

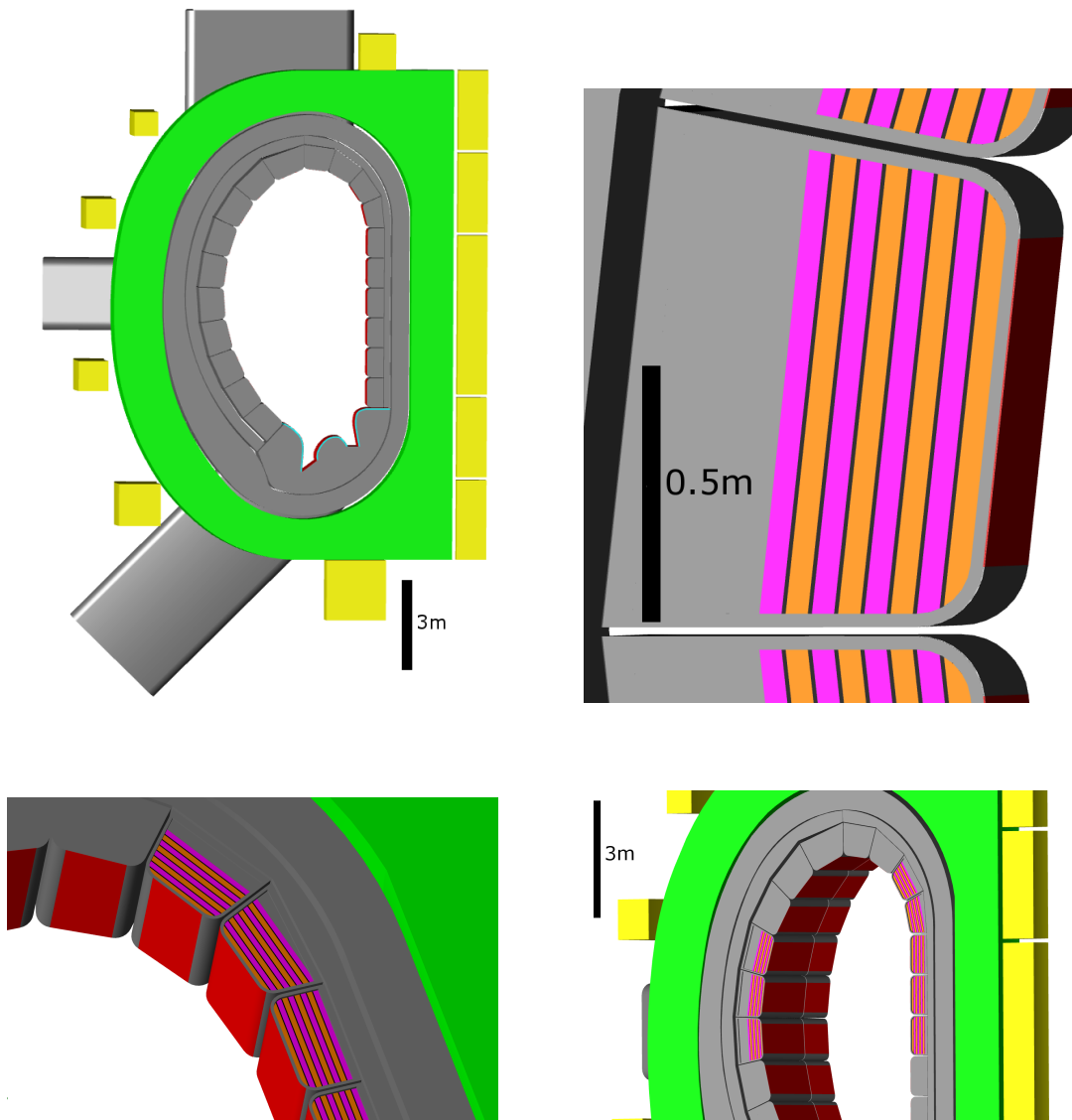


Fig. 6.1 Various views of the modified DEMO model used, showing the vacuum vessel, divertor and blanket casing (grey) ■, toroidal field coils (green) □, poloidal field coils (yellow) ▲, blanket (alternating layers orange □ and pink □) and tungsten armour (red) ▢ are included. Image generated using [200].

6.3 Results

Figure 6.2 shows the maximum TBR values achievable with uniform blankets and 70% and 100% ${}^6\text{Li}$ enrichment. The maximum TBR values were found to be 1.062 and 1.096 respectively. The additional ${}^6\text{Li}$ enrichment increased the TBR as expected. To find the maximum TBR values for uniform composition breeder blankets 200 simulations were performed. The optimal multiplier fractions for 70% and 100% ${}^6\text{Li}$ enrichment were found to be 0.66 and 0.72 respectively. A higher ${}^6\text{Li}$ enrichment has previously been shown (see Chapter 2) to require a higher multiplier ratio to maximise the TBR.

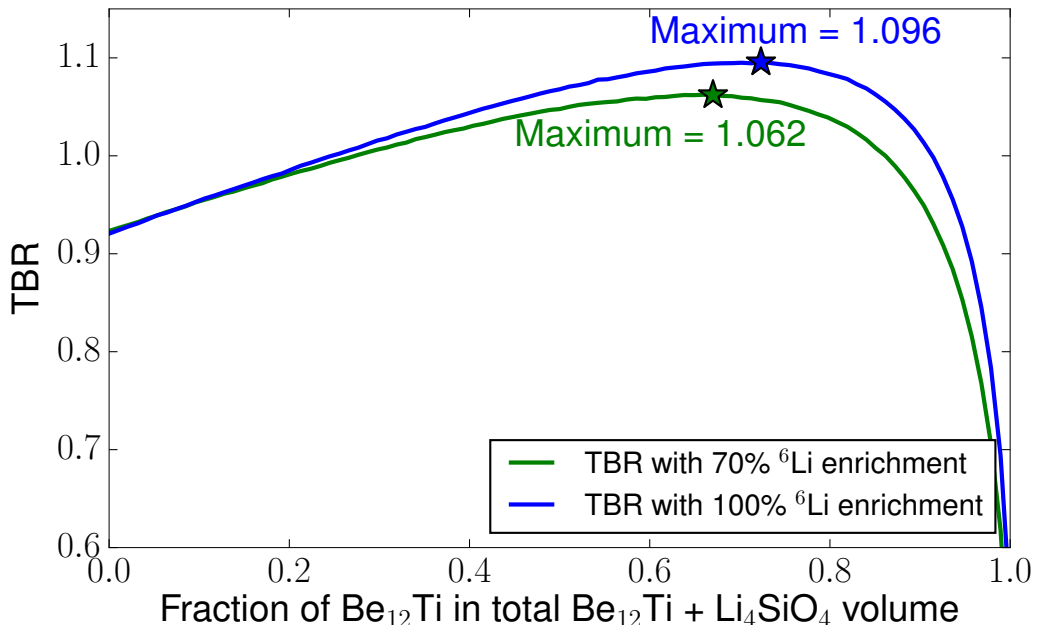


Fig. 6.2 Optimising the composition of a uniform blanket for two different enrichments of ${}^6\text{Li}$

Figure 6.3 shows typical results produced by a round. From these results it is clear to see that decreasing the ${}^6\text{Li}$ enrichment by 2% in any of the blanket layers results in reduced TBR. Increasing the ${}^6\text{Li}$ enrichment in any of the eight layers was not simulated in this particular batch as the starting design was already enriched to the ${}^6\text{Li}$ limit. Other variations are shown to reduce the TBR of the blanket, for instance, increasing the multiplier fraction in either of the first two layers of the blanket would decrease the TBR. In contrast to this, decreasing the multiplier fraction in either of the first two layers would increase the TBR. It was common to find that increasing or decreasing the multiplier fraction in an individual layer has opposite impacts on the TBR. This is to be expected and gives some confidence to the results. Ideally it would have been beneficial to run the simulations with more particle histories (2×10^7 was used), as this would decrease the size of the error bars. Due to the limitations in computational power it was not possible to increase the number of particle histories run with each round. It is possible that due to overlapping error bars an incorrect win was chosen in some rounds. As the non uniform blanket composition approached high TBR values, the compositional changes made resulted in less and less difference in TBR values.

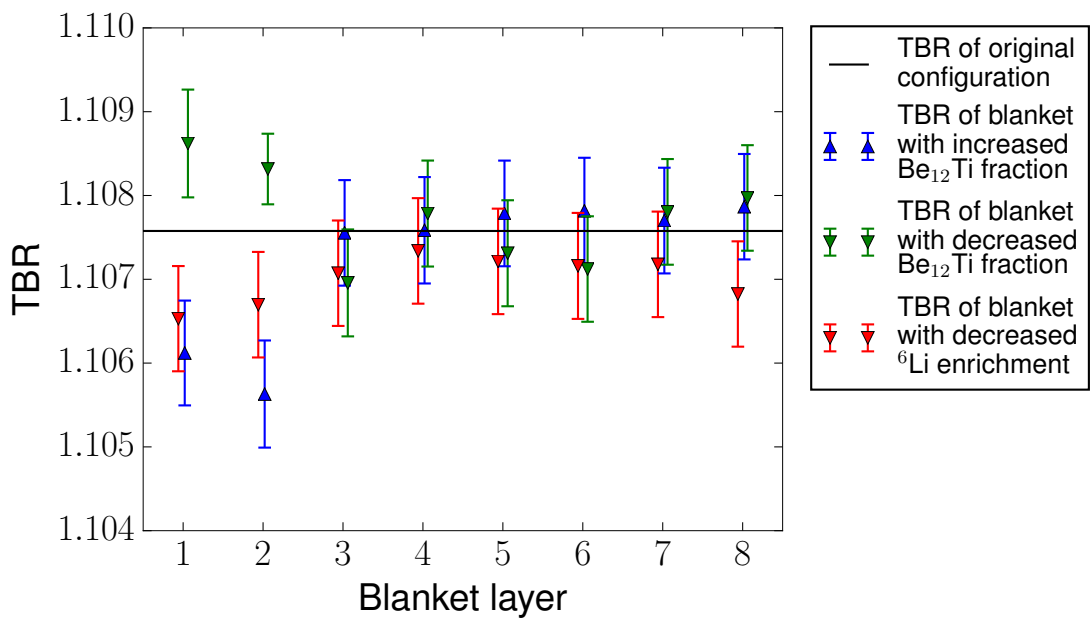


Fig. 6.3 Results showing the TBR values of 24 variations to the starting design. Error bars shown are derived from statistical error data produced by MCNP and show a 1 sigma confidence.

Figures 6.4 and 6.5 show the composition found after 51 rounds of simulations were completed. It is important to note that this final composition may not be the optimal composition possible and this was not an exhaustive search. However, in both cases the multiplier fraction towards the rear of the blanket has been decreased. Also the multiplier fraction in the first layer is lower than the second layer. These observations are well supported by the cross sections of the important reactions involved. For instance, the reduction of beryllium at the rear of the blanket is well founded, as the neutrons have been moderated to some degree when they reach the rear. The ${}^9\text{Be}(\text{n},2\text{n})$ reaction is threshold and requires neutrons above 1.8MeV. The reduction of beryllium at the front could be due to the scattering properties of beryllium. Having too much beryllium at the front of the blanket could be acting as a reflector, prohibiting neutrons from entering the blanket.

These results also have a bearing on the work carried out in Chapter 5. Chapter 5 showed that a linear variation in multiplier fraction was better (higher TBR) than a uniform multiplier fraction throughout the blanket.

Also, the final variation in multiplier fraction of the blanket is not well approximated by a straight line. The work carried out in Chapter 5 found that the TBR could be increased (compared to a uniform blanket) by linear variations in the breeder fraction. These two figures indicate that non linear variations in multiplier fractions are preferable when seeking to optimise the TBR.

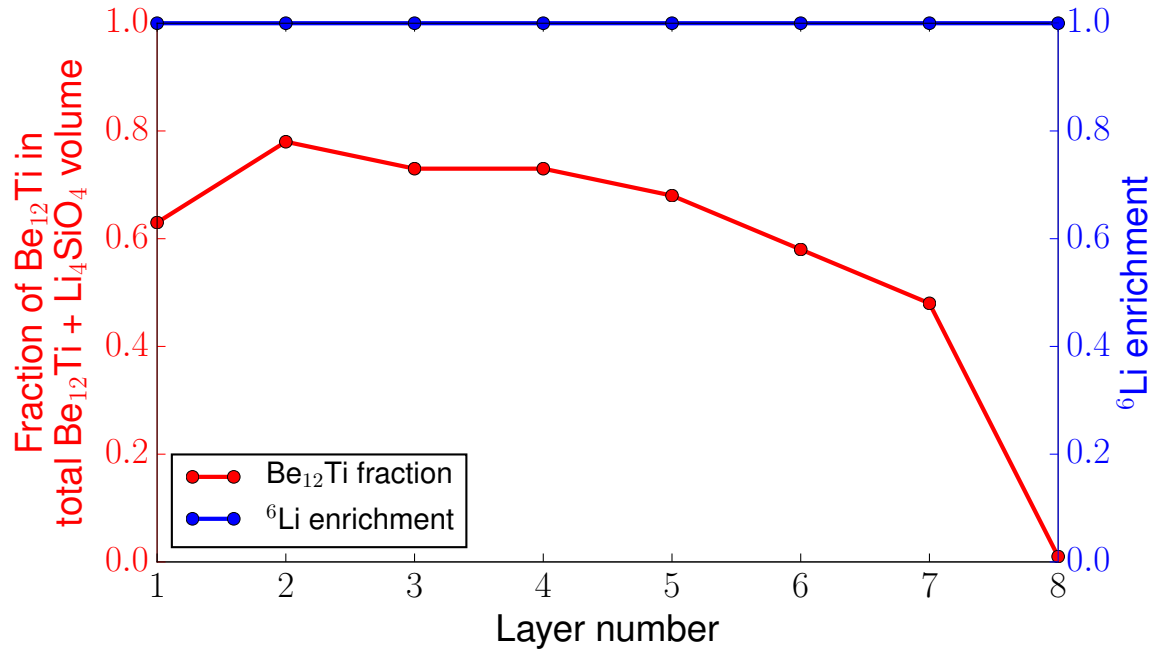


Fig. 6.4 Final composition found when the ${}^6\text{Li}$ enrichment was limited to 100%

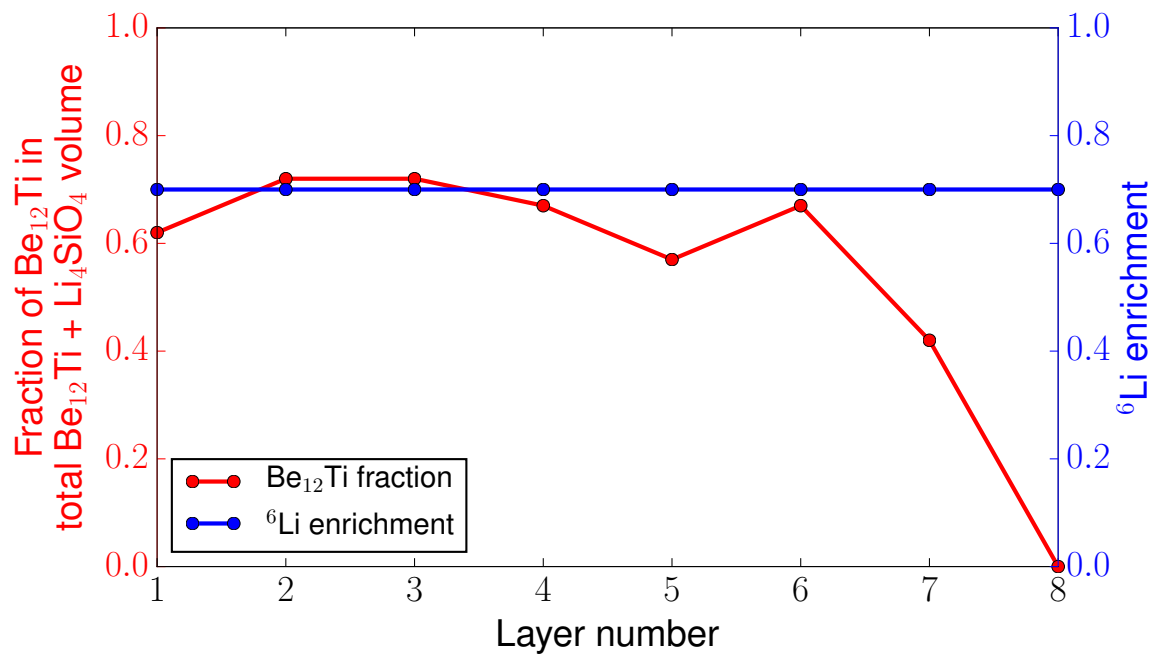


Fig. 6.5 Final composition found when the ${}^6\text{Li}$ enrichment was limited to 70%

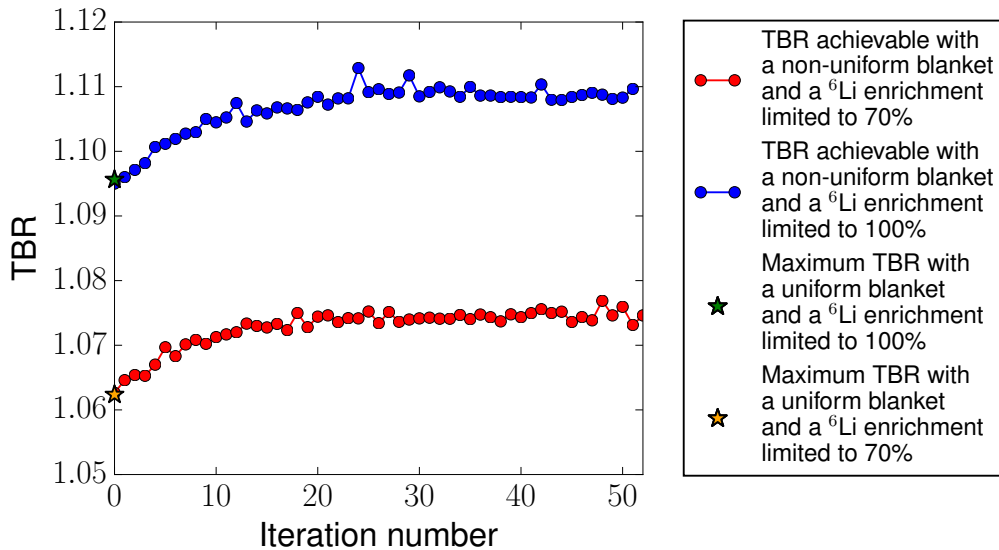


Fig. 6.6 Maximum TBR achieved with each iteration of the blanket composition.

	Uniform composition blanket	Non uniform composition blanket
Maximum TBR with 70% enriched ${}^6\text{Li}$	1.062	1.073
Maximum TBR with 100% enriched ${}^6\text{Li}$	1.096	1.109

Table 6.2 Comparison of TBR value achievable when using the uniform and non uniform blankets.

The process of continually selecting the highest performing design and simulating variations of this design, resulted in gradually increasing values of TBR achieved by the blanket. The maximum TBR achievable with the uniform blanket design was improved upon in both of the example ${}^6\text{Li}$ enrichments. The improvement was most rapid with the initial changes to the blanket composition. Occasionally an erroneously high TBR value can be observed. This is due to statistical variation in the simulated TBR values. After ~ 20 iterations the value of TBR achieved plateaued. The final improvement, by switching from uniform to non uniform, was +0.013 for the 100% ${}^6\text{Li}$ enrichment example and +0.011 for the 70% ${}^6\text{Li}$ enrichment example. A comparison of the TBR performance of the two blanket designs can be seen in Table 6.2.

6.4 Conclusion

This preliminary study has shown that by moving to non uniform blankets the TBR of blankets can be increased. The example ${}^6\text{Li}$ enrichments considered in this study showed that an increase of over 0.01 is achievable with moderate changes to the blanket composition. The reduction of the Be_{12}Ti towards the rear of the blanket was found to increase the TBR. This finding is supported by the cross sections involved in important reactions within the blanket (as discussed in Chapter 5). This study highlights the potential increase in TBR achievable. If DEMO designs require the volume available for breeder blankets to be reduced then this is one potential method of compensating. Other suggestions such as using cellular breeding material could potentially also increase the TBR achievable. If further work is to be carried out on varying the composition then more optimal numerical methods for finding the optimal composition should be considered. Also it would be interesting to look at variation of the composition as a function of width as well as depth. Breeder material at the periphery of the blanket's width receive a different neutron spectrum compared to the central region; this is due to the nearby structural material required for the first wall. The blanket might benefit from breeder material at the periphery of the blanket offering reduced neutron multiplication and increased tritium production. This is simply due to the probability of neutron leakage which is related to the distance from the edge of the blanket. Neutrons born at the periphery have a greater chance of escaping the blanket module compared to neutrons born in the centre of the blanket.

Chapter 7

Isotopically Enriched Structural Materials

7.1 Introduction

Material selection in fusion breeder blankets is particularly challenging, due to the environmental conditions. Selection criteria include neutronic considerations such as low activation and low gas production as well as engineering requirements, such as high melting point, high tensile strength and chemical compatibility with other materials. The work presented in this chapter looks at the effect of isotopic enrichment on the neutronics properties of two candidate materials (CuCrZr and Eurofer).

CuCrZr is a candidate material for plasma facing components and is also used for bonding materials to tungsten [34]. In both of the potential uses CuCrZr will be subject to intense neutron fluxes. Production of helium gas through (n,α) reactions leads to helium embrittlement and ultimately to material failure. Helium preferentially collects at grain boundaries forming small bubbles of high pressure gas. The strain can initiate cracks which propagate along the grain boundaries and reduce the structural integrity of the material. This process has been studied and there is evidence to suggest that the lifetime of materials in fusion reactors such as CuCrZr will be limited by helium embrittlement [70]. The expected lifetime of materials is dependant upon variables such as grain size, position within the reactor and

material composition.

Eurofer steel is a candidate material for structural parts of the breeder blanket. Traditionally, the composition of low activation materials (LAMs) such as Eurofer has been chosen based on the elemental properties [99]. Nuclear properties of elements with a natural abundance of isotopes present were considered. Elements such as Al, B, Co, Cu, Mo, Nb, and Ni have been limited or removed from LAMs because their elemental composition was prone to activation [98] [89] [99]. The limiting or removal of these elements can have negative impact on the engineering properties of the material (e.g reduced fracture toughness and yield stress). This is certainly true in the case of addition of Ni in steel which has been shown to mitigate against irradiation embrittlement [85] and the addition of Mo has been shown to increase the hardenability of steel [116]. It is feasible that Ni and Mo additions to Eurofer steel will bring similar benefits.

While individual isotopes of the same element have similar mechanical and chemical properties they differ in their nuclear properties. Materials made using elements in their natural abundances will have different nuclear properties when compared to enriched materials that are comprised of different isotopic abundances. The nuclear properties of the different isotopes of the same elements can be very diverse. In certain cases enriching an individual isotope (e.g. ^{235}U , ^{64}Zr , ^6Li and ^{10}B) results in very different nuclear properties when compared to the properties of the natural element. Isotopic enrichment is required to achieve the desired result. Isotopically enriched low activation materials (ITLAMs) are introduced as a possible method of improving the material's properties, while avoiding detrimental nuclear consequences. Isotopic tailoring of materials for fusion applications has been previously researched:

- Lithium is enriched to improve the tritium producing performance of some breeder blankets. Using D_2O instead of H_2O as the coolant has also been considered to increase tritium production [112].
- The enrichment of structural steels to achieve low activation has previously been researched [28] [119] [177].
- Enrichment of particular elements such as titanium [178] and silicon [138] to achieve

low activation and reduced gas production.

The research on isotopic enrichment in fusion reactors carried out to date looks at reducing the activity or increasing the TBR. The research carried out in this chapter builds on the existing work in the field and aims to show additional potential benefits of isotopic enrichment. Research that I have carried out and presented in this chapter has also been published in a journal article on the isotopic enrichment [132].

The production of gas (He) in CuCrZr is investigated and the dominant cause of helium production is identified as an individual isotope of Cu. Enrichment of Cu is then considered to mitigate against excessive helium production and prolong the estimated lifetime of the material.

Adding previously prohibited elements (Ni and Mo) back into the LAMs (Eurofer) is also considered. The isotopic composition of the reintroduced elements is enriched so that the nuclear properties of the element can be improved in comparison to the natural element. The irradiation of Eurofer with additional enriched Ni and Mo was simulated and the activity of the resulting materials was found to be comparable with unaltered Eurofer.

7.2 Theory

Cu accounts for the vast majority of material within CuCrZr (98.95% of mass). Two isotopes are present in natural Cu and they differ in their capacity to create helium from incident neutrons (see Figure 7.1). ^{63}Cu is a more prolific producer of helium compared to ^{65}Cu . As Cu has only two natural isotopes, depleting ^{63}Cu and enriching ^{65}Cu appears relatively straightforward. There appears to be potential for reduced helium production as the $^{63}\text{Cu}(n,\alpha)$ cross-section is larger than $^{65}\text{Cu}(n,\alpha)$ at all energies.

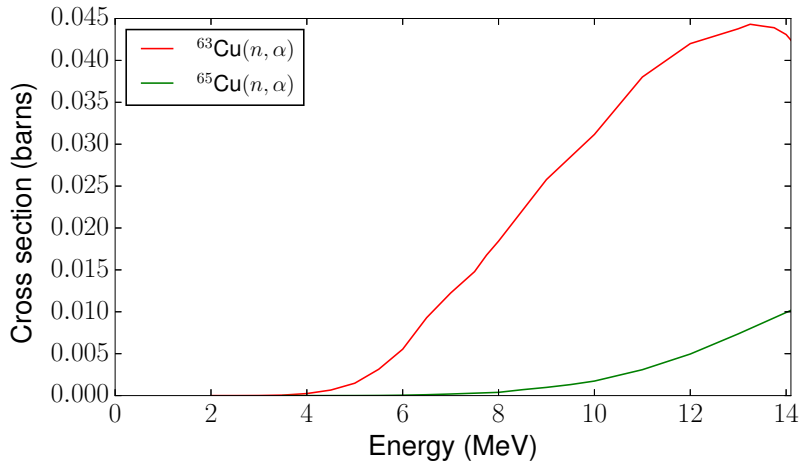


Fig. 7.1 (n, α) cross-sections for the two stable Cu isotopes. Data from the ENDF/B-VII.1 library [22].

The critical bulk concentration of helium atoms in copper can be calculated using the method described in [70]. The method used assumes the material is pure copper and assumes unimpeded migration of He atoms to the grain boundaries. The method does not account for helium atoms being pinned at dislocations or escaping the material. Therefore the method suggested by [70] over predicts the critical bulk concentrations and further work is needed to refine this diffusion model. However, as a representative figure the critical bulk concentration in copper is found to be 615ppm. Once this concentration of helium is reached, the material cracks along the grain boundaries and fails.

The activation of the isotopes belonging to the same element vary. The isotopes making up the elements have different neutron disappearance cross-sections (see Figures 7.2 and

7.3). Neutron disappearance is the sum of all reaction channels that involve an incident neutron and do not produce a neutron as one of the products. In the ENDF cross-section tables [22], reactions have unique MT numbers [182] assigned to them and (n ,disappearance) is the sum of MT numbers 102-117, 155, 182, 191-193 and 197). Not only do the isotopes differ in terms of their neutron absorption but they also produce different daughter products when they decay. This results in each isotope producing a unique distribution of daughter products following irradiation. Some of the daughter products produced will be stable (e.g. $^{60}\text{Ni}(n,\gamma)^{61}\text{Ni}$), while others could be radioactive (e.g. $^{60}\text{Ni}(n,p)^{60}\text{Co}$).

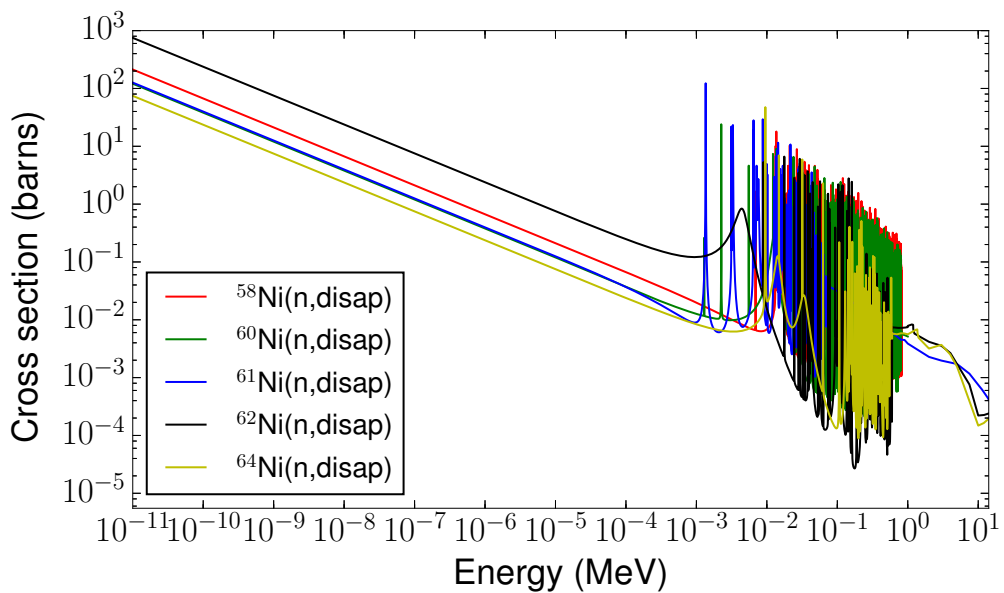


Fig. 7.2 Neutron disappearance cross-sections for the different Ni isotopes.

In summary, the nuclear data presented supports the theory that there are potential reductions in gas production of CuCrZr as well as reductions in Ni and Mo activation.

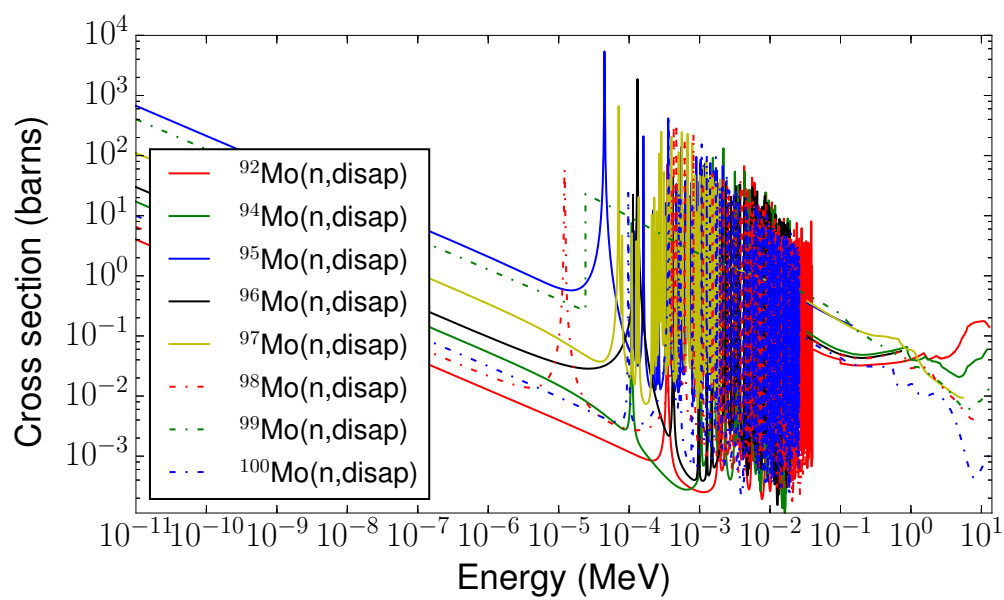


Fig. 7.3 Neutron disappearance cross-sections for the different Mo isotopes.

7.3 Materials and methods

A DEMO model generated with the HERCULES code was used [144] in order to assess the impact of ITLAMs. The HERCULES code is capable of creating MCNP compatible models of fusion devices based on primary parameters (e.g. major radius of the device and aspect ratio). A thermal power of 1GW and other primary inputs that were consistent with recent DEMO studies were used [94]. The reactor was assumed to operate at 70% [185] availability for 5 years before the blankets are changed. Figure 7.4 shows the resulting DEMO model generated. The DT neutron source simulated [51] was based on primary plasma parameters and the source spatial distribution is included in Figure 7.4. The advantage of using parameters to generate models is the ability to adapt the model quickly and perform iterative scoping studies. This is often necessary as DEMO designs are continually refined.

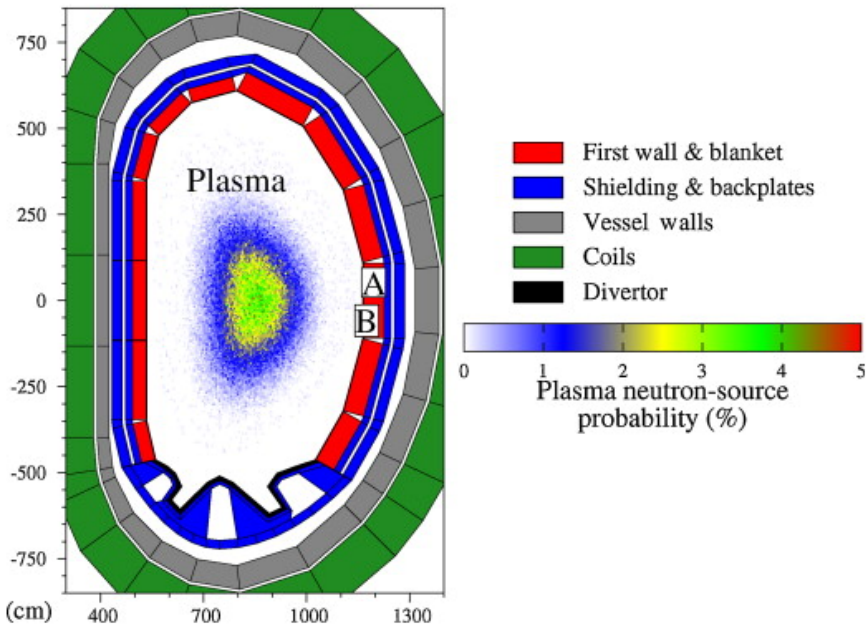


Fig. 7.4 View of the HCPB DEMO model used. Individual components of the fusion reactor and the plasma source intensity are shown. The location of the Eurofer within the blanket (A) and the CuCrZr as a plasma facing component (B) are shown. Image source [132].

Material choices were consistent with existing HCPB blanket designs and produced as part of the HERCULES output code. The material choices are largely the same as the materials used in previous chapters. The main difference is the use of an homogenised first

wall consisting of Eurofer, water and tungsten with volume fractions of 72%, 18% and 10% respectively. Previous chapters have used a semi-heterogeneous first wall and employed helium as a coolant, however both coolants are currently considered viable.

The particle transport was simulated using MCNP 6.0 together with FENDL 3.0 [61] nuclear data. The neutron spectra averaged over the blanket (position A in Figure 7.5) and averaged over the first wall (position B in Figure 7.5) were found using track length (F4) tallies with a 709 energy group structure (see [179] for details on the energy group structure). The neutron spectrum was then used as an input for FISPACT-II which is able to track nuclide reactions and decays as a function of time. Additional FISPACT inputs were TENDL 2012 nuclear data library [104], a description of the material composition and a DEMO relevant irradiation duration (5 years). FISPACT is able to predict the activity at specified times and this information was used to produce Figures 7.7-7.8. FISPACT is also able to produce inventory files that specify the number density of the nuclides present in the material; this information was used to track helium production and was used to generate Figure 7.10. The breeder blanket (position A) experiences a softer neutron spectrum when compared to the first wall (position B) and an increase in thermal neutron flux. This is caused by neutron interactions within the first wall and the blanket, such as inelastic scattering which moderates the energy of the neutrons. The spectrum for the breeder blanket was obtained with an MCNP F4 tally and was averaged over the bulk material of all the breeder blanket modules. The spectrum for first wall is averaged over the entire first wall of the model.

When enriching or depleting elements it is necessary to know the natural abundance of each constituent isotope. The natural abundances of isotopes from [31] were used (see Table 7.1). Enriching a particular isotope requires depleting the other isotopes so that the sum of all isotopes remains at 100%. This is simple in the case of copper as only two isotopes are present and enriching one isotope by a certain amount results in an equal depletion of the other isotope. In elements with more than two isotopes (Mo and Ni) the abundance of depleted isotopes was set proportionally to the natural abundance.

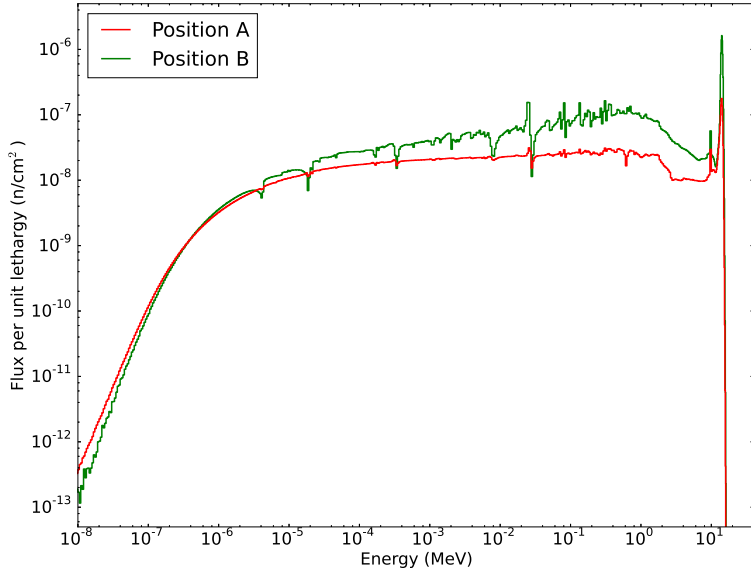


Fig. 7.5 MCNP F4 tallies showing the neutron spectra for the breeder blanket (position A) and the first wall (position B) shown in Figure 7.4.

Element	Isotope	Natural abundance
Mo	⁹² Mo	0.1453
	⁹⁴ Mo	0.0915
	⁹⁵ Mo	0.1584
	⁹⁶ Mo	0.1667
	⁹⁷ Mo	0.0960
	⁹⁸ Mo	0.2439
	¹⁰⁰ Mo	0.0982
Ni	⁵⁸ Ni	0.68077
	⁶⁰ Ni	0.26223
	⁶¹ Ni	0.011399
	⁶² Ni	0.036346
	⁶⁴ Ni	0.009255
Cu	⁶³ Cu	0.6915
	⁶⁵ Cu	0.3085

Table 7.1 Natural abundance of isotopes in each of the three elements that were selected for enrichment, data from [31].

7.4 Results

7.4.1 Additional Mo in Eurofer

Additional Mo was added to Eurofer in natural and enriched forms, in each case 2% of the Eurofer mass was replaced with Mo. The addition of natural Mo into Eurofer causes additional activation (see Figure 7.6). This results in a higher activity particularly in the 100-200 year time frame. The additional activity is caused predominantly by the activation of ^{92}Mo and ^{98}Mo (see Figure 7.7). ^{92}Mo produces ^{93}Mo , while ^{98}Mo produces ^{99}Tc , both of which are radioactive and have relatively long half-lives compared to other products of Mo irradiation. ^{93}Mo has a half-life of 4×10^3 years and ^{99}Tc has a half-life of 2.14×10^5 years [142]. The addition of Mo with highly reduced ^{92}Mo and ^{98}Mo content does not result in significant production of these long half-life radioactive products and can have very similar activity to Eurofer without Mo. There are several ways to achieve a reduced amount of the long half-life radioactive products mentioned. Either ^{92}Mo and ^{98}Mo could be depleted or ^{94}Mo , ^{95}Mo , ^{96}Mo , ^{97}Mo or ^{100}Mo could be enriched, as shown in Figure 7.7.

Figure 7.6 shows that additional Mo in the form of highly enriched ^{97}Mo results in similar activities to Eurofer without any additional Mo.

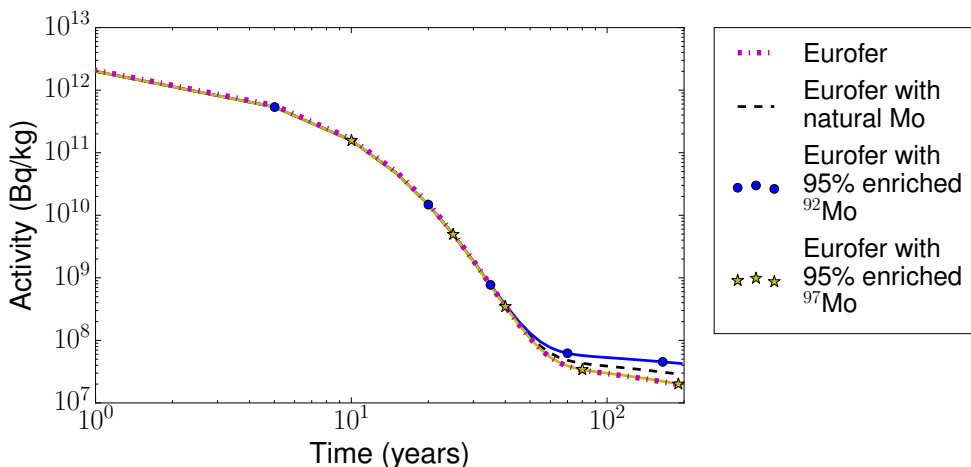


Fig. 7.6 The simulated activity of regular Eurofer compared to Eurofer with an additional 2% Mo mass.

Figure 7.7 shows the impact of adding additional Mo with different isotopes enriched. Enriching ^{92}Mo or ^{98}Mo results in additional activity while enriching ^{94}Mo , ^{95}Mo , ^{96}Mo , ^{97}Mo or ^{100}Mo results in reduced activity compared to natural Mo. Adding highly enriched (100%) ^{94}Mo , ^{95}Mo , ^{96}Mo , ^{97}Mo or ^{100}Mo can achieve the same low activity as Eurofer with no additional Mo.

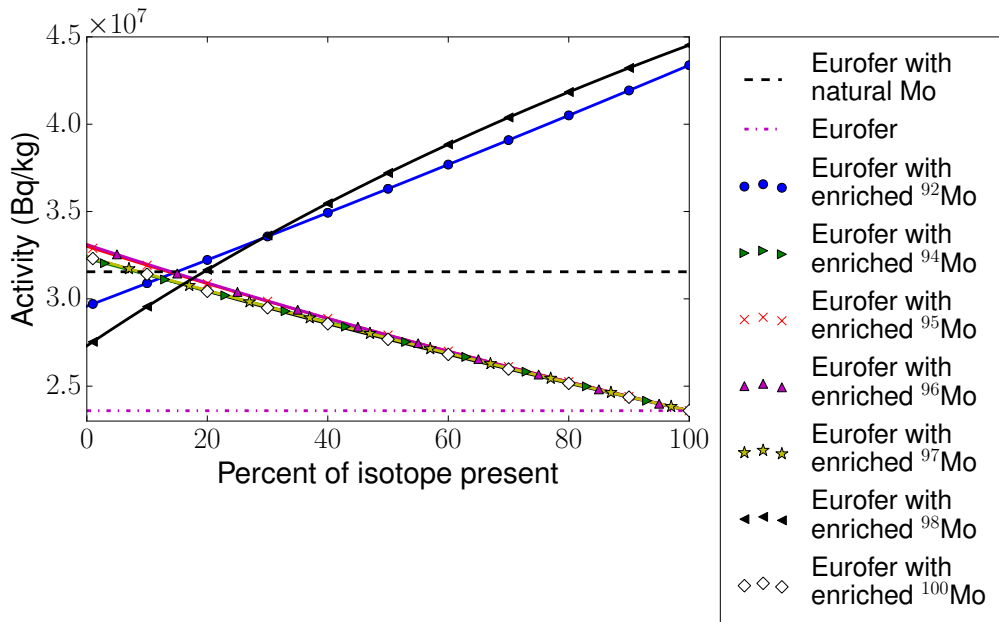


Fig. 7.7 The simulated activity of Eurofer containing 2% mass Mo additions with varying isotopic enrichments. For comparison, regular Eurofer and Eurofer with additional natural Mo are also plotted. The figure shows the activity 100 years after the end of irradiation.

7.4.2 Additional Ni in Eurofer

Additional Ni was added to Eurofer in natural and enriched forms. In each case 2% of the Eurofer mass was replaced with Ni. The addition of natural Ni into Eurofer causes additional activation (see Figure 7.8). This results in a higher activity which is particularly noticeable after 100 years. The additional activity is caused predominantly by the activation of ^{62}Ni (see Figure 7.9). ^{62}Ni produces ^{63}Ni via a (n,γ) reaction, the product is radioactive and has a long half-life (93 years). ^{58}Ni is the second most problematic isotope in natural Ni. Activation of ^{58}Ni also results in non-negligible quantities of ^{59}Ni produced via (n,γ)

reactions; the product is radioactive and has a very long half-life (76,000 years). The addition of Ni with highly enriched ^{60}Ni and ^{64}Ni content results in less activity than Eurofer with additional natural Ni. However, in all cases of additional Ni, the activity is above that of Eurofer without Ni.

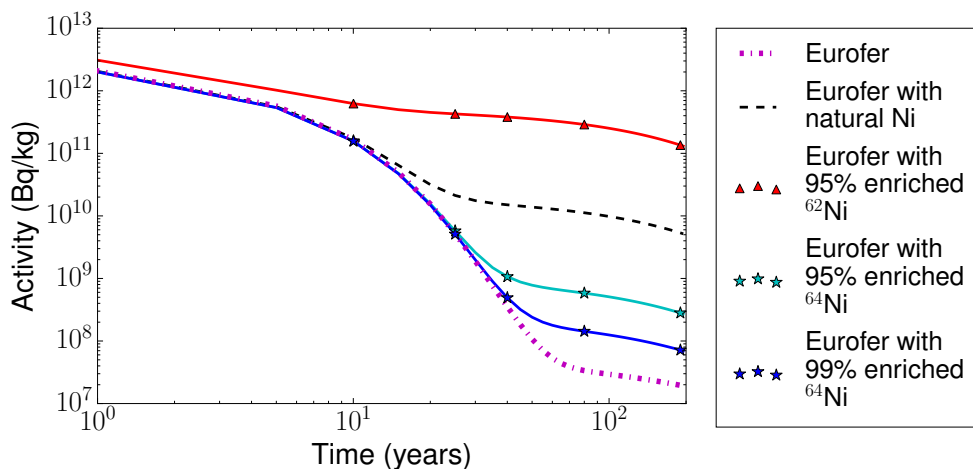


Fig. 7.8 The activity of regular Eurofer compared to Eurofer with an additional 2% Ni mass.

Figure 7.9 shows the impact of adding additional Ni with different isotopes enriched. Enriching ^{62}Ni results in additional activity while enriching ^{58}Ni , ^{60}Ni , ^{61}Ni or ^{64}Ni results in reduced activity compared to natural Ni.

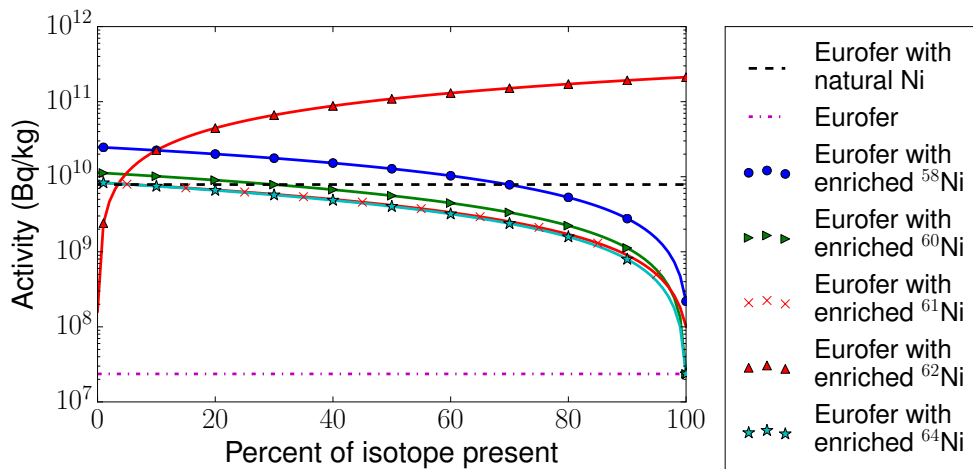


Fig. 7.9 The activity of Eurofer containing 2% mass Ni additions with varying isotopic enrichments. For comparison regular Eurofer and Eurofer with additional natural Ni are also plotted. The figure shows the activity 100 years after the end of irradiation.

7.4.3 Helium production in CuCrZr

Helium production within CuCrZr was investigated. The simulated results presented in Figure 7.10 show helium production within natural CuCrZr. The vast majority of helium is generated by ^{63}Cu (92%) which is consistent with the (n,α) cross-sections (see Figure 7.1). During the simulated neutron irradiation, ^{63}Cu produced approximately five times more He per atom compared to ^{65}Cu . CuCrZr containing natural copper produced 64 ppm He atoms per year. However, by enriching the copper content to 95% ^{65}Cu , He production was decreased to 20 ppm per year.

The critical bulk ppm concentration in Cu (615 ppm) would be achieved in 9.6 years using natural copper or this could be increased to 32.4 years using copper enriched to 95% ^{65}Cu . If the neutron flux was increased, then a linear relationship with helium production would be expected. The 1GW thermal plant simulated is representative of current EU DEMO designs. Whilst other DEMO designs offer similar power outputs some are smaller and more compact [180]. This would result in larger neutron fluxes and the critical bulk ppm would be reached sooner.

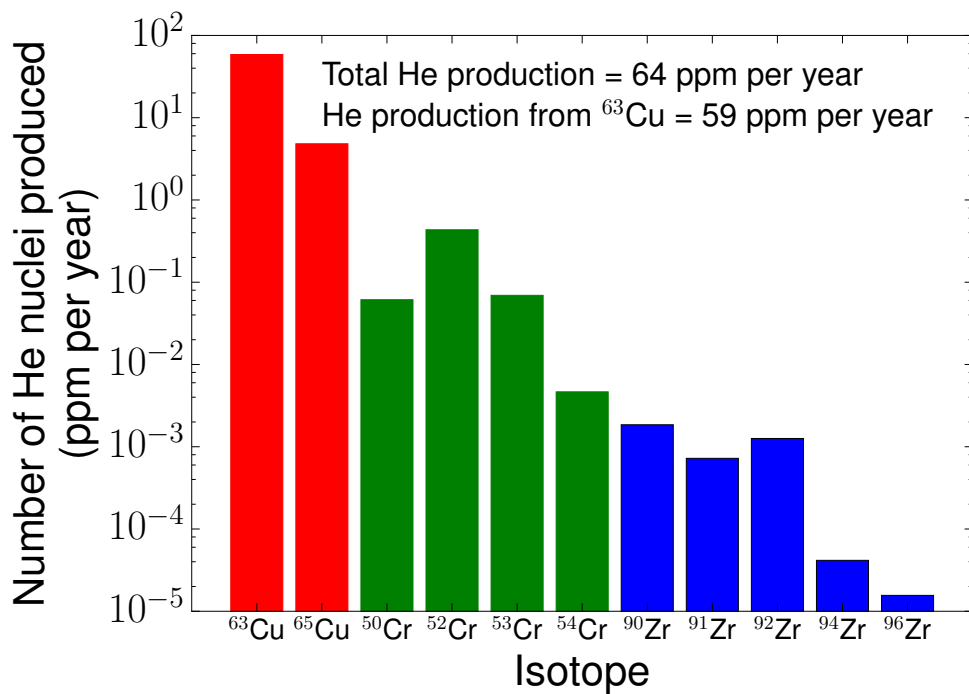


Fig. 7.10 The helium production (^3He and ^4He collectively) in CrCuZr

7.5 Costs involved

The cost of achieving the enrichment scenarios specified are considered in order to perform cost benefit analysis. Separative Work Units (SWU) describe the amount of effort required to enrich or deplete individual isotopes and can be used to approximate the cost of enrichment. The dominant technology are gaseous centrifuges and typically cost £160 per SWU [155]. Both Ni and Mo can be enriched using centrifuges however it is not possible to enrich Cu using current centrifuge technology. Methods such as electromagnetic separation are able to enrich copper but the cost is prohibitive (£20,000 per SWU).

The amount of effort or SWUs needed to enrich an element can be calculated using Equations 7.1-7.5 where W is the mass of waste (also referred to as tails), P is the mass of the product and F is the mass of feedstock. x_W , x_P and x_F are the fraction of the enriched isotope in the waste, product and feedstock respectively. The value function $V(x)$ can be found by knowing the concentration (x) of the given assay. The quantity of feedstock required to produce a known amount of product can be found using Equations 7.3-7.5 and the natural abundances of the isotopes involved (see [20] for more details).

$$\text{SWU} = P.V(x_p) + W.V(x_W) - F.V(x_F) \quad (7.1)$$

$$V(x) = (2x - 1)\ln\left(\frac{x}{1-x}\right) \quad (7.2)$$

$$P = F - W \quad (7.3)$$

$$\frac{F}{P} = \frac{x_p - x_w}{x_f - x_w} \quad (7.4)$$

$$\frac{W}{P} = \frac{x_f - x_p}{x_w - x_f} \quad (7.5)$$

The same product can be produced with different amounts of feedstock. This is achieved by varying the depletion in the waste assay. Finding a compromise between using large quantities of feedstock and mildly depleting the waste assay, or using small amounts of feedstock and highly depleting the waste assay is referred to as optimising the tails. The optimal solution depends on the relative costs of enrichment compared to the cost of the feedstock and any resale value related to the depleted tails. In the case of Ni and Mo enrichment the tails will have a resale value due to the range of non-nuclear uses for both elements. To calculate the cost of Ni, Mo and Cu enrichment several assumptions have been made.

- The costs of feedstock for natural Ni, Mo and Cu are £8,833 per tonne, £16,739 per tonne and £4002 per tonne respectively [1].
- The depleted tails produced have a resale value of 90% of the purchase price.
- The mass of Ni, Mo and Cu required is 40,000kg, 40,000kg and 7.7kg respectively.
- The enrichment costs of Ni, Mo and Cu are £160 per SWU, £160 per SWU and £20,000 per SWU respectively.
- Ni, Mo and Cu are enriched from their natural abundance (see Table 7.1).

The proposed amount of Eurofer containing enriched alloys is 200 tonnes; this equates to approximately 10% of the Eurofer in the blankets of a typical DEMO device. The mass contribution of enriched Ni or Mo to Eurofer is 2% of the Eurofer mass which results in 40,000kg of enriched Ni or Mo.

Assuming a thickness of 0.008mm is required to bond tungsten to Eurofer [204] then approximately 863cm³ of Cu will be needed to bond the tungsten first wall armour to Eurofer. The proposed mass of Cu to be enriched is therefore 7.7kg.

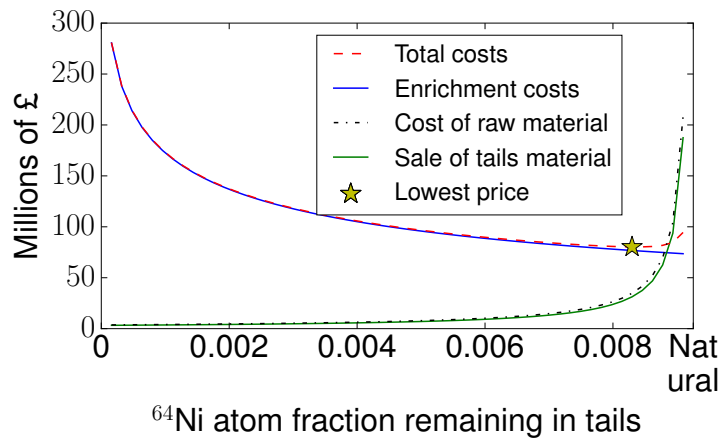


Fig. 7.12 Optimising the depletion level of the tails for ^{64}Ni enrichment.

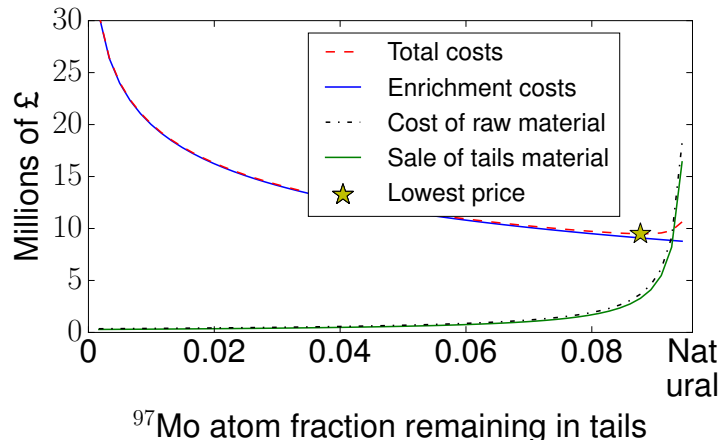


Fig. 7.13 Optimising the depletion level of the tails for ^{97}Mo enrichment.

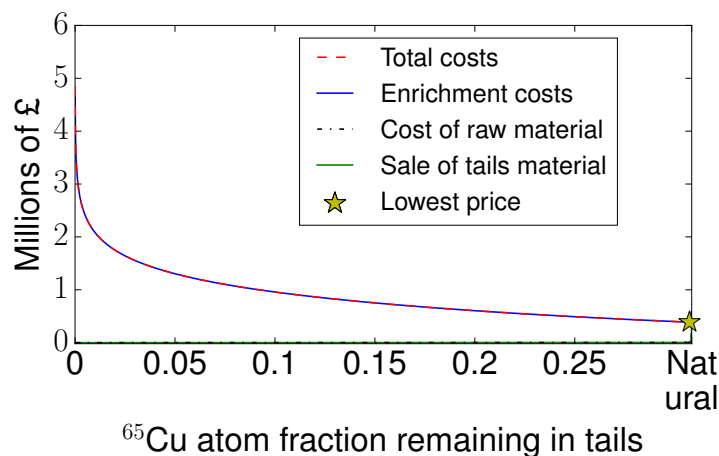


Fig. 7.14 Optimising the depletion level of the tails for ^{65}Cu enrichment.

The estimated costs for providing 40,000kg of 95% enriched ^{64}Ni and ^{97}Mo are £80 million and £9.5 million respectively (see Figures 7.13 and 7.12). The most economic depletion level for the tails in ^{64}Ni and ^{97}Mo enrichment was found to be 0.0083 and 0.0877 respectively. The costs for Cu enrichment are significantly higher per SWU but due to the small quantities required for bonding (7.7kg) the enrichment cost was estimated to be £0.4 million. The most economic depletion level for the tails in ^{65}Cu was found to be 0.3074 which is close to the natural abundance (0.3085). This is due to the relatively low raw material costs compared to the cost of enrichment. The costs stated here depend heavily upon the assumptions made. Companies such as Urenco currently offer Ni and Mo isotope enrichment services [2] and therefore the up front costs of establishing an enrichment facility have not been included.

For isotopic enrichment to be financially viable the additional capital costs involved must be offset by increased revenue. Possible advantages of ITLAMs are: improved material longevity and the ability to operate at increased temperatures. Improved longevity due to reduced helium production or improved radiation tolerance could result in increased reactor availability. Increased blanket temperatures would result in higher efficiencies when converting thermal power to electrical power. Both of these improvements would result in additional revenue for a fusion power plant.

Disadvantages include the additional upfront costs of the enrichment. The enrichment might act as a bottleneck in the operations and could possibly lengthen the construction time of the plant. The introduction of another technology into the process increases the risk and uncertainty of the overall plant cost.

Quantifying the potential increased availability and increased thermal efficiency resulting from the reintroduction of alloying elements such as Ni and Mo or enrichment of Cu is beyond the scope of this neutronics study. However, it is reasonable to ascertain the revenue increase required to offset the specified enrichment scenarios. Further materials based research would need to be performed to quantify the improved material properties of ITLAMs, if indeed there are any improvements.

In order to assess the potential revenue increases further assumptions about the power

plant are required, these are:

- The availability of the fusion power plant is 70%.
- The blanket's lifetime is 5 years before it is replaced.
- The wholesale price of electricity of £45 per MWh.
- The inlet coolant and outlet coolant temperatures are 300°C and 500°C respectively.
- The plant produces 1GW of thermal power.
- The revenue of the reactor can be approximated using Equation 7.6.

$$\text{Revenue} = \text{thermal power} \times \text{efficiency} \times \text{availability} \times \text{price per unit energy} \quad (7.6)$$

Currently the temperature of blankets is limited by the materials [208], however adding important alloying elements into the material could potentially increase their upper temperature ranges. Increasing the operation temperature of the breeder blankets would increase the thermodynamic efficiency of the plant. The resulting increase in thermal efficiency for a certain temperature rise can be calculated using the Carnot Cycle [21]. The thermodynamic efficiency (η_{th}) can be found using is dependent upon the temperature of the hot reservoir (T_H) and the temperature of the cold reservoir (T_C) as shown by Equation 7.7.

$$\eta_{th} \leq 1 - \frac{T_C}{T_H} \quad (7.7)$$

The thermodynamic efficiency is a key factor in deciding the cost of electricity for a fusion power plant [192]. Assuming coolant inlet and outlet temperatures of 300°C (573K) and 500°C (773K) then the thermal efficiency is a maximum of 25.9%. If the structural steel was able to tolerate an increase of just 10°C in the outlet temperature then this would result in an efficiency of 26.8%. This additional efficiency could generate additional electricity and increase the yearly revenue by approximately £2.5M. Figure 7.15 shows how raising the outlet temperature relates to additional revenue.

The availability is another significant variable which determines the revenue generated by a fusion power plant [192]. Additional alloying elements such as Ni have been shown

to reduce the severity of radiation embrittlement in steel [85]. It is also conceivable that reduced helium production (particularly in welds) could result in fewer material failures. Using the previously assumed wholesale price and thermal power, the revenue generated by an increase in availability of 0.01 would be approximately £1M. Figure 7.15 uses Equation 7.7 to illustrates the correlation between additional revenue and increased temperature or availability.

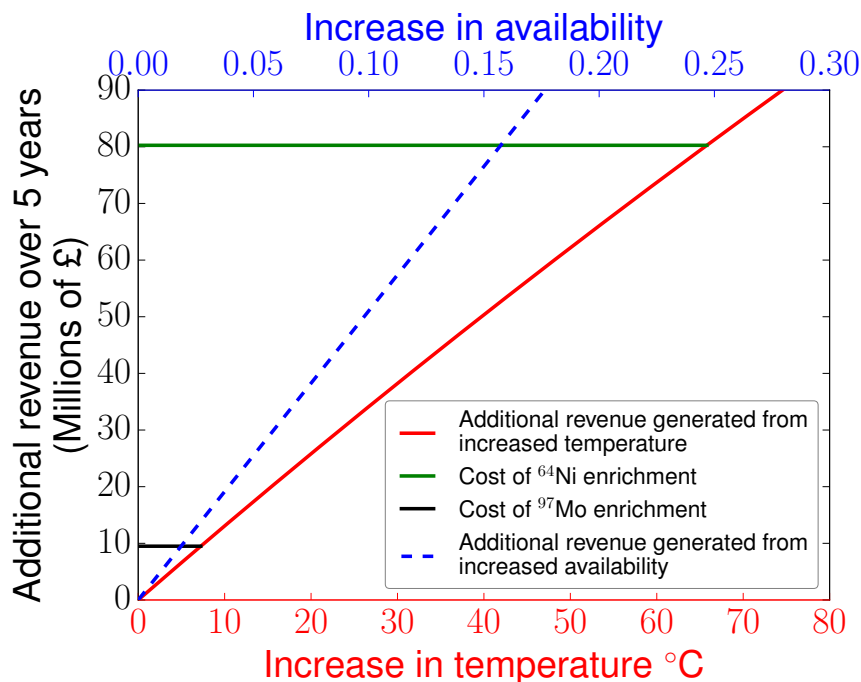


Fig. 7.15 The additional availability or temperature required to cover the costs of isotope enrichment.

The use of ITLAMs could be offset against an increase in availability or temperature or an increase in both. To finance the capital cost of 40,000kg of enriched Ni (95% ^{64}Ni) an increase of 66°C in temperature or 0.157 in availability would be required. The substantial increase in temperature or availability required to finance this ^{64}Ni enrichment scenario seems too ambitious. ^{97}Mo is significantly cheaper to enrich due to the higher natural abundance of ^{97}Mo and an increase of 7.2°C in temperature or 0.019 in availability would cover the enrichment costs. The enrichment of Cu for use in CuCrZr would only require marginal increases in temperature (1.5°C) or availability (0.004) to increase the revenue by £0.4 mil-

lion.

Whilst this research is unable to quantify the profitability of ITLAMs it presents feasible mechanisms for ITLAMs to offset the cost of enrichment. It is reasonable to assume that reintroducing important alloying elements back into LAMs would have beneficial effects on the material properties. It is possible that the addition of key alloying elements into LAMs could achieve increased revenue from increased temperature and increased availability. This preliminary estimate of the financial incentive strengthens the case for ITLAMs but any suggested improvement in material properties needs to be supported by experiment. This is currently not possible as there are no material testing facilities that can provide DEMO relevant irradiation with 14.1MeV neutrons.

It should be noted however that there is flexibility to vary the amount of enriched material (currently 40,000kg for Ni 40,000kg for Mo and 7.7kg for Cu) or the amount of enrichment (currently 95%) which would vary the cost of enrichment. Figure 7.16 shows how the amount of material or the enrichment can affect the resulting price. It is conceivable that ITLAMs are not financially viable at certain combinations of enrichment and quantity but feasible at others. For example it might be better to add enriched ^{64}Ni to a smaller percent of the Eurofer in the blanket, previously 10% had been assumed. Adding enriched Eurofer to only 5% of the Eurofer in the breeder blankets would halve the cost. However not all of the scenarios shown in Figure 7.16 result in the same activity. More precisely, using lower enrichment levels (below 95%) would result in additional activity (see Figure 7.9). If additional enriched Ni, Mo or Cu is shown to be beneficial experimentally then more thorough cost benefit analysis would be needed to optimise the quantity and enrichment fraction of the additives.

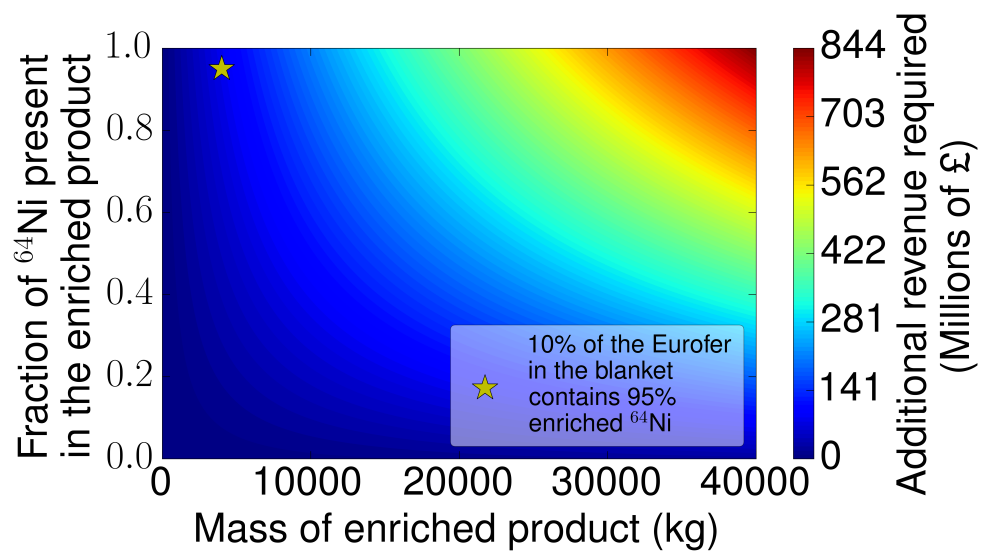


Fig. 7.16 The cost of different enrichment scenarios and the resulting activity.

7.6 Conclusion

The production of gas (He) in CuCrZr is investigated and the dominant cause of helium production is identified as an individual isotope of Cu. The enrichment of Cu is then considered to mitigate against excessive helium production. The helium production in CuCrZr is shown to decrease if enriched ^{65}Cu is used instead of natural Cu. However, Cu enrichment is not possible using current centrifuge enrichment technology and alternative techniques were found to be more expensive. The overall cost of enriching the CuCrZr used for bonding tungsten to Eurofer was £0.4 million due to the small amount of Cu required (7.7kg)

The research presented in this chapter also re-evaluates the selection of elements permitted in LAMs. Adding previously disallowed elements (Ni and Mo) back into the LAMs (Eurofer) is considered. The isotopic composition of the reintroduced elements is enriched so that the mechanical properties of the material can be improved without adding the activation associated with the natural element. The activation of Eurofer with additional enriched Ni and Mo was simulated and the activity of the resulting materials was found. It was possible to reintroduced enriched Mo without causing additional activity (compared to Eurofer without Mo). Reintroducing Ni was found to increase the activity compared to Eurofer without Ni. However, enriched Ni additions were shown to have a lower activity than natural Ni additions.

The financial case for isotopically tailored low activation materials (ITLAMs) is argued and possible ways to offset the cost of enrichment are discussed. Increases in temperature or availability which may result from the improved materials were suggested as possible methods of covering the costs of enrichment.

The research carried out in this chapter builds on the existing work and finds that additional enriched Ni and Mo content in Eurofer is potentially beneficial to material properties. Also possible opportunities of offsetting the enrichment costs of Ni, Mo and Cu were discussed. In the case of Cu enrichment, isotopic tailoring is shown to be beneficial as the He production can be reduced.

Chapter 8

Thesis conclusion

The thesis started by investigating the simulation of tritium production in breeder blankets as they age. The research carried out shows that fine material segmentation is required to avoid over-estimating tritium production. Being able to accurately predict the amount of tritium produced is essential for designing a successful DEMO reactor. Parts of the work presented in this chapter have been published in Fusion Engineering and Design [171].

The thesis moves on to consider solid-type breeder blankets made from different material compositions (different ${}^6\text{Li}$ enrichments and breeder fractions). The tritium production as well as the additional material costs of producing surplus tritium were explored. The additional material costs required to produce surplus tritium were found to be more economical than current and proposed tritium production facilities. The material cost of breeder blankets was dominated by the cost of Be_{12}Ti . The range of compositions were also compared in terms of their energy multiplication and their ability to maintain a consistent TBR value during the blanket's lifetime (5 years). Undesirable blanket compositions in terms of the four criteria investigated (costs, TBR degradation, energy multiplication and TBR) were found to be avoidable. The work presented in Chapter 3 has been used to enhance systems codes for fusion reactors [105] and has been submitted to Fusion Engineering and Design for consideration.

The production of surplus tritium researched in the Chapter 2 would allow reactors to provide a start-up inventory for subsequent reactors. However, the worldwide shortage of

tritium is only partly addressed by designing blankets capable of breeding excess tritium. Early reactors such as DEMO may not have any preceding tritium breeding reactors to rely on. Starting up a reactor in DT operation without an external supply of tritium has previously been proposed. The method considered is to use a DD plasma bred tritium. Optimisations of the breeder blankets to maximise the tritium production from DD neutrons was therefore investigated. It was possible to increase tritium production in the blankets by over 10%, although this improvement did not result in substantial benefit in terms of the duration of DD plasma required to achieve DT start-up. Chapter 4 highlighted the importance of collaboration with international partners on the topic and the author plans to contribute to a future publication in the field.

The cost of Be_{12}Ti was found to be the dominant cost in breeder blankets. Beryllium is also considered a precious element as it is particularly rare and has a range of high value uses. The thesis investigates a method of reducing the beryllium content without negative consequences in terms of key performance criteria (TBR, cost, peak heating and energy multiplication). Linear variation in material composition was found to be an improvement compared to uniform composition breeder blankets. It was found to be possible to reduce the quantity of beryllium required by the blanket while also improving the blanket's performance in all four criteria. Parts of the work presented in this chapter have been published in Fusion Engineering and Design [170].

It was also found that non uniform breeder blankets offer the potential to increase the TBR compared to uniform breeder blankets. More flexible variations in radial composition were investigated as a method of further increasing the TBR. By allowing material composition to vary radially it was shown that the TBR could be increased to values unobtainable with uniform blanket compositions. This is particularly useful for fusion reactors with limited space for breeder blankets, such as double null diverter designs and some high aspect ratio designs that have no inner blanket modules.

Finally, structural parts of breeder blankets were investigated. Methods of adding important alloying elements back into fusion relevant materials (Eurofer and CuCrZr) were considered. Isotopic enrichment allows certain isotopes to be separated from other less de-

sirable isotopes of the same element. During the development of Eurofer, several elements have been prohibited due to their tendency to become highly activated. Unfortunately some of the prohibited elements such as Mo and Ni are desirable for their alloying properties. The research showed that it is possible to reintroduce prohibited elements (provided that they are highly enriched) without detrimental effects on the activation. The enrichment of Cu in Cu-CrZr was also considered as a strategy for reducing the amount of helium produced. This increases the expected lifetime of the material as well as its reweldability. Parts of the work presented in Chapter 7 has been published in Fusion Engineering and Design [132].

Collectively the body of work contained within this thesis has made recognised contributions to the field of fusion neutronics ([171] and [132]). Existing research in the field of start-up without external tritium supplies has been enhanced and new avenues of research such as non-uniform composition breeder blankets have been initiated. The general over arching theme of this thesis is that materials should be tailored to suit the neutron spectra that they experience. Improvements can be made to the overall performance of breeder blankets by judicious tailoring of the material. Improvements to the activation, peak heating, energy multiplication, tritium production, material usage and cost have all been demonstrated in this thesis.

References

- [1] (2015). The London Metal Exchange. <http://www.lme.com/>. 2015-6-9.
- [2] (2015). Urenco enrichment company. <http://www.urencocom>. 2015-06-17.
- [3] Abdou, M. (1983). Tritium Breeding in Fusion Reactors. *Nuclear Data for Science and Technology*, pages 293–312.
- [4] Alvani, C. et al. (2000). Li₄SiO₄ pebbles reduction in He + 0.1% H₂ purge gas and effects on tritium release properties. *Journal of Nuclear Materials*, 208.
- [5] Andreani, R. et al. (2006). Overview of the European Union fusion nuclear technologies development and essential elements on the way to DEMO. *Fusion Engineering and Design*, 81.
- [6] Andreev, B. et al. (2001). Separation of hydrogen isotopes in the H₂O/H₂S system. *Separation Science and Technology*, 36:1833–1834.
- [7] Artsimovich, L. et al. (1967). Thermal insulation of plasma in the tokamaks. *Soviet Atomic Energy*, 22:656–665.
- [8] Atkinson, R. et al. (1924). Zur Frage der Aufbaumoglichkeit der Elements in Sternen. *Zeitschrift fur Physik*, 54:656–665.
- [9] Aures, A. et al. (2013). Tritium self-sufficiency of HCPB blanket modules for DEMO considering time-varying neutron flux spectra and material compositions. *Fusion Engineering and Design*, 88:2436–2439.
- [10] B. LaBombard and others (2014). ADX: a high field, high power density advanced divertor tokamak experiment - A white paper submitted to the FESAC Strategic Planning Panel.
- [11] Bank, O. D. (2006). The JEFF-3.1 Nuclear Data Library. JEFF Report 21. NEA/OECD: No. 6190. ISBN92-64-02314-3.
- [12] Berwald, D. et al. (1985). Assessment of beryllium resources for fusion applications. *Fusion Technology*, 8.
- [13] Bethe, H. (1993). The fusion hybrid. *Physics Today*, 32.
- [14] Beyond Petroleum (2014). BP Statistical Review of World Energy. <http://www.bp.com/en/global/corporate/about-bp/energy-economics/statistical-review-of-world-energy.html>.

References

- [15] Boccaccini, L. et al. (2004). Materials and design of the european DEMO blankets. *Journal of Nuclear Materials*, 329-333, Part A:148 – 155. Proceedings of the 11th International Conference on Fusion Reactor Materials (ICFRM-11).
- [16] Boccaccini, L. et al. (2011). Present status of the conceptual design of the EU test blanket systems. *Fusion Engineering and Design*, 86:478–483.
- [17] Bolt, H. et al. (2004). Materials for the plasma-facing components of fusion reactors. *Journal of Nuclear Materials*, 329-333:55–73.
- [18] Bradshaw, A. (2011). Is fusion a sustainable energy form? *Fusion Engineering and Design*, 86:2770–2773.
- [19] Brysk, H. (1973). Fusion Neutron Energies and Spectra. *Plasma Physics*, 15:611–617.
- [20] Cacuci, D. (2010). Handbook of Nuclear Engineering, Volume 1 Nuclear Engineering Fundamentals. ISBN: 978-0-387-98130-7. Springer.
- [21] Carnot, P. (1824). Reflexions sur la puissance motrice du feu et sur les machines propres à développer cette puissance. Chez Bachelier, Libraire.
- [22] Chadwick, M. et al. (2011). ENDF/B-VII.1 nuclear data for science and technology: cross sections, covariances, fission product yields and decay data. *Nucl. Data Sheets*, 112:2887–2996.
- [23] Chaudhuri, P. et al. (2014). Progress in engineering design of Indian LLCB TBM set for testing in ITER. *Fusion Engineering and Design*, 89:1362–1369.
- [24] Chen, H. et al. (2014). Conceptual design and analysis of the helium cooled solid breeder blanket for CFETR. *Fusion Engineering and Design*, proceedings Symposium on Fusion Technology 2014.
- [25] Chen, Y. et al. (2003). The EU power plant conceptual study – neutronic design analyses for near term and advanced reactor models, FZKA 6763. <http://bibliothek.fzk.de/zb/berichte/FZKA6763.pdf>.
- [26] Chitrakar, R. et al. (1961). Recovery of lithium from seawater using manganese oxide adsorbent ($H_{1.6}Mn_{1.6}O_4$) Derived from $Li_{1.6}Mn_{1.6}O_4$. *Industrial & Engineering Chemistry Research*, 40:1833–1834.
- [27] Colling, B. et al. (2012). Development of fusion blanket technology for the DEMO reactor. *Applied Radiation and Isotopes*, 70:1370–1372.
- [28] Conn, R. et al. (1978). Minimizing radioactivity and other features of elemental and isotopic tailoring of materials for fusion reactors. *Nuclear Technology*, 41:389–400.
- [29] Cook, E. et al. (1979). The helium question. *Science*, 206:4423.
- [30] Cook, I. et al. (2002). Prospects for economic fusion electricity. *Fusion Engineering and Design*, 63-64:25–33.

- [31] Coursey, J. et al. (2015). Atomic weights and isotopic compositions with relative atomic masses. NIST Physical Measurement Laboratory, www.nist.gov/pml/data/comp.cfm.
- [32] Craig, H. et al. (1961). Standard for reporting concentrations of deuterium and oxygen-18 in natural waters. *Science*, 133 no. 3467:1833–1834.
- [33] D. Spong (2015). Scientific visualization of 3-dimensional optimized stellarator Configurations. <http://www.physics.ucla.edu/icnsp/Html/spong/spong.htm>.
- [34] Davis, J. et al. (1996). Use of tungsten coating on ITER Plasma-facing components. *Journal of nuclear materials*, 1237:604–608.
- [35] Dean, S. et al. (1976). Fusion Power by Magnetic Confinement Program Plan. Energy Research and Development Administration report ERDA-76/110.
- [36] Dean, S. et al. (1998). Fusion power by magnetic confinement program plan. *Fusion Energy*, 17.
- [37] Dombrowski, D. (1997). Manufacture of beryllium for fusion energy applications. *Fusion Engineering and Design*, 37 (2).
- [38] Dorn, C. (12-5-2014). personal communication.
- [39] Dorn, C. et al. (2009). A review of physical and mechanical properties of titanium beryllides with specific modern application of TiBe₁₂. *Fusion Engineering and Design*, 84:319–322.
- [40] Dylst, K. (2008). Removing tritium and other impurities during industrial recycling of beryllium from a fusion reactor. *Fusion Science and Technology*, 54.
- [41] Eckhardt, D. et al. (1995). Nuclear fuels for low-beta fusion reactors: lithium resources revisited. *Journal of Fusion Energy*, 14:329–341.
- [42] EFDA (2013). Fusion Electricity A roadmap to the realisation of fusion energy. <https://www.euro-fusion.org/wpcms/wp-content/uploads/2013/01/JG12.356-web.pdf>.
- [43] Ehrlich, K. et al. (1998). Ifmif – an international fusion materials irradiation facility. *Nuclear Instruments and Methods in Physics Research Section B: Beam Interactions with Materials and Atoms*, 139:72–81.
- [44] El-Guebaly, L. (2009). Toward the ultimate goal of tritium self-sufficiency: Technical issues and requirements imposed on ARIES advanced power plants. *Fusion Eng. Des.*, 84:2072–2083.
- [45] El-Guebaly, L. (2011). Comments on aries-act strawman. http://fti.neep.wisc.edu/presentations/lae_comments_aries0411.pdf. 2014-09-30.
- [46] Enerdata Global Energy Intelligence (2015). Global Energy & CO₂ Data. <http://www.enerdata.net/enerdatauk/knowledge/subscriptions/database/energy-market-data-and-co2-emissions-data.php>.

References

- [47] Enoda, M. et al. (2014). R&D status on water cooled ceramic breeder blanket technology. *Fusion Engineering and Design*, 89:1131–1136.
- [48] EUROfusion (2015). ITER CAD diagram. <http://www.euro-fusion.org>.
- [49] European Commission, E. (2010). European Fusion Development Agreement Experimental Facilities. http://europa.eu/rapid/press-release_MEMO-10-165_en.htm.
- [50] Fasel, D. et al. (2005). Availability of lithium in the context of future D-T fusion reactors. *Fusion Engineering and Design*, 75-79.
- [51] Fausser, C. et al. (2012). Tokamak D-T neutron source models for different plasma physics confinement modes. *Fusion Engineering and Design*, 87:787–792.
- [52] Federici, G. et al. (2014). Overview of EU DEMO design and R and D activities. *Fusion Engineering and Design*, 89:882–889.
- [53] Feng, K. et al. (2014). New progress on design and R&D for solid breeder test blanket module in China. *Fusion Engineering and Design*, 89:1119–1125.
- [54] Ferronsky, V. et al. (2012). Isotopes of the Earth’s Hydrosphere. ISBN 978-94-007-2856-1.
- [55] Fietz, W. et al. (2013). Prospects of high temperature superconductors for fusion magnets and power applications. *Fusion Engineering and Design*, 88(6–8):440–445.
- [56] Fischer, U. (1988). Optimal use of beryllium for fusion reactor blankets. *Fusion Technology*, 13, no. 1:143–152.
- [57] Fischer, U. et al. (2005). Neutronic design optimisation of modular HCPB blankets for fusion power reactors. *Fusion Engineering and Design*, 75-79:751–757.
- [58] Fischer, U. et al. (2014). Neutronic analysis and tools development efforts in the european demo programme. *Fusion Engineering and Design*, 89:1880–1884.
- [59] Fischer, U. et al. (2015). Neutronics requirments for a DEMO fusion power plant. *Fusion Engineering and Design*, In Press.
- [60] Fleischmann, M. et al. (1989). Electrochemically induced nuclear fusion of deuterium. *Journal of Electroanalytical Chemistry*, 261.
- [61] Forrest, R. et al. (2012). FENDL-3 library - Summary document. INDC(NDS)-628.
- [62] Fribe, S. et al. (2015). Deuterium/Hydrogen permeation through different molecular sieve membranes: ZIF, LDH, Zeolite. *Microporous and Mesoporous Materials*.
- [63] Fusion For Energy (2014). Annual Reports. <http://fusionforenergy.eu/mediacorner/annualreport.aspx>.
- [64] Gan, Y. et al. (2010). Computer simulation of packing structure in pebble beds. *Fusion Engineering and Design*, 85:1782–1787.
- [65] Gernstner, E. et al. (2009). The hybrid returns. *Nature*, 460:25–28.

- [66] Giancarli, L. (2012). Overview of the ITER TBM Program. *Fusion Engineering and Design*, 87.
- [67] Giancarli, L. et al. (2006). Breeding Blanket Modules testing in ITER: An international program on the way to DEMO. *Fusion Engineering and Design*, 81:393–405.
- [68] Gierszewski, P. (1989). Tritium supply for near-term fusion devices. *Fusion Engineering and Design*, 10:399–403.
- [69] Gierszewski, P. (1995). Ceramic pebble bed development for fusion blankets. *Fusion Engineering and Design*, 27:167–178.
- [70] Gilbert, M. et al. (2012). An integrated model for materials in a fusion power plant: transmutation, gas production, and helium embrittlement under neutron irradiation. *Nuclear Fusion*, 52.
- [71] Glaser, A. et al. (2012). Proliferation risks of magnetic fusion energy: clandestine production, covert production and breakout. *Nuclear Fusion*, 52(4):043004.
- [72] Gohar, Y. (1980). Neutronics optimization of solid breeder blankets for starfire design.
- [73] Gonfiantini, K. et al. (1991). Tritium in the global atmosphere: Distribution patterns and recent trends. *Journal of Physics G: Nuclear and Particle Physics* 17.S.
- [74] Goorley, J. et al. (2013). Initial MCNP 6 Release Overview - MCNP 6 version 1.0.
- [75] Gorley, M. et al. (2014). Critical assessment 12: Prospects for reduced activation steel for fusion plant. *Material Science and Technology*.
- [76] Grosjean, C. et al. (2012). Assessment of world lithium resources and consequences of their geographic distribution on the expected development of the electric vehicle industry. *Renewable and Sustainable Energy Reviews*, 16.
- [77] H. Batemann (1910). The solution of a system of differential equations occurring in the theory of radio-active transformations. *Proceedings of the Cambridge Philosophical Society, Mathematical and physical sciences*.
- [78] Hazeltine, R. et al. (2010). Research needs workshop for magnetic fusion energy science. *Fusion Engineering and Design*, 85.
- [79] Hirai, T. (2013). ITER full tungsten divertor qualification program and progress. *Physica Scripta*, 2014:T159.
- [80] Hiwatari, R. et al. (2005). Demonstration tokamak fusion power plant for early realization of net electric power generation. *Nuclear Fusion*, 45:96–109.
- [81] Hodgson, P. (1971). The nuclear optical model. *Reports on Progress in Physics*, 34.
- [82] Hoshino, T. et al. (2011). Basic technology for 6Li enrichment using an ionic-liquid impregnated organic membrane. *Journal of Nuclear Materials*, 417:696–699.
- [83] Igitkhanov, Y. et al. (2013). Applicability of tungsten EUROFER blanket module for the DEMO first wall. *Journal of Nuclear Materials*, 438:440–444.

References

- [84] Ihli, T. et al. (2008). Review of blanket designs for advanced fusion reactors. *Fusion Engineering and Design*, 83.
- [85] International Atomic Energy Agency (2005). Effects of nickel on irradiation embrittlement of light water reactor pressure vessel steels. ISBN:92-0-103305-2.
- [86] International Energy Agency (2015). R&D statistics database. <http://www.iea.org/stats/rd.asp>.
- [87] J. Freidberg and others (2015). Research Needs for Fusion-Fission Hybrid Systems, United States department of Energy. http://web.mit.edu/fusion-fission/Hybrid_Report_Final.pdf.
- [88] Jackson, G. et al. (2013). An analytic expression for the tritium burnup fraction in burning-plasma devices. *Fusion Science and Technology*, 64.
- [89] Jones, R. (1999). Low activation materials. *Journal of Nuclear Materials*, 271 and 272:518–525.
- [90] Kasada, R. et al. (2015). A system dynamics model for stock and flow of tritium in fusion power plant. *Fusion Engineering and Design*.
- [91] Kataoka, K. et al. (2009). Crystal growth and structure refinement of monoclinic Li_2TiO_3 . *Materials Research Bulletin*, 44:168–712.
- [92] Kawamura, H. et al. (2002). Application of beryllium intermetallic compounds to neutron multiplier of fusion blanket. *Fusion Engineering and Design*, 61-62.
- [93] Kawamura, H. et al. (2003). Development of advanced blanket materials for a solid breeder blanket of a fusion reactor. *Nucl. Fusion*, 43.
- [94] Kemp, R. et al. (2013). DEMO1 parameters. EFDA report, EFDA_D_2LK7PH, PROCESST output files, <https://idm.euro-fusion.org/?uid=2MAWHP>.
- [95] Khanbabaei, B. et al. (2014). Deuterium-tritium catalytic reaction in fast ignition: Optimum parameter approach. *Pramana - Journal of Physics*, 83.
- [96] Kim, K. et al. (2015). Design concept of k-demo for near-term implementation. *Nuclear Fusion*, 55.
- [97] Kleykamp, H. (1999). Chemical interactions in the EXOTIC-7 experiment. *Journal of Nuclear Materials*, 272 (2).
- [98] Klueh, R. (2004). Elevated-Temperature Ferritic and Martensitic Steels and Their Application to Future Nuclear Reactors. Oak Ridge National Laboratory (ORNL/TM-2004/176).
- [99] Klueh, R. et al. (2004). Reduced-activation bainitic and martensitic steels for nuclear fusion applications. *Current Opinion in Solid State and Materials Science*, 8:239–250.
- [100] Knitter, R. (10-3-2014). personal communication.

- [101] Knitter, R. et al. (2013). Recent developments of solid breeder fabrication. *Journal of Nuclear Materials*, 442:S420–S424.
- [102] Kogan, B. et al. (1975). Beryllium, Report LN302-88, USSR Ministry of Geology.
- [103] Kolbasov, B. et al. (2008). Russian concept for a DEMO-S demonstration fusion power reactor. *Fusion Engineering and Design*, 83:870–876.
- [104] Koning, A. et al. (2012). Modern nuclear data evaluation with the TALYS code system. *Nuclear Data Sheets*, 113(12):2841 – 2934. Special Issue on Nuclear Reaction Data.
- [105] Kovari, M. et al. (2014). “PROCESS”: A systems code for fusion power plants Part 1: Physics. *Fusion Engineering and Design*, 89:3054–3069.
- [106] Krupka, M. et al. (Third Int. Conf. on Alternative Energy Sources, Miami Beach (1980)). Energy, helium and the future-II. <http://library.lanl.gov/cgi-bin/getfile?00237166.pdf>.
- [107] Kushnir, D. et al. (2012). The time dimension and lithium resource constraints for electric vehicles. *Resources Policy*, 37.
- [108] Kwon, M. et al. (2008). A strategic plan of Korea for developing fusion energy beyond ITER. *Fusion Engineering and Design*, 83:883–888.
- [109] Kwon, S. et al. (2013). Operation scenario of DT fusion plant without external initial tritium. *Fusion Engineering and Design*, 2013 IEEE 25th Symposium on Fusion Engineering, pages 1–5.
- [110] Lawson, J. (1957). Some Criteria for a Power Producing Thermonuclear Reactor. *Proceedings of the Physical Society, Section B* 70, no. 1.
- [111] Lee, C. et al. (2012). Sensitivity of the homogenized model in the neutronics analysis for the Korea Helium Cooled Solid Breeder Test Blanket Module. *Fusion Engineering and Design*, 87:575–579.
- [112] Lee, Y. et al. (2013). An effect of heavy water in a Korean DEMO water cooled ceramic blanket (WCCB). *Fusion Engineering and Design*, 88:2306–2308.
- [113] Leonard, B. et al. (1973). A review of fusion-fission (hybrid) concepts. *Nuclear Technology*, 20:161–178.
- [114] Lin, M. et al. (2015). An ultrafast rechargeable aluminium-ion battery. *Nature*, 520:324–328.
- [115] Lindau, R. et al. (2005). Present development status of EUROFER and ODS-EUROFER for application in blanket concepts. *Fusion Engineering and Design*, 75-79:989–996.
- [116] Lindsley, B. et al. (2008). Effects of molybdenum content in PM steels. *Advances in Powder Metallurgy and Particulate Materials*, 26.

References

- [117] Liu, S. et al. (2014). Conceptual design of a water cooled breeder blanket for CFETR. *Fusion Engineering and Design*, 89:1380–1385.
- [118] Lui, R. et al. (2014). Integral neutronics experiments in analytical mockups for blanket of a hybrid reactor. *Fusion Engineering and Design*, 89.
- [119] Lyakishev, N. (1996). Prospect of development and manufacturing of low activation metallic materials for fusion reactor. *Journal of Nuclear Materials*, 233:1516–1522.
- [120] Maisonnier, D. (2007). Power plant conceptual studies in Europe. *Nucl. Fusion*, 47, (11).
- [121] Maki, K. et al. (1988). Energy Multiplication in High Tritium Breeding Ratio Blanket with Front Breeder Zone for Fusion Reactors. *Journal of Nuclear Science and Technology*, 25:72–80.
- [122] Meade, D. et al. (2009). 50 years of fusion research. *Nuclear Fusion*, 50, no. 1:440–444.
- [123] Menard, J. et al. (2011). Prospects for pilot plants based on the tokamak, spherical tokamak and stellarator. *Nuclear Fusion*, 51.
- [124] Miller, A. (2001). Heavy Water: A Manufacturers' Guide for the Hydrogen Century. *Canadian Nuclear Society Bulletin*, 22, no. 1.
- [125] Miyai, Y. et al. (1988). Recovery of lithium from seawater using a new type of ion-sieve adsorbent based on MgMn₂O₄. *Separation Science and Technology*, 23.
- [126] Moeslang, A. et al. (2006). The IFMIF test facilities design. *Fusion Engineering and Design*, 81:863–871.
- [127] Moore, G. et al. (1965). Cramming more components onto integrated circuits. *Electronics*, 38, no. 8.
- [128] Moosavi, M. et al. (2007). Investigation of fuel energy gain for tritium-poor fuels in fast ignition fusion approach. *Plasma Science and Technology*, 15:996.
- [129] Morgan, L. (2012). *Inertial Confinement Fusion Neutronics*. PhD thesis, The University of York, Department of Physics.
- [130] Morgan, L. et al. (2013a). The impact of time dependant spectra on fusion blanket burn-up. *Fusion Engineering and Design*, 88:100 – 105.
- [131] Morgan, L. et al. (2013b). The development of a fusion specific depletion interface code FATI. *Fusion Engineering and Design*, 88(11):2891 – 2897.
- [132] Morgan, L. et al. (2015). Isotopically enriched structural materials in nuclear devices. *Fusion Engineering and Design*, 90:79–87.
- [133] Motojima, O. et al. (2008). Progress of design studies on an LHD-type steady state reactor. *Fusion Engineering and Design*, 83.

- [134] Murphy, D. et al. (1993). Reclamation of tungsten from activated fusion reactor components. *Fusion Engineering and Design*, 22.
- [135] N. Balshaw and others (2015). All the World's Tokamaks Poster. <http://www.tokamak.info/>.
- [136] Ni, M. (2013). Tritium supply assessment for ITER and DEMOnstration power plant. *Fusion Engineering and Design*, 9-10:2422–2426.
- [137] Ninomiya, H. et al. (2006). JT-60 upgrade device for confinement and steady state studies. *Plasma Devices and Operations*, 1:1.
- [138] Noda, T. et al. (1998). Silicon isotope enrichment for low activation. *Fusion Engineering and Design*, 41:173–179.
- [139] Nuttall, W. et al. (2012a). Helium from the air. The Future of Helium as a Natural Resource, Routledge, Abingdon/New York, p. 118.
- [140] Nuttall, W. et al. (2012b). Stop squandering helium. *Nature*, 485.
- [141] Okano, K. et al. (2014). DEMO design activities in the broader approach under Japan/EU collaboration. *Fusion Engineering and Design*, 89:2008–2012.
- [142] Packer, L. et al. (2010). The European Activation File: EAF-2010 Decay Data Library, CCFE-R (10)02. http://www.ccfc.ac.uk/easy-data/eaf2010/Docs/EAF_Decay_2010.pdf.
- [143] Packer, L. et al. (2011). Tritium self-sufficiency time and inventory evolution for solid-type breeding blanket materials for DEMO. *J. Nucl. Mat.*, 417:718–722.
- [144] Pampin, R. et al. (2006). Fusion power plant performance analysis using the HERCULES code. *Fusion Engineering and Design*, 81:1231–1237.
- [145] Park, J. et al. (2014). Pre-conceptual Design Study on K-DEMO Ceramic Breeder Blanket. *Fusion Engineering and Design*, proceedings of The 28th Symposium on Fusion Technology.
- [146] Peng, Y. et al. (2005). A component test facility based on the spherical tokamak. *Plasma Phys. Control. Fusion*, 47.
- [147] Pereslavtsev, P. et al. (2010). Neutronic analysis of the HCPB TBM in ITER utilizing an advanced integral approach. *Fusion Engineering and Design*, 85:1653–1658.
- [148] Pereslavtsev, P. et al. (2013). Generation of the MCNP model that serves as a common basis for the integration of the different blanket concepts. *EFDA D 2M7GA5 V.1.0*.
- [149] Piazza, G. et al. (2002). Characterisation of ceramic breeder materials for the helium cooled pebble bed blanket. *Journal of Nuclear Materials*, 307-311:811–816.
- [150] Puma, A. et al. (2006). Breeding blanket design and systems integration for a helium-cooled lithium-lead fusion power plant. *Fusion Engineering and Design*, 81:469–476.

References

- [151] Ragheb, M. et al. (1985). Alternate approach to inertial confinement fusion with low tritium inventories and high power densities. *Journal of Fusion Energy*, 4.
- [152] Rhinehammer, T. et al. (1978). *Evaluation of fuel resources and requirements for the magnetic fusion energy program*.
- [153] R.Hiwatari et al. (2010). Plasma Commissioning Scenario and Initial Tritium Inventory for Demo-CREST. *23rd International Atomic Energy Agency Fusion Energy Conference*, page 446.
- [154] Romanelli, F. et al. (2011). The role of JET for the preparation of the ITER exploitation. *Fusion Engineering and Design*, 86.
- [155] Rothwell, G. et al. (2009). Market power in uranium enrichment. *Science Global Security: The Technical Basis for Arms Control, Disarmament, and Nonproliferation Initiatives*, 17.
- [156] Russell, D. (2002). Validation suite for MCNP. Biennial Topical Meeting of the American Nuclear Society, Radiation Protection and Shielding Division.
- [157] Ryutov, D. et al. (2007). Geometrical properties of a snowflake divertor. *Physics of Plasmas*, 14.
- [158] Sanchez, J. (2014). Nuclear fusion as a massive, clean, and inexhaustible energy source for the second half of the century: brief history, status and perspective. *Energy Science and Engineering*, 2:165–176.
- [159] Sato, S. et al. (2012). Effects of lithium burn-up on TBR in DEMO reactor SlimCS. *Fusion Engineering and Design*, 87:680–683.
- [160] Satoshi, K. (2000). Possible scenario to start up DT fusion plant without initial loading of tritium. *Plasma Physics and Fusion Technology*, 76:1309–1312.
- [161] Sawan, M. et al. (2006). Physics and technology conditions for attaining tritium self-sufficiency for the DT fuel cycle. *Fusion Engineering and Design*, 81:1131–1144.
- [162] Scaffidi-Argentina, F. et al. (1998). Critical assessment of beryllium pebbles response under neutron irradiation: Mechanical performance and tritium release. *Journal of Nuclear Materials*, 258-263 (1).
- [163] Schaaf, B. et al. (2003). The development of EUROFER reduced activation steel. *Fusion Engineering and Design*, 69.
- [164] Schwarz, R. et al. (1999). A microsoft windows version of the MCNP visual editor. *Transactions of the American Nuclear Society*, 31:256–257. .
- [165] Schwochau, K. et al. (1984). Extraction of metals from sea water. *Inorganic Chemistry Topics in Current Chemistry*, 124.
- [166] Shanliang, Z. et al. (2002). Neutronics optimization of tritium breeding blanket for the FDS. *Plasma Science and Technology*, 4 (2).

- [167] Shibata, K. et al. (2011). Jendl-4.0: a new library for nuclear science and engineering. *J. Nucl. Sci. Technol.*, 48:1–30.
- [168] Shimomura, Y. et al. (2001). ITER-FEAT operation. *Nuclear Fusion*, 41.
- [169] Shimwell, J. et al. (2015a). A parameter study of time-varying tritium production in solid-type breeder blankets. *Fusion Engineering and Design*, 104, pages =.
- [170] Shimwell, J. et al. (2015b). Reducing beryllium content in mixed bed solid-type breeder blankets. *Fusion Engineering and Design*, In press.
- [171] Shimwell, J. et al. (2015c). Spatially and temporally varying tritium production in solid-type breeder blankets. *Fusion Engineering and Design*, 98-99:1868–1871.
- [172] Someya, Y. et al. (2011). Simplification of blanket system for SlimCS fusion DEMO reactor. *Fusion Engineering and Design*, 86:2269–2272.
- [173] Someya, Y. et al. (2015). Design study of blanket structure based on a water-cooled solid breeder for DEMO. *Fusion Engineering and Design*, page In Press.
- [174] Son, S. et al. (2004). Aneutronic fusion in a degenerate plasma. *Physics Letters A*, 329:76–82.
- [175] Srinivasan, R. et al. (2008). Strategy for the Indian DEMO design. *Fusion Engineering and Design*, 83:7–9.
- [176] Stott, P. E. (2005). The feasibility of using D-³He and D-D fusion fuels. *Plasma Physics and Controlled Fusion*, 47:1305–1338.
- [177] Sublet, J. et al. (1994a). The neutronic basis for elemental substitution in martensitic steels. *Journal of Nuclear Materials*, 212-215, Part 1:695–700.
- [178] Sublet, J. et al. (1994b). The potential of isotopic tailoring for titanium. *Journal of Nuclear Materials*, 208:8–17.
- [179] Sublet, J.-C. et al. (2012). The FISPACT-II User Manual. [http://www.ccfc.ac.uk/assets/Documents/CCFE-R\(11\)11.pdf](http://www.ccfc.ac.uk/assets/Documents/CCFE-R(11)11.pdf).
- [180] Sutherland, D. et al. (2014). The dynamak: An advanced spheromak reactor concept with imposed-dynamo current drive and next-generation nuclear power technologies. *Fusion Engineering and Design*, 89:412–425.
- [181] Sykes, A. et al. (1992). First results from the START experiment. *Nuclear Fusion*, 32, no. 4.
- [182] T-2 Nuclear Information Service (1998). Introduction to the ENDF Formats: ENDF MT Values. <http://t2.lanl.gov/nis/endf/mts.html>.
- [183] Taczanowski, S. (1980). Neutron multiplier alternatives for fusion reactor blankets. *Annals of Nuclear Energy*, 8:29–35.
- [184] Tamm, I. et al. (1959). Theory of the magnetic thermonuclear reactor. part I *Plasma Physics and the Problem of Controlled Thermonuclear Reactions (transl)*, page 3–19.

References

- [185] Taylor, N. et al. (2000). A model of the availability of a fusion power plant. *Fusion Engineering and Design*, 51-52:363–369.
- [186] Thomas, R. et al. (1998). Observation of Alpha Heating in JET DT Plasmas. *Physics Review Letters*, 80.
- [187] Tranqui, D. (1979). Crystal structure of ordered Li₄SiO₄. *Acta Crystallographica Section B, Structural Crystallography and Crystal Chemistry*, 35.
- [188] United States Geological Survey (2015). Commodity Statistics and Information. <http://minerals.usgs.gov/minerals/pubs/commodity/>.
- [189] Ushigusa, K. et al. (1996). Steady State Operation Research in JT-60U. *16th IAEA Fusion Energy Conference, IAEA-CN-64/01-3*.
- [190] Valanju, P. et al. (2008). Conceptual design of a component test facility based on the spherical tokamak. *Fusion Engineering and Design*, 83:1648–1653.
- [191] W. Stacey (2008). *Fusion Plasma Physics*. Wiley, ISBN: 9783527405862.
- [192] Ward, D. (2000). The impact of physics assumptions on fusion economics. *Fusion Energy 2000*, 18th Conference Proceedings, Sorrento, October 2000, Pub. IAEA Vienna, 2001, Paper FTP2/20.
- [193] Ward, D. et al. (2005). The economic viability of fusion power. *Fusion Engineering and Design*, 75-79:1221–1227.
- [194] Wegener, L. et al. (2009). Status of Wendelstein 7-X construction. *Fusion Engineering and Design*, 84:Proceeding of the 25th Symposium on Fusion Technology — (SOFT-25).
- [195] Willms, S. (2003). Tritium Supply Considerations. *Fusion Development Paths Workshop*.
- [196] Wittenberg, L. (1990). Comparison of tritium production reactors. *9th Topical Meeting on the Technology of Fusion Energy*, 7-11.
- [197] Wolf, R. et al. (2010). From Wendelstein 7-X to a Stellarator Reactor. *Plasma and Fusion Research*, 5:S1011–1 – S1011–6.
- [198] Wong, C. et al. (2010). An overview of the US DCLL ITER-TBM program. *Fusion Engineering and Design*, 85:1129–1132.
- [199] Wu, Y. et al. (2006). Conceptual design activities of FDS series fusion power plants in China. *Fusion Engineering and Design*, 81:2713–2718.
- [200] Wu, Y. et al. (2007). CAD-based interface programs for fusion neutron transport simulation. *Fusion Engineering and Design*, 84:1987 – 1992.
- [201] X-5 Monte Carlo Team (2008). MCNP - A General Monte Carlo N-Particle Transport Code, Version 5.

- [202] Xi, Z. et al. (2005). Thermal–hydraulic analysis and optimization of breeder unit for EU helium cooled pebble bed blanket. *Fusion Engineering and Design*, 75-79:785–788.
- [203] Y. Asaoka (2001). Commissioning of a DT fusion reactor without external supply of tritium. 18th Fusion Energy Conference, International Atomic Energy Agency.
- [204] Yang, Z. (2014). Tungsten/steel diffusion bonding using Cu/W–Ni/Ni multi-interlayer. *Transactions of Nonferrous Metals Society of China*, 24:2554–2558.
- [205] Youssef, M. et al. (2001). The breeding potential of ‘flinabe’ and comparison to ‘flibe’ in ‘CLiFF’ high power density concept. *Fusion Engineering and Design*, 61-62:497–503.
- [206] Zerkin, V. et al. (2015). Experimental nuclear reaction data (EXFOR). <https://www-nds.iaea.org/exfor/exfor.htm>.
- [207] Zheng, S. et al. (2015). Study of impacts on tritium breeding ratio of a fusion DEMO reactor. *Fusion Engineering and Design*, 98-99:1915–1918.
- [208] Zinkle, S. (2009). Structural materials for fission and fusion energy. *Materials Today*, 12, (11):12–19.

